



**REPUBLIC OF TURKEY  
ADANA ALPARSLAN TÜRKER SCIENCE AND TECHNOLOGY  
UNIVERSITY**

**GRADUATE SCHOOL OF NATURAL AND APPLIED SCIENCES  
DEPARTMENT OF ELECTRICAL AND ELECTRONICS  
ENGINEERING**

**DESIGN AND IMPLEMENTATION OF A FLOATING  
PHOTOVOLTAIC SYSTEM FOR HYDROGEN PRODUCTION**

**Emre GÜLLÜ  
MASTER OF SCIENCE**



**REPUBLIC OF TURKEY**  
**ADANA ALPARSLAN TÜRKESİ SCIENCE AND TECHNOLOGY**  
**UNIVERSITY**

**GRADUATE SCHOOL OF NATURAL AND APPLIED SCIENCES**  
**DEPARTMENT OF ELECTRICAL AND ELECTRONICS**  
**ENGINEERING**

**DESIGN AND IMPLEMENTATION OF A FLOATING**  
**PHOTOVOLTAIC SYSTEM FOR HYDROGEN PRODUCTION**

**EMRE GÜLLÜ**  
**MASTER OF SCIENCE**

**SUPERVISOR**  
**ASSOC. PROF. DR. BAŐAK DOĐRU MERT**

**ADANA 2021**

I hereby declare that all information in this thesis has been obtained and presented in accordance with academic rules and ethical conduct. I also declare that, as required by these rules and conduct, I have fully cited and referenced all information that is not original to this work.

[Signature]

Emre GÜLLÜ

# ABSTRACT

## DESIGN AND IMPLEMENTATION OF A FLOATING PHOTOVOLTAIC SYSTEM FOR HYDROGEN PRODUCTION

Emre GÜLLÜ

Department of Electrical and Electronics Engineering

Supervisor: Assoc. Prof. Dr. Başak DOĞRU MERT

Ocak 2021, 96 pages

One of the most important steps to slow down or stop global warming is to replace fossil fuel-based energy production with renewable energy sources. In this study, firstly, the efficiency of the floating solar panel was examined both practically in the field and by simulating on Matlab Simulink in order to minimize the panel temperature factor that negatively affects the panel efficiency while obtaining solar energy, which is one of the renewable energy types. Then, the electrochemical process in converting the generated energy into hydrogen in order to be able to use it when needed, especially to meet the energy needs of sea vehicles, was discussed practically. In order to determine the positive contribution of floating solar panels mounted on water to the efficiency of the panel, a land mounted (non-floating) 10 W solar panel and one 10 W floating solar panel were installed. As a result of the experiments, the power obtained from the panel at 37 ° C air temperature was 11% higher in the floating panel compared to the land-mounted panel. MATLAB Simulink results also largely overlapped with experimental data.

In the laboratory for hydrogen production, graphite (G), nickel coated graphite (G / Ni) and cobalt decorated nickel coated graphite (G / NiCo) were used as working electrodes in 1 M KOH solution, and the dissociation voltages of these electrodes were determined. In addition, hydrogen gas production of electrodes at different potentials was investigated. As a result of the experiments, the highest hydrogen volume was obtained with G / NiCo.

**Keywords:** floating photovoltaic panel, solar energy, hydrogen production, graphite, sea vehicle

# ÖZET

## HİDROJEN ÜRETİMİ İÇİN YÜZEN FOTOVOLTAİK SİSTEMİN TASARIMI VE UYGULAMASI

Emre GÜLLÜ

Elektrik Elektronik Mühendisliği Anabilim Dalı

Danışman: Doç. Dr. Başak DOĞRU MERT

Ocak 2021, 96 sayfa

Küresel ısınmanın yavaşlatılması ya da durdurulabilmesi için en önemli adımlardan biri fosil yakıtlara dayalı enerji üretiminin yerine yenilenebilir enerji kaynaklarının kullanılmasıdır. Bu çalışmada ilk olarak yenilenebilir enerji türlerinden olan güneş enerjisi vasıtasıyla elektrik enerjisi elde ederken panel verimine olumsuz etki eden panel sıcaklığı faktörünü azaltmak üzere yüzen güneş panelinin verimi hem sahada uygulamalı olarak hem Matlab Simulink üzerinden simülasyon yapılarak incelenmiştir. Daha sonra üretilen enerjinin ihtiyaç duyulduğunda kullanılabilmesi, özellikle deniz taşıtlarının enerji ihtiyacının karşılanabilmesi için hidrojene dönüştürülmesindeki elektrokimyasal süreç uygulamalı olarak ele alınmıştır.

Yüzen güneş panelinin panel verimine olumlu katkısının belirlenmesi amacıyla bir adet karaya montajlı (yüzmeyen) 10 W güneş paneli ve bir adet 10 W su üzerinde yüzen güneş paneli kurulmuştur. Deneyler sonucunda 37°C hava sıcaklığında panelden elde edilen güç yüzen panelde karaya montajlı panele göre % 11 daha fazla olduğu tespit edilmiştir. MATLAB Simulink sonuçları da deneysel verilerle büyük oranda örtüşmüştür.

Hidrojen üretimi için laboratuvarında, 1 M KOH çözeltisi içerisinde çalışma elektrodu olarak sırasıyla grafit (G), nikel kaplı grafit (G/Ni) ve kobaltla dekore edilmiş nikel kaplı grafit (G/NiCo) kullanılmış ve bu elektrotların ayrışma gerilimleri belirlenmiştir. Ayrıca elektrotların farklı potansiyellerdeki hidrojen gazı üretimleri incelenmiştir. Deneyler sonucunda en yüksek hidrojen hacmi G/NiCo ile elde edilmiştir.

**Anahtar Kelimeler:** yüzen güneş paneli, solar enerji, hidrojen üretimi, grafit, deniz taşıtları



*dedication*

*I would like to dedicate my thesis to my wife Gülay and my daughter Ceyda*

## ACKNOWLEDGEMENTS

In the preparation of this thesis, I would like to thank my respected supervisor Assoc. Prof. Dr. Bařak DOĐRU MERT for her contributions, guiding, motivating and patiently answering my questions.

I would also like to thank dear Assoc. Prof. Dr. TuĐçe DEMİRDELEN, who supported and guided the thesis during the thesis and the process until the thesis period.

I would also like to thank dear Res. Asst. Hüseyin NAZLIGÜL, dear Res. Asst. Burak ESENBOĐA, dear Res. Asst. Abdurrahman YAVUZDEĐER, my dear colleague Hasan KART and my dear friend Dr. ÇaĐatay TÜLÜ for their assistance in technical matters during the thesis.

Finally, I would like to thank my dear wife Gülay GÜLLÜ, who showed understanding about my thesis and motivated me, and my dear daughter Ceyda GÜLLÜ who did not upset me.

# TABLE OF CONTENTS

TABLE OF CONTENTS.....	ix
LIST OF FIGURES .....	xii
LIST OF TABLES .....	xiv
NOMENCLATURE.....	xvi
<b>1. INTRODUCTION.....</b>	<b>1</b>
<b>1.1. Fossil fuels .....</b>	<b>3</b>
<b>1.1.1. Coal .....</b>	<b>4</b>
<b>1.1.2. Oil.....</b>	<b>4</b>
<b>1.1.3. Natural gas .....</b>	<b>4</b>
<b>1.1.4. Nuclear energy .....</b>	<b>5</b>
<b>1.1.5. The effect of fossil fuels .....</b>	<b>5</b>
<b>1.1.5.1. Greenhouse effect.....</b>	<b>6</b>
<b>1.1.5.2. Acid rains.....</b>	<b>6</b>
<b>1.1.5.3. Nuclear wastes.....</b>	<b>6</b>
<b>1.2. Renewable energy sources .....</b>	<b>7</b>
<b>1.2.1. Wind energy .....</b>	<b>8</b>
<b>1.2.2. Biomass energy .....</b>	<b>11</b>
<b>1.2.3. Geothermal energy .....</b>	<b>12</b>
<b>1.2.4. Wave power.....</b>	<b>13</b>
<b>1.2.5. Hydroelectric energy .....</b>	<b>14</b>
<b>1.2.6. Solar energy.....</b>	<b>15</b>
<b>1.2.6.1 Structure of photovoltaic panels.....</b>	<b>18</b>
<b>1.2.6.2 Mathematic model of photovoltaic panel .....</b>	<b>22</b>
<b>1.3. Hydrogen production .....</b>	<b>23</b>
<b>1.3.1. Electrolysis .....</b>	<b>25</b>
<b>1.3.2. Electrocatalysis .....</b>	<b>28</b>
<b>1.3.3. Hydrogen economy .....</b>	<b>29</b>
<b>1.3.4. Storage and novel applications of hydrogen .....</b>	<b>30</b>
<b>2. LITERATURE REVIEW .....</b>	<b>33</b>
<b>3. MATERIALS AND METHODS .....</b>	<b>46</b>

3.1. Solar panel experiment materials .....	46
3.2. Hydrogen production experiment materials .....	49
3.3.. Methods .....	51
3.4.. Simulation Method .....	52
<b>4. RESULTS AND DISCUSSIONS .....</b>	<b>54</b>
4.1. Solar energy production in non-floating design.....	54
4.2. Solar energy production in floating design .....	59
4.3. Comparison of floating solar panel and land mounted solar panel .....	65
4.4. Hydrogen production experiment .....	70
4.4.1. The performance of graphite .....	70
4.4.2. The performance of nickel plated graphite .....	73
4.4.3. The performance of cobalt decorated nickel plated graphite .....	76
<b>5. CONCLUSIONS .....</b>	<b>82</b>
<b>6. RECOMMENDATIONS.....</b>	<b>84</b>
<b>REFERENCES .....</b>	<b>85</b>
<b>CURRICULUM VITAE.....</b>	<b>96</b>

## LIST OF FIGURES

<b>Figure 1.1.</b> Change of renewable energy production by years in the world.....	2
<b>Figure 1.2.</b> Renewable energy source types. ....	7
<b>Figure 1.3.</b> The interior structure of a wind tribune .....	9
<b>Figure 1.4.</b> Wind energy density of Turkey .....	10
<b>Figure 1.5.</b> Adana Province wind speed map.....	11
<b>Figure 1.6.</b> Cycle of biomass energy .....	12
<b>Figure 1.7.</b> The geothermal energy potential of Turkey.....	13
<b>Figure 1.8.</b> Structure of a hydroelectric power plant.....	15
<b>Figure 1.9.</b> Solar panel system in early 1900's .....	16
<b>Figure 1.10.</b> Basic structure of a passive solar house.....	17
<b>Figure 1.11.</b> Typical structure of a solar panel and a solar cell.....	19
<b>Figure 1.12.</b> Variation of PV panel power according to panel temperature.....	20
<b>Figure 1.13.</b> Average highest temperatures of Adana from 1928 to 2018 .....	21
<b>Figure 1.14.</b> Average daily sunbathing durations of Adana from 1928 to 2018.....	22
<b>Figure 1.15.</b> Equivalent circuit a) one diode b) two diodes c) simplified circuit model.....	23
<b>Figure 1.16.</b> Hydrogen production by water electrolysis .....	26
<b>Figure 1.17.</b> Classification of electrolysis methods .....	27
<b>Figure 1.18.</b> An example of an energy system in hydrogen economy .....	30
<b>Figure 1.19.</b> Hydrogen storage methods .....	32
<b>Figure 2.1.</b> PVcells electrical and thermal yielding in 35 °C.. .....	33
<b>Figure 2.2.</b> Block diagram of integrated system. ....	36
<b>Figure 2.3.</b> Schematic diagram of PVT based hydrogen production. ....	37
<b>Figure 2.4.</b> Schematic of hydrogen production through wind energy.....	38
<b>Figure 2.5.</b> Different renewable energy systems that are considered for the simulation.....	38
<b>Figure 2.6.</b> Hydrogen production system. ....	39
<b>Figure 2.7.</b> Some pathways for hydrogen production. ....	40
<b>Figure 2.8.</b> Block diagram of the proposed topology.....	42
<b>Figure 2.9.</b> PEC and photochemical water seperation methods. ....	42
<b>Figure 2.10.</b> The largest floating PV system in the world which is installed in China. ....	45

<b>Figure 3.1.</b> The appearance of solar panel back. ....	47
<b>Figure 3.2.</b> The Appearance of solar panel from side. ....	47
<b>Figure 3.3.</b> Installed solar panel floating on water .....	48
<b>Figure 3.4.</b> View of the experimental setup .....	50
<b>Figure 3.5.</b> MATLAB Simulink equivalent circuit of panel .....	53
<b>Figure 4.1.</b> Obtained curve belonging to potential (U/V) and current (I/A) at 6°C .....	55
<b>Figure 4.2.</b> Obtained curve belonging to potential (U/V) and current (I/A) at 16°C .....	56
<b>Figure 4.3.</b> Obtained curve belonging to potential (U/V) and current (I/A) at 24°C .....	57
<b>Figure 4.4.</b> Obtained curve belonging to potential (U/V) and current (I/A) at 37°C .....	58
<b>Figure 4.5.</b> Obtained curve belonging to potential (U/V) and current (I/A) at different temperatures .....	58
<b>Figure 4.6.</b> Obtained curve belonging to potential (U/V) and current (I/A) at 6°C in floating design. ....	59
<b>Figure 4.7.</b> Obtained curve belonging to potential (U/V) and current (I/A) at 16°C in floating design. ....	60
<b>Figure 4.8.</b> Obtained curve belonging to potential (U/V) and current (I/A) at 24°C in floating design. ....	62
<b>Figure 4.9.</b> Obtained curve belonging to potential (U/V) and current (I/A) at 37°C in floating design. ....	64
<b>Figure 4.10.</b> Obtained curve belonging to potential (U/V) and current (I/A) at different temperatures in floating design. ....	65
<b>Figure 4.11.</b> Pmax comparison floating with non-floating design. ....	66
<b>Figure 4.12.</b> Current (I / A) - voltage (U / V) graph obtained as a result of 6°C temperature in MATLAB Simulink. ....	67
<b>Figure 4.13.</b> Current (I / A) - voltage (U / V) graph obtained as a result of 16°C temperature in MATLAB Simulink. ....	68
<b>Figure 4.14.</b> Current (I / A) - voltage (U / V) graph obtained as a result of 24°C temperature in MATLAB Simulink. ....	68
<b>Figure 4.15.</b> Current (I / A) - voltage (U / V) graph obtained as a result of 37°C temperature in MATLAB Simulink. ....	69
<b>Figure 4.16.</b> The voltage - current density curve of G-I/bare (●) and G-II/bare (○) in 1 M KOH at 298 K.. ....	70
<b>Figure 4.17.</b> The voltage - current curve of G-I/bare (●) in 1 M KOH at 298 K... ..	71

<b>Figure 4.18.</b> Hydrogen production volume by applied voltage with G-I/bare.....	72
<b>Figure 4.19.</b> The voltage - current density curve of G-I /Ni (◇) in 1 M KOH at 298 K.....	74
<b>Figure 4.20.</b> The voltage - current density curve of G-I/bare (●) and G-I/Ni (◇) in 1 M KOH at 298 K.....	74
<b>Figure 4.21.</b> Hydrogen production volume by applied voltage with G-I/Ni.....	75
<b>Figure 4.22.</b> The voltage - current density curve of G-I /NiCo (■) in 1 M KOH at 298 K.....	77
<b>Figure 4.23.</b> The voltage - current density curve of G-I/bare (●), G-I/Ni (◇) and G-I/NiCo (■) in 1 M KOH at 298 K.....	78
<b>Figure 4.24.</b> Hydrogen production volume by applied voltage with G-I/NiCo.....	79
<b>Figure 4.25.</b> Comparison of the hydrogen amounts generated by the G-I/bare, G-I/Ni and G-I/NiCo electrodes.....	79

## LIST OF TABLES

<b>Table 1.1.</b> Current state of development of electrolysis methods. ....	28
<b>Table 2.1.</b> Hydrogen generating expense in some places and with some renewable energy resources.....	35
<b>Table 3.1.</b> Technical datas of the solar panel.. ....	46
<b>Table 4.1.</b> Obtained current(I/A) and potential(U/V) values at temp 6°C in non-floating design... ..	54
<b>Table 4.2.</b> Obtained current(I/A) and potential(U/V) values at temp 16°C in non-floating design.. ..	55
<b>Table 4.3.</b> Obtained current(I/A) and potential(U/V) values at temp 24°C in non-floating design.....	56
<b>Table 4.4.</b> Obtained current(I/A) and potential(U/V) values at temp 37°C in non-floating design.....	57
<b>Table 4.5.</b> Obtained current(I/A) and potential(U/V) values at temp 6°C in floating design.....	59
<b>Table 4.6.</b> Obtained current(I/A) and potential(U/V) values at temp 16°C in floating design.....	60
<b>Table 4.7.</b> Obtained current(I/A) and potential(U/V) values at temp 24°C in floating design.....	61
<b>Table 4.8.</b> Obtained current(I/A) and potential(U/V) values at temp 37°C in floating design.....	63
<b>Table 4.9.</b> Pmax values at different temperatures in two design.....	66
<b>Table 4.10.</b> Produced hydrogen volume with G-I/bare at the end of 30 minutes.....	71
<b>Table 4.11.</b> Produced hydrogen volume with G/Ni at the end of 30 minutes.. ..	75
<b>Table 4.12.</b> Produced hydrogen volume with G-I/NiCo at the end of 30 minutes.....	78

## NOMENCLATURE

kWh	: kilowatt hour
MWh	: megawatt hour
TWh	: terawatt hour
W	: watt
kW	: kilowatt
MW	: megawatt
GW	: gigawatt
V	: volt
A	: amper
g	: gram
kg	: kilogram
m	: meter
m <sup>2</sup>	: meter square
cm	: centimeter
cm <sup>2</sup>	: centimeter square
l	: liter
ml	: milliliter
%	: percent
s	: second
°C	: celcius
°F	: fahranheit
°K	: kelvin
U	: voltage
I	: current
E <sub>d</sub>	: dissociation voltage
I <sub>d</sub>	: current density
E	: energy
m	: mass
c	: speed of light
Ag	: silver

K	: potassium
AgCl	: silver chloride
KCl	: potassium chloride
G	: graphite
G/Ni	: nickel plated graphite
G/NiCo	: cobalt decorated nickel plated graphite
Zn	: zinc
Pt	: platinum
O <sub>2</sub>	: oxygen
H <sub>2</sub>	: hydrogen
N	: nitrogen
CO <sub>2</sub>	: carbon dioxide
CH <sub>4</sub>	: methane
Na	: sodium
NaOH	: sodium hydroxide
KOH	: potassium hydroxide
Cl <sub>2</sub>	: chlorine
NaCl	: sodium chloride
Cu	: copper
Bi	: bismuth
B	: boron
S	: sulfur
M	: molar
H <sub>2</sub> SO <sub>4</sub>	: sulfuric acid
NASA	: national aeronautics and space administration
e <sup>-</sup>	: electron
B.C.	: before Christ
PV	: photovoltaic

# 1. INTRODUCTION

Due to fast developing technology, increasing population, expanding cities and industrial structures, obtaining energy at the most cost-effective has become more important in recent years.

Rapidly developing technology, diversifying production processes, increasing demand in the end user increase the need for energy day after day. According to the BP (British Petrol) 2019 World Energy Statistics Report, energy consumption worldwide increased by 2.9 percent compared to the previous year, reaching approximately 13.8 billion tons of oil equivalent. This increase was recorded as the biggest increase on an annual basis since 2010.

There is a positive correlation between countries' energy consumption and their gross national product. At the same time, although the carbon emission is high due to the industry in developed countries, the renewable energy installed power is also high. In this respect, the renewable energy installed capacity of the country gives an important idea about its development.

Turkey in 2017, 289 billion 975 million 177 thousand kWh of electricity consumed, an increase of 0.75 percent in 2018, this figure rose to 292 billion 171 million 619 thousand kWh. According to the compilation made from the Ministry of Energy and Natural Resources data, the country's electricity consumption increased last year compared to the previous year.

According to data published by BP, the most electricity in the world was produced from coal last year with 10 thousand 100 terawatt hours. Electricity production from coal increased by 3 percent compared to the previous year According to the BP 2019 World Energy Statistics Report, total global electricity production reached 26,614 TWh in 2018.

In Turkey, 55% of the electricity produced in June and 57.5% of the total electricity generated in thermal power plants in July.

The need for renewable energy has been increasing more and more due to the depletion of fossil fuels and the negative impact of fossil fuel use on global warming. However, energy production from renewable sources is increasing rapidly each year, as shown in figure 1.1.

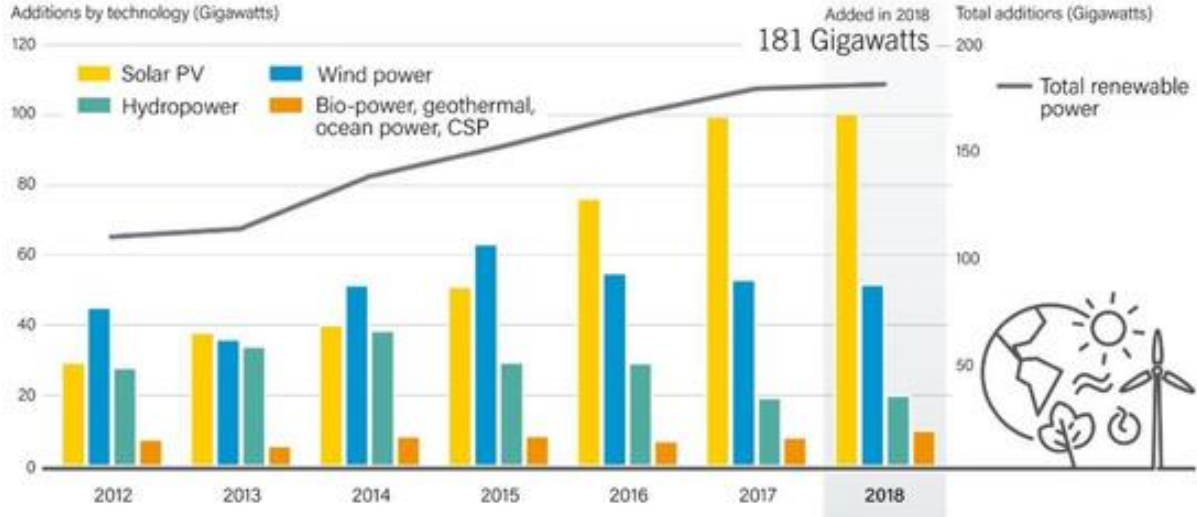


**Figure 1.1.** Change of renewable energy production by years in the world (Aleem et al, 2020).

However, renewable energy resources have been exposed serious changes according to daily weather events, which makes it unpredictable. The energy needs to be provided clean, safe and uninterruptedly and delivered to the point where it will be consumed. However, the efficiency of photovoltaic panels is highly influenced by parameters such as sunshine duration, humidity, temperature and dust. In addition, the electrical energy must be consumed at the moment it is produced and must be stored, which raises the cost of storage.

In this respect, producing hydrogen from an electrolysis system that will be designed with a renewable energy supply and storing the produced hydrogen in suitable tanks seems to be one of the optimum solutions. Hydrogen is one of the new generation fuel types and its usage area has been increasing day by day. With stored hydrogen, energy can be used whenever needed.

The harm caused by carbon emissions to the environment in recent years has been serious. R&D (research and development) activities such as carbon capture and storage aimed at reducing environmental damage are aimed at reducing gas emissions. Most of the carbon emissions in nature arise from the use of fossil resources in energy production. Energy

consumption and carbon emissions increase in direct proportion. Fossil fuels used in energy production leave residues in solid and gaseous form after burning. These residues can not be utilized in any way and cause environmental pollution.

There are basically two sources of energy production: fossil fuels and renewable resources. For example, almost all of the energy in the United States and other industrialized countries is derived from fossil fuels such as coal and natural gas. During its use, it is not taken into account how energy is produced or the environmental damage it will cause. Its supply is limited as non-renewable energy sources are found as a constant stock in nature. Based on the current consumption level of 2010, it is estimated that the world coal reserves will be exhausted within 150 years, oil reserves 30 years and natural gas reserves will be exhausted in 50 years if there are no new reserves. Despite its limited supply, it is observed that the demand for non-renewable resources in the world is gradually increasing.

### **1.1. Fossil Fuels**

Fossil is the remains of living creatures that lost their lives for many years without deterioration. All energy resources such as coal, oil and natural gas, which have hydrocarbon content, are called fossil fuels.

Fossil fuels are formed by the thermochemical reactions of plant and animal wastes under the soil. This shows that fossil fuels are available in certain regions and at limited levels.

While coal gained importance after the invention of the steam engine, benefiting from the kinetic energy of water gained importance with the invention of dynamo. And oil gained great importance when internal combustion engines were invented in 1900s and internal combustion diesel engines in 1910.

These fuels can be categorized as follows; coal, oil and natural gas. When we look at the rate of these fuels in the world; seventy percent consists of coal, fourteen percent oil, fourteen percent natural gas, and the remaining two percent are other fossil fuels.

### **1.1.1. Coal**

Coal, meaning fossilized carbon mineral, is a combustible black or brown-black sedimentary rock in which layers of rock are formed in layers or veins called coal deposits or coal seams. It consists of carbon with varying amounts of hydrogen, sulfur, oxygen and nitrogen. Throughout history, coal has mainly been used as a burnt energy source for electricity and / or heat generation and is also used for industrial purposes such as refining metals. It is estimated that it was started to be used for heating the houses in Great Britain in the 16th century. Its use in China for the same purpose is estimated to be goes back to the 22nd century.

### **1.1.2. Oil**

Oil (petroleum) is a mixture consisting of a high percentage of various hydrocarbons and at the same time containing a low percentage of nitrogen and sulfur in its structure. These elements consist of complex molecular structures.

Oil is a fuel that has played a key role in the industry, especially in the production sector and logistics. The search for alternative energy sources instead of oil has accelerated as the negative effects of global warming on the world are felt concretely. As will be mentioned later in the study, solar energy and hydrogen fuel cells are some of the most important of these.

### **1.1.3. Natural gas**

Natural gas is a petroleum derivative gas containing methane gas, which is a high proportion of hydrocarbon group. Compounds in the structure of natural gas other than methane are propane, butane and ethane. It also contains very small amounts of carbon dioxide, helium, nitrogen and hydrogen sulfide. It can be said that it is the cleanest fuel among fossil fuels. Its use in history dates back to 1000s before the Asian continent.

Natural gas is extracted in almost all regions of the world. Russia, Iran, USA and Netherlands are the leading producers. Natural gas, which becomes liquid under high pressure, is transported by this method or through pipelines. It is calculated that all the reserves of natural gas in the world can be used for a maximum of eighty more years and then this energy source will be exhausted. Considering this situation, it is certain that it cannot play a role as the

energy of the future, even if it does not have a negative impact on global warming as much as other fossil fuel types.

#### **1.1.4. Nuclear energy**

Nuclear energy is the energy released by methods such as combining or breaking down subatomic particles, which are the smallest units of matter. The combination process is called fusion, and the disintegration process is called fission.

Energy is obtained by fission reaction in nuclear power plants. For this, uranium, one of the radioactive elements, is used. In the fission reaction, a high speed neutron is applied to the element uranium. A huge amount of energy is released from the element uranium that is broken down in this way.

The high amount of heat emitted by the generated energy creates strong steam waves by boiling the water in giant boilers. These steam waves rotate the generator turbines and produce electrical energy.

Nuclear energy waste problem is one of the controversial energy sources because of the high risk of accidents and the size that can threaten large masses. On the other hand, it plays an important role in reducing energy costs in developed countries. France, one of these countries, obtains almost 80 percent of its energy needs from nuclear power plants. Continue building a nuclear power plant in Mersin Akkuyu in halihair in Turkey.

#### **1.1.5. The Effects of fossil fuels**

The biggest disadvantage of fossil fuels is that they emit greenhouse gases into the atmosphere when they are burned to generate energy.

Under normal conditions, rays reaching the earth from the sun are absorbed by seas and land surfaces, and the natural greenhouse gases in the atmosphere prevent this heat from dispersing into space. However, as the greenhouse gases released by the burning of fossil fuels increase the amount of heat that is prevented from dispersing, they cause global warming.

### **1.1.5.1. Greenhouse effect**

The greenhouse effect (global warming) is defined as the gradual rise of greenhouse gases in the world. The greenhouse effect is the situation where the heat reaching the earth with the sun rays is trapped by the atmosphere. Greenhouse gases, which accumulate more than normal in the sky, prevent the spread of the heat that should be spread from the earth's surface to a certain extent, causing the earth to become warmer.

### **1.1.5.2. Acid rains**

It has an acidic effect in terms of pH value such as carbon dioxide, sulfur dioxide and nitrogen dioxide emitted into the aura of the world. The occurrence of these gases coming down to the earth with rain and snow is known as acid rain. Acid rain disrupts the pH balance of fresh water resources on earth. It reduces the quality of the soil in agricultural areas.

### **1.1.5.3. Nuclear wastes**

In nuclear snatrals, tools, parts, filters and equipment that constantly work with radioactive materials become radioactive after a while. After the end of their life, these substances become nuclear waste. As they cannot be released to the nature, they must be stored by considering the half-life periods of the substance.

Our country, which is dependent on foreign sources in terms of energy raw materials, has significant environmental pollution as a result of accidents that may occur during fuel transportation.

According to the new policy scenario of the International Energy Agency (IEA) covering the 2010-2035 period, it is expected that the demand for coal will increase by 27%, the demand for oil and nuclear energy will increase by 15% and the demand for natural gas will increase by 35% in the period from 2010 to 2035.

The International Energy Agency expects a 70% increase in oil demand and a 130% increase in carbon emissions by 2050. Most of the carbon dioxide emissions that cause greenhouse effects are use of fossil fuels. Therefore, a tax policy that will encourage the reduction of fossil fuel use and the use of renewable energy sources that do not harm the environment

instead of fossil resources will contribute to the reduction of environmental externalities. (Çoban and Kılınç, 2012)

## 1.2. Renewable energy resources

Renewable energy sources are a source of energy production that constantly renews itself and pollutes the nature less. These sources do not contain CO<sub>2</sub> like fossil sources.

Solar, wind, biomass, geothermal, wave power and hydro energies are the main types of renewable energy sources, as seen in Figure 1.2 Another advantage of renewable energy sources is that they can be found all over the world depending on their geographical and geopolitical conditions. In other words, these are natural energy sources. Countries do not need to import them, these sources alleviate the problem of energy dependency. It contributes to reduce the difference between the levels of international development.

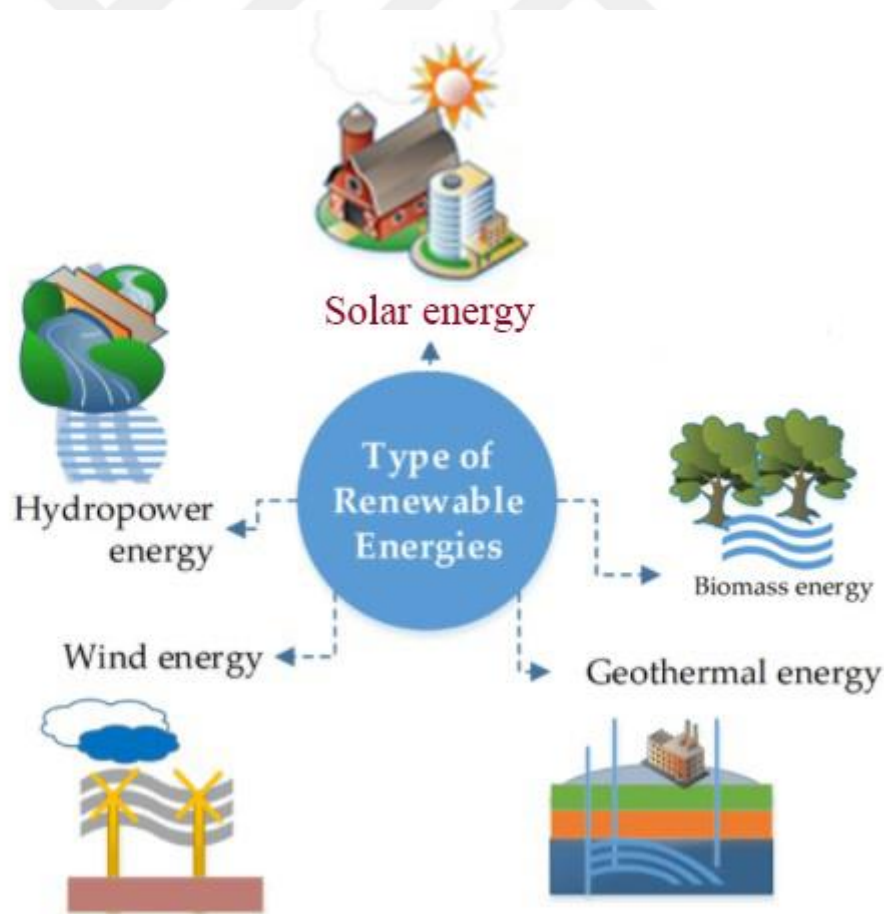


**Figure 1.2.** Renewable energy source types (Shamik, 2015).

### **1.2.1. Wind energy**

The variation of air properties such as temperature, humidity and pressure according to locations causes air currents. Electricity is produced thanks to the motion energy of the air flow or wind. Basically, wind is formed by the rise of warmed air and the descent of the cooled air, and this physical effect causes the displacement of air masses.

If you pay attention, it will be understood that the source of this energy is the sun. In fact, some of the heat effect of the sun is spent on wind formation. Wind energy has a long history. It dates back to 3000 BC.

The amount of wind formed in every region on the earth is not the same. Wind maps showing the wind potentials of the regions are prepared in order to monitor the energy generation potentials and to evaluate whether the wind farm investment is reversible.

Wind power plants, like many similar electricity generation systems, generate electricity by directing the movement created by the wind to the rotating turbines and rotating a rotor connected to the turbines in magnetic flux. Developed countries are very advanced in wind energy, as in other renewable energy types. In our country, wind power investments have been increasing rapidly in recent years.

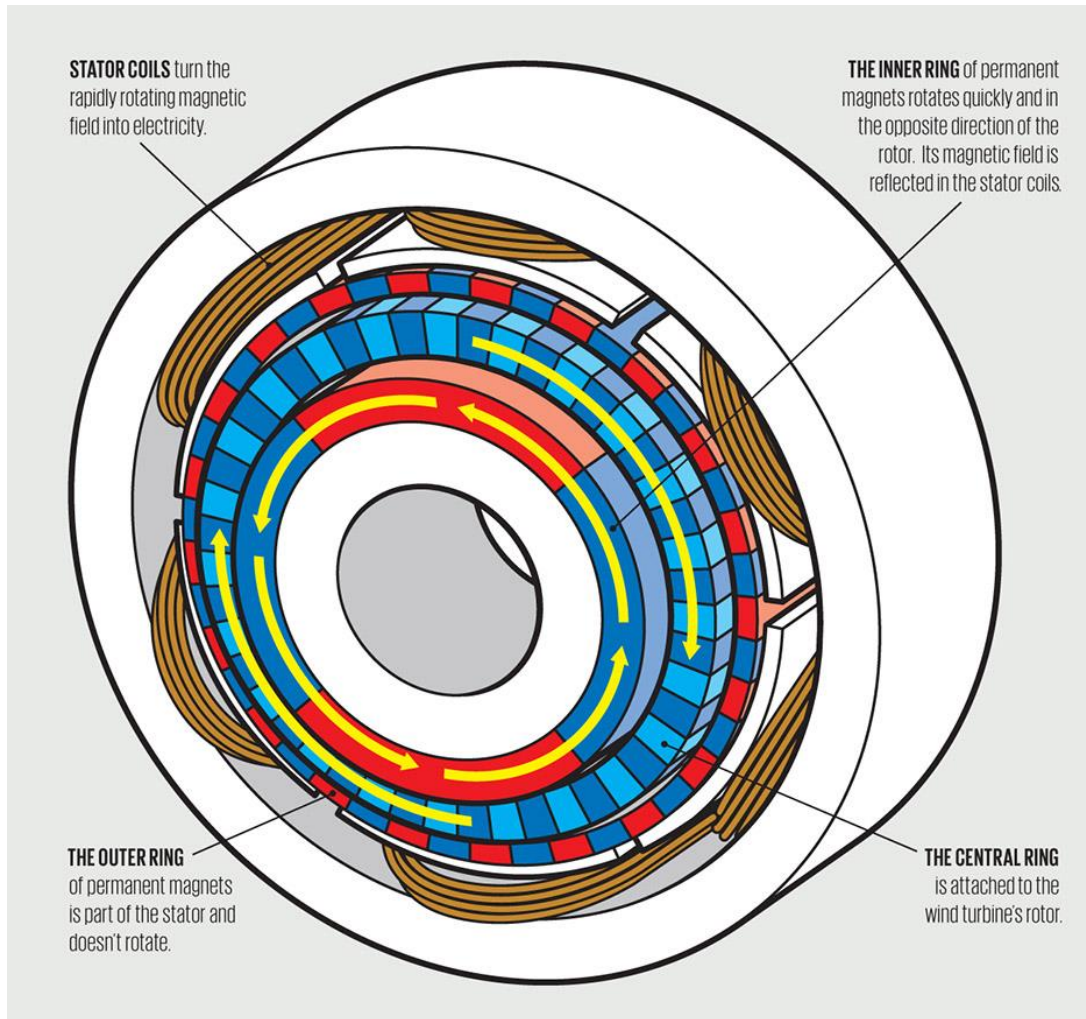


**Figure 1.3.** The interior structure of a wind tribune (IEEE, 2019).

Turkey's annual wind energy potential,  $100\text{-}500 \text{ W} / \text{m}^2$  is around according to recent measurements. Turkey's wind power installed capacity has exceeded 8000 MW.

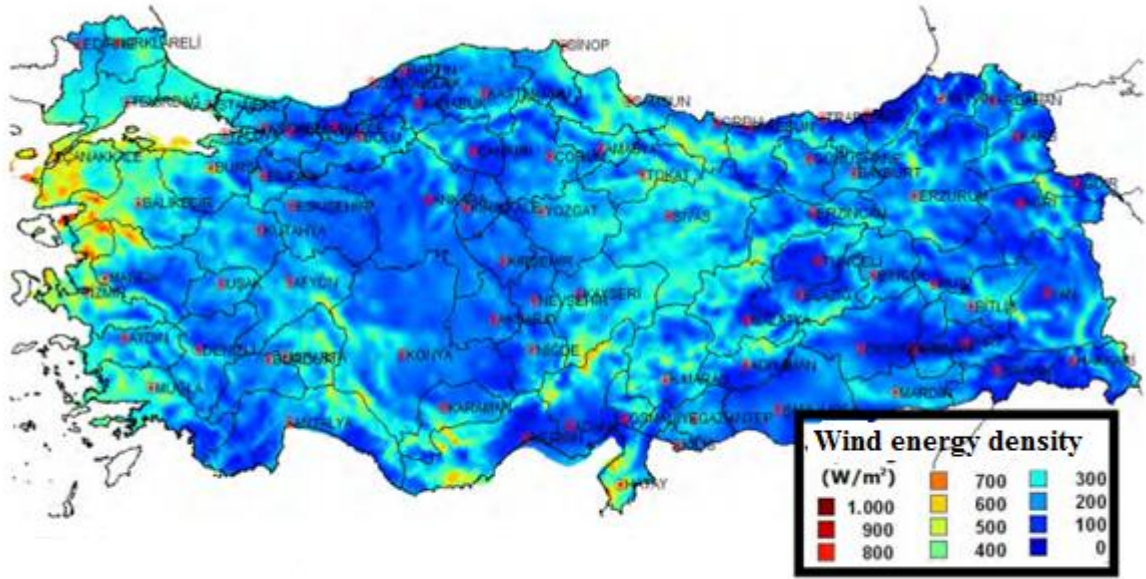


**Figure 1.4.** Wind energy density of Turkey (General Directorate of Meteoroloji, 2018).

Adana Province assessed in terms of wind potential and wind potential maps which is prepared by the Turkish Directorate General of Renewable Energy were examined. For a wind power plant investment to be economical, the average wind speed in the region where the power plant will be installed must be at least 7 m / s. Looking at the Adana Province Center, it is seen that the average wind speed is well below the desired value, as seen in figure 1.4. and 1.5.

Therefore, it was concluded that establishing the wind tribune is not advantageous in terms of regional conditions.

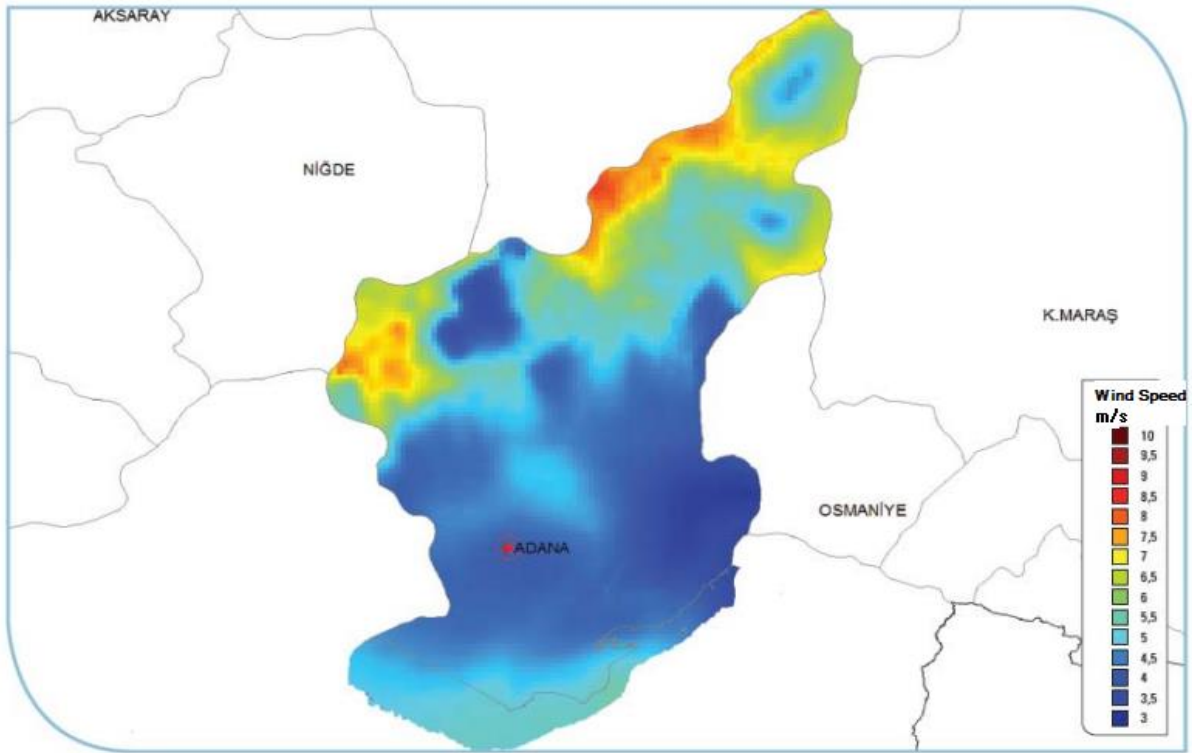


**Figure 1.5.** Adana Province wind speed map (YEGM, 2015).

### 1.2.2. Biomass energy

The heaps consisting of all kinds of wastes of all living organisms, plants and animals, are called biomass. Biomass energy is obtained by converting the heat obtained from the burning of the gases released by these wastes after a certain period of time into electrical energy. Electricity is generated from biomass by combustion and indirect combustion.

Energy production by direct burning of biomass resources is the most advanced and common technology. It is suitable for production in a range of capacity from a few MW to 100 MW and above.

Figure 1.6 shows the cycle of biomass energy in nature.

Biomass energy will not be used in this study due to the fact that existing facilities are not suitable in terms of access to biomass resources.

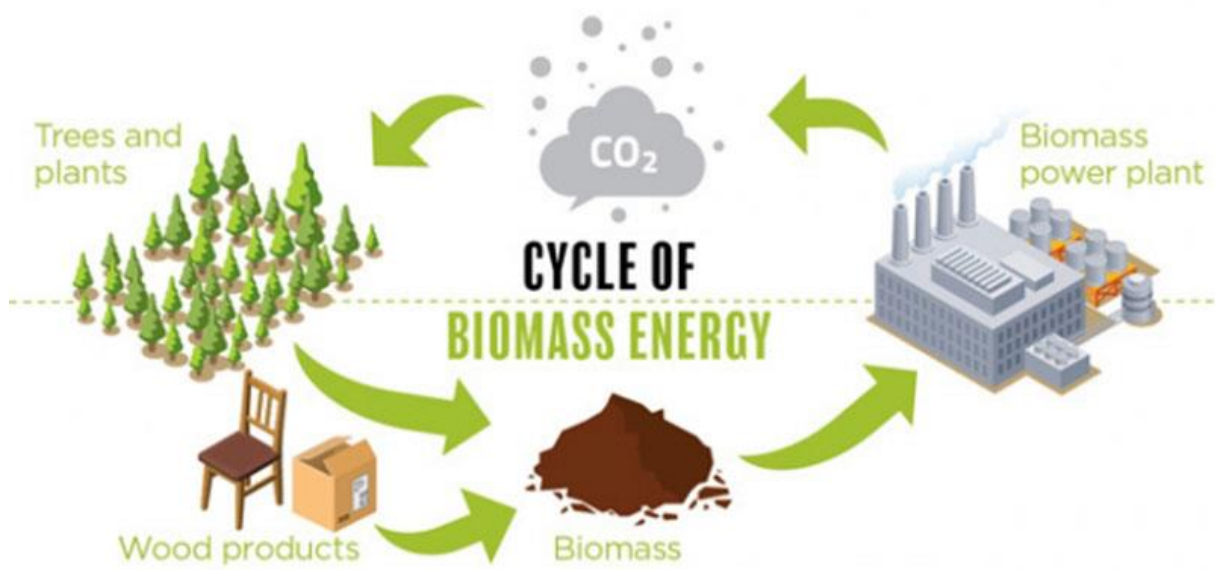


**Figure 1.6.** Cycle of biomass energy (semanticscholar.org, 2019).

### 1.2.3. Geothermal energy

The energy obtained by directing the heat generated in the lower layers of the earth and the steam of water heated by the effect of this heat to suitable turbines is called geothermal energy.

Geothermal energy is generally obtained from the surface waters or specially drilled boreholes using weak zones formed by cracks and fractures reaching the earth surface.

Geothermal energy is the most important among alternative energy sources to fossil fuels. However, the use of geothermal energy was not planned in the study due to the lack of geothermal resources in Adana Province as seen in Figure 1.7.

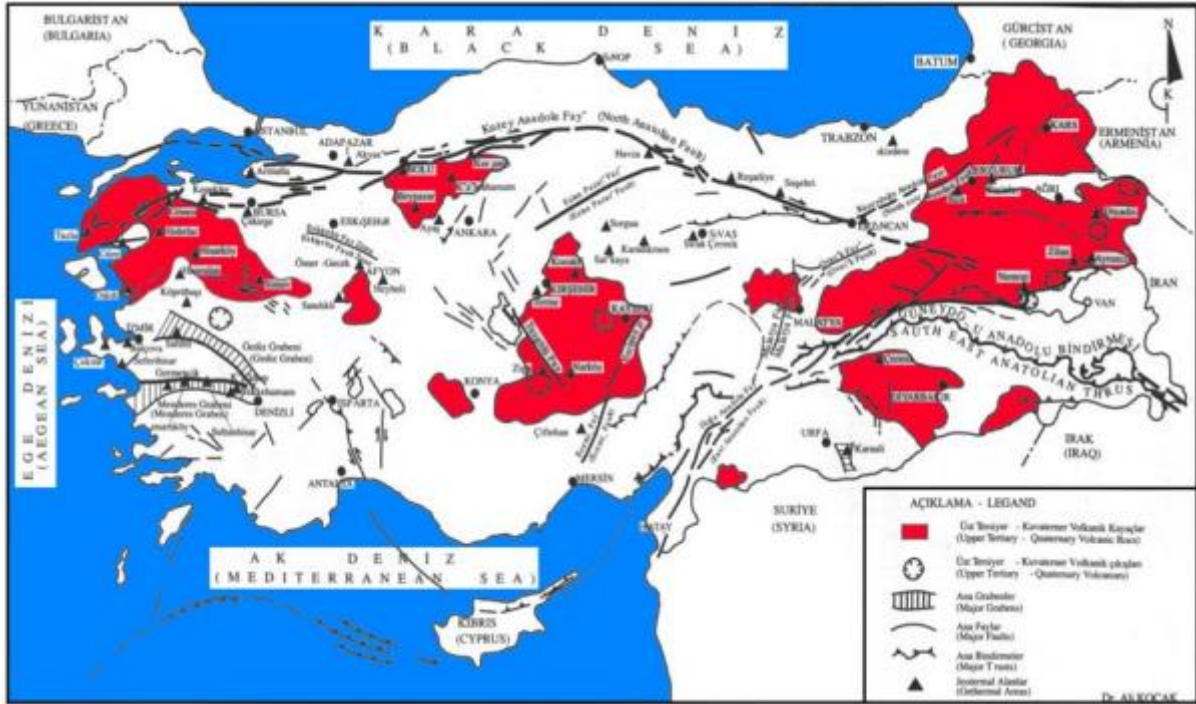


**Figure 1.7.** The geothermal energy potential of Turkey (Chamber of Mechanical Engineers, 2000).

#### 1.2.4. Wave Power

Wave energy is derived from the wave surface or from wave pressures below the surface. Wave energy is produced by winds blowing on the surface of the sea or oceans. In many parts of the world, the wind blows regularly and continuously enough to create continuous waves.

It has been calculated that wave energy is at least 10 times more efficient than other renewable energy sources. (Arslan et al., 2016)

There are several methods of obtaining electrical energy from wave power. The first is that plates placed on water rise abruptly by wave power. Second, the water rising with the wave is accumulated in the reservoir at a higher position. Third, the water is confined in a pipe and the pressure generated by the force of the wave is struck by the turbines.

However, wave energy technologies have not developed much, not only in our country but all over the world. The wave potential of the sea closest to the area where the study will be conducted is below the desired level. Therefore, this type of energy was not used in the study.

### **1.2.5. Hydroelectric energy**

Water accumulated in dams or a reservoir is a renewable energy source with the largest share of installed power in our country.

A hydroelectric power station uses the flow energy of water to generate electricity. Large concrete blocks are pulled over the flowing water (river, stream, stream, etc.) and accumulation is ensured. The accumulated water up to a certain height has significant potential energy. This potential energy is first transformed to kinetic energy (mechanical energy) by means of turbines and then into electrical energy by the rotation of the generator motor connected to the turbine wheel, according to the principle of energy conversion with various mechanisms within the dam as seen in figure 1.8.

Hydroelectric energy is one of the most widely used energy sources in the world. The installed power of hydroelectric energy (water power), which is a renewable resource with a share of more than 25% in the world electricity production, is approximately 900 GW.

According to 2017 data, 628 hydroelectric power plants (HEPPs) and these power plants have an installed capacity of 27.273 MW in our country. This installed power corresponds to approximately 32% of the total installed power.

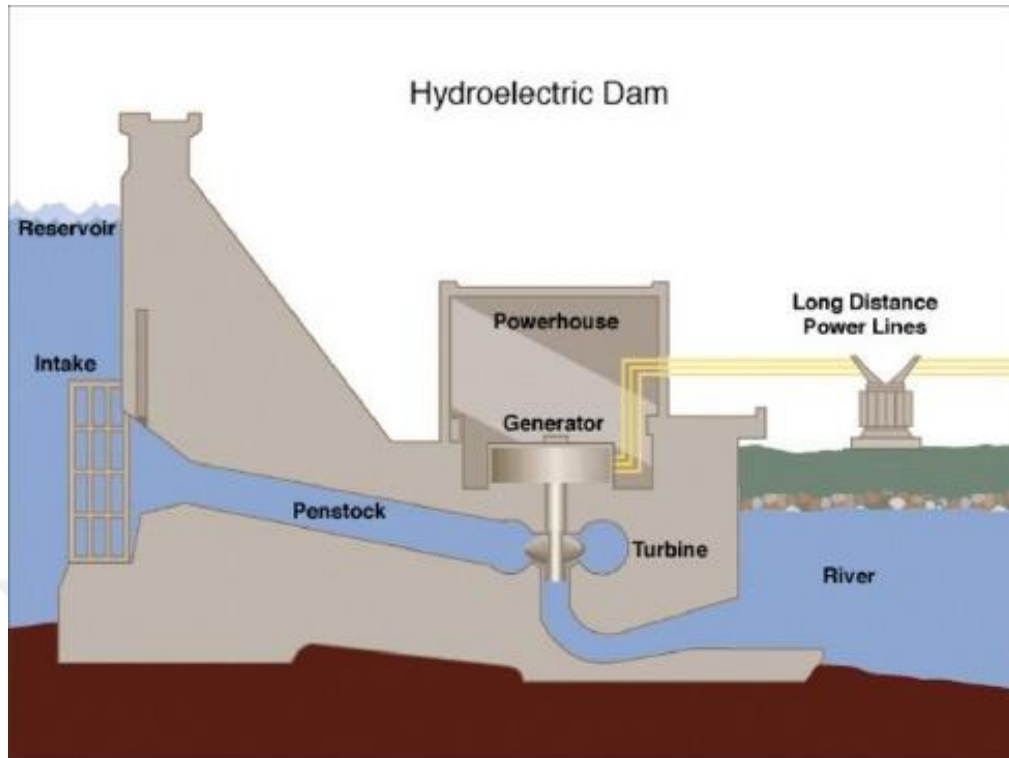


**Figure 1.8.** Structure of a hydroelectric power plant (Ministry of Energy and Natural Resources of Turkish Republic, 2015).

Hydroelectric power plants are a very advantageous type of renewable energy because dams have a life of 30-40 years, the system can be activated when the power demand increases, a fixed energy can be produced, and it is a clean energy because it does not cause carbon emission.

However, this type of energy was not preferred because there are many applications and studies on hydroelectric energy.

### 1.2.6. Solar energy

The use of solar energy by humanity dates back to 6000 BC. It is believed that for the first time in this period, the Chinese considered the fact that the sun's rays reach the building more in architecture. It is also known that the famous thinker Socrates emphasizes the importance of the angle from which the sun's rays come. In the 1760s, Swiss scientist Horace de Saussure invented a rectangular box with glass lids for solar collectors used to heat water. In the early 19th century, Europe and the USA developed models that could be called the basis of today's solar systems as seen in Figure 1.9. During this period, it was discovered that some materials

produce electric current if exposed to light energy. In 1878 a steam engine powered by solar energy was produced by a French mathematician. (Jones and Boumanne, 2012) In the late 19th and early 20th century, approximately fifty articles about solar energy were published in the American Scientific Journal. (Perlin, 2013)

However, the fact that fossil fuels were inexpensive and did not require high technology until the World War II prevented the commercial spread of solar energy.



**Figure 1.9.** Solar panel system in early 1900's (makeuseof.com, 2015).

The first solar houses were designed and started to be used in Germany after the First World War. In the passive solar houses, windows, walls, doors, ceilings are made to collect, store and distribute solar energy in the form of heat in winter and to protect it from solar heat in the summer as shown in figure 1.9. (US Department of Energy, 2001).

In the 1930s, researchers from the Massachusetts Institute of Technology (MIT) developed the pump and storage system in the passive solar building. The same researchers operated an air conditioning device of that period with the electrical energy they obtained from the solar panel in 1938, and by the Boston industrialist, "the art of converting the energy of the sun to the use of man "award.

The foundation of today's modern solar cells was laid when the researcher Russel Ohl, who worked at Bell Labs in the USA, found a silicon solar cell. While working on the behavior of crystals in different environments, Ohl discovered the PN barrier and then the P-N junction. Ohl later produced the diode, which would be a very useful circuit element, making use of the semiconductor property of the super-purity Germanium element. With the development of semiconductor technology, Ohl produced the first silicon solar cell in 1946 and patented it under the name "Light Sensitive Device" (Jones and Bouamane, 2012).

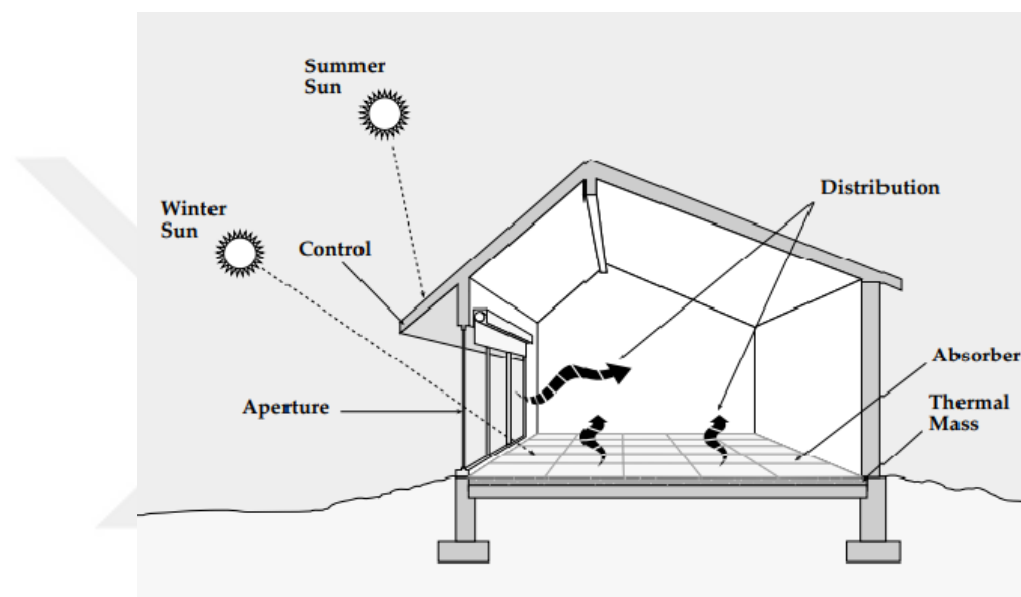


**Figure 1.10.** Basic structure of a passive solar house (US Ministry of Energy web page energy.gov, 2020).

Solar cell technology has progressed, albeit slowly, after this date, but no significant progress has been made as fossil fuels are cheap and easily available. However, the oil crisis in the 1970s concentrated some countries on nuclear energy, it made some countries think more seriously about wind and solar energy.

However, the real rise in solar energy occurred after 2000s with the increasing danger of global warming. As of 2010, with the elevation of energy storage technologies, the improvement of converters, inverters, filters and energy quality elements, the use of photovoltaic panels has become quite widespread, and solar energy has started to have a significant share in energy production in developed countries.

Again, it seems inevitable that smart grid systems have become widespread recently, the need for charging stations for electric cars, the management of different types of renewable energy sources within the same grid system, and widespread smart home applications and PV panels continue to be the area of interest for researchers.

#### **1.2.6.1. Structure of Photovoltaic Panels**

The PV panel is one of the most crucial renewable energy resources. It produces energy by absorbing sunlight with photovoltaic cells, generating direct current (DC) energy. If the PV panel is to be used to supply AC loads, an AC / DC converter is required. However, since the hydrogen production station will be produced by electrolysis, DC energy will be used and therefore no alternative current will be needed.

Photovoltaic structure consists of two-layer silicon structure. There is a thin P type material on the N type base. When the light falls on the junction of these two materials, a tension occurs in which the N-type material is positive relative to the P-type. The output voltage depends on the light intensity falling on the element. When a load is connected to the output, a current will flow. The intensity of this current depends on the light intensity falling on the element and the surface area of the element. By connecting these cells (batteries) in series or parallel, the intensity of the current and voltage to be obtained can be increased.

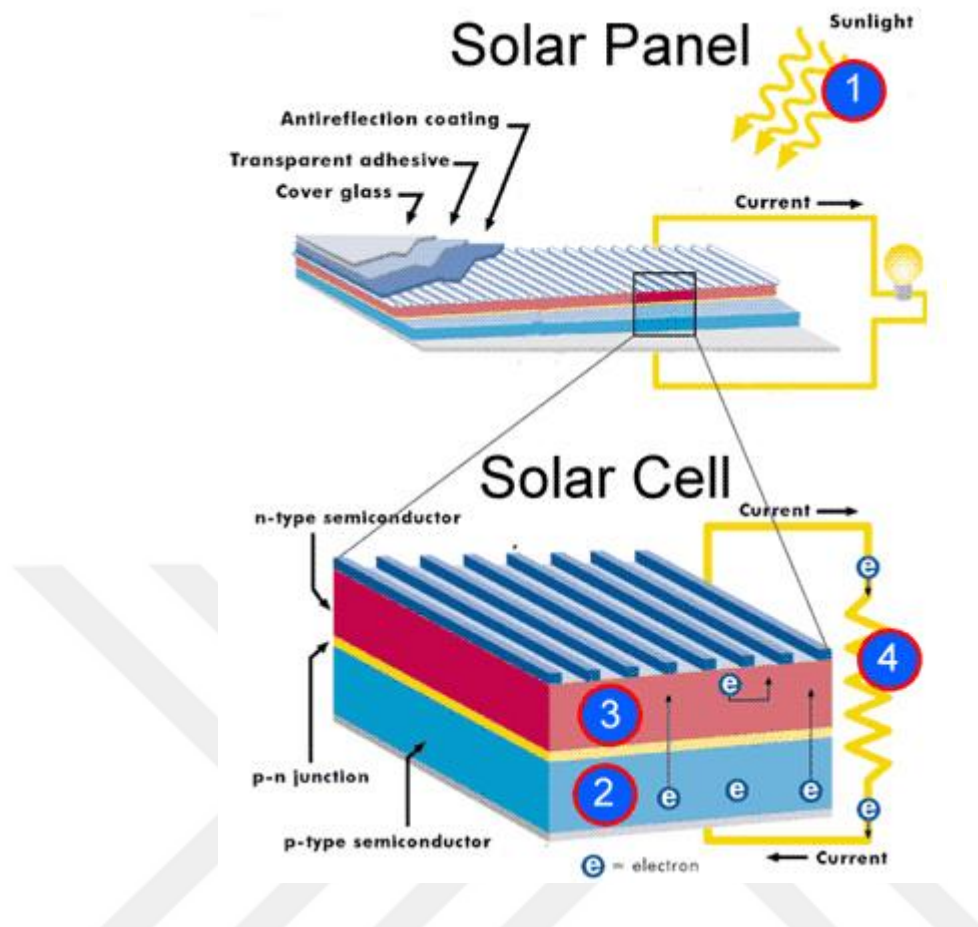


**Figure 1.11.** Typical structure of a solar panel and a solar cell (Bauer et al, 2009).

The top layers of solar panel cells consist of anti-reflection coatings and protections to prevent cracking, breakage and energy loss. Below these layers are N-type and P-type semiconductor materials as shown in Figure 1.11. N and P type materials are formed as a result of the controlled doping of semiconductor materials with the desired materials in the molten state. Multicrystalline polycrystalline silicon is mostly used as semiconductor material in solar cells.

When the figure 1.12. is examined it will be seen that; the output power of PV panels decreases considerably due to temperature. In addition, dust accumulated on the panel reduces the efficiency of the panel. Again, the decrease of clean and usable water resources with the effect of global warming necessitates the protection of these waters with more economical methods.

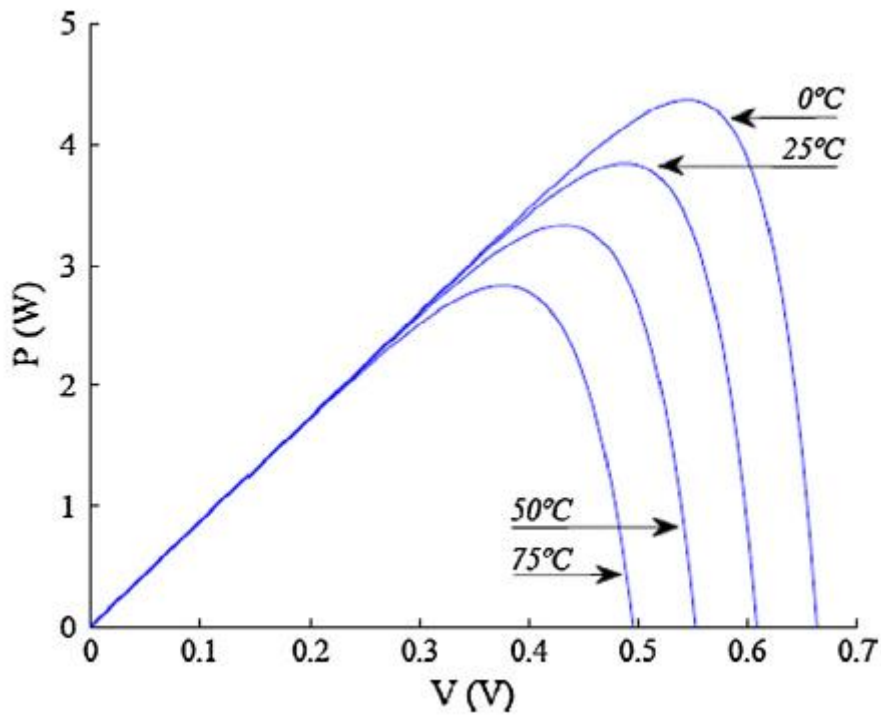


**Figure 1.12.** Variation of PV panel power according to panel temperature (Moharram et al, 2013).

Therefore, the PV panel floating on the water will keep the panel temperature below a certain degree and the dust accumulated on the panel will be washed.

At this point, the evaporating water does not take place in the desired yield, which descends back to the earth with the cycle in nature and enters the groundwater. Solar panels floating on the water will also reduce the evaporation of the water and the amount of water available on the earth will be preserved.

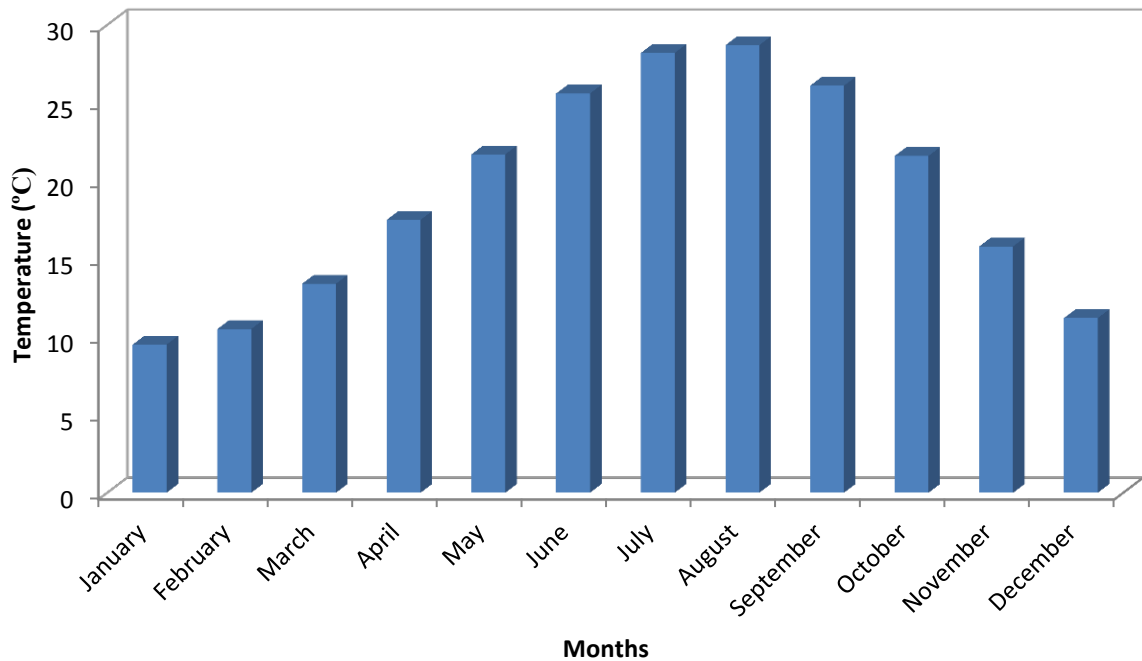


**Figure 1.13.** Average highest temperatures of Adana from 1928 to 2018 (General Directorate of Meteoroloji, 2020).

In order to reduce the temperature of the panel exposed to sunlight to exceed the optimum values, in this study, the panel will be positioned on the water and a floating solar panel will be obtained.

Passive cooling elements will be used to increase the contact surface of the panel with water. Float connection will be made on all four sides so that the panel can stay on the water.

The characteristics of the geography selected for the experimental study were examined. Adana Region, where the study will be implemented, is a region with a high number of sunny days, although the summers are hot, cloudless and without rain, and winters receive precipitation as seen in figure 1.13 and figure 1.14.

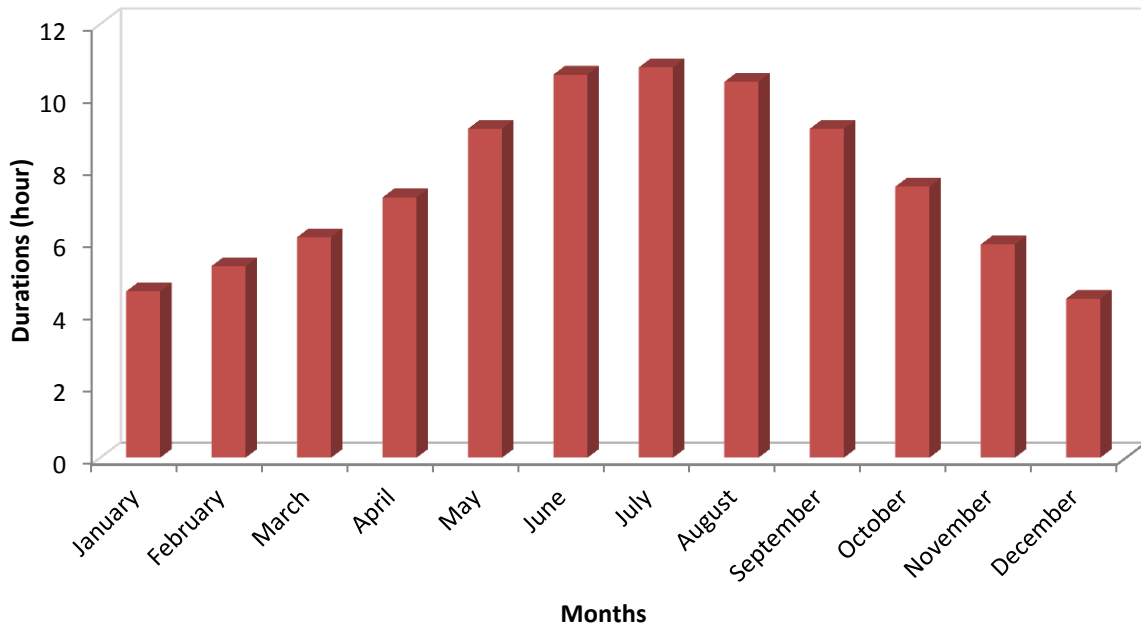


**Figure 1.14.** Average daily sunbathing durations of Adana from 1928 to 2018 (General Directorate of Meteoroloji, 2020).

When the figure 1.14 is examined, sunshine duration of up to average of 11 hours per day are achieved in the city center, especially in the summer months. Even in winter, the region has an average of 4 hours of sunlight per day.

### 1.2.6.2. Mathematic model of photovoltaic panel

The mathematical expression of the relationship between the solar panel's output voltage and current is shown below. (Equation 1)

$$I = I_L - I_D$$

$$I = I_L - I_0 \left[ \exp\left(\frac{V + IR_s}{\alpha}\right) - 1 \right] \quad (1)$$

I: load current (A)

$I_L$ : light current (A)

$I_0$ : saturation current (A)

V: output voltage (V)

$R_s$ : serial resistance ( $\Omega$ )

$\alpha$ : heat voltage factor (V)

Solar cell output I-V relationship; It can be explained by light current, saturation current and series resistance. The mathematical formula for this is shown below. (Equation 2)

$$I_L = \frac{\Phi}{\Phi_{ref}} \cdot [I_{L,ref} + \mu_{I,sc} \cdot (T_c - T_{c,ref})] \quad (2)$$

$\Phi$ : irradiation ( $\text{W}/\text{m}^2$ )

$\Phi_{ref}$ : reference irradiation ( $1000 \text{ W}/\text{m}^2$ )

$I_{L,ref}$ : light current at reference condition

$T_c$ : cell heat ( $^{\circ}\text{C}$ )

$T_{c,ref}$ : reference heat ( $25^{\circ}\text{C}$ )

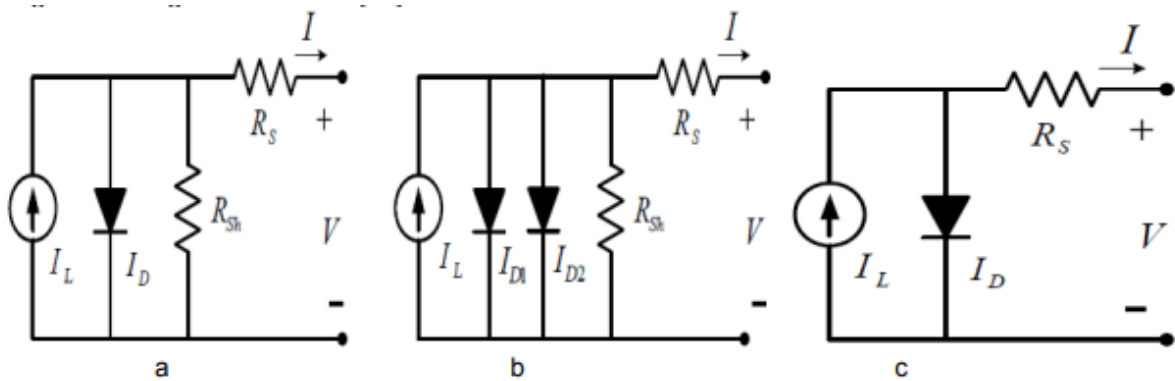


**Figure 1.15.** Equivalent circuit a) one diode b) two diodes c) simplified circuit model (Sinha et al, 2014).

### 1.3. Hydrogen production

Hydrogen was discovered in the 1500s, its flammability was realized in the 1700s, it is the simplest and most abundant element of the universe, it is a colorless, odorless gas 14.4 times lighter than air and completely non-toxic.

In the process that started with the invention of steam in the 19th century and continued with the Industrial Revolution, the need for energy increased continuously with the increase in the need for machine power rather than human power. In order to meet this energy need, many resources have been used, from wood to coal, and later to fossil fuels of hydrocarbon origin. Thus, living standards reached higher levels and reached today.

It can be said that hydrogen has been mentioned in the literature in 1974 at the "Hydrogen Economy Miami Conference" organized by the University of Miami Clean Energy Institute in

Florida, USA. With this meeting, the International Hydrogen Energy Association (IHEA) was established.

The use of hydrogen as a fuel in aircraft was first tried in 1956 in the USA. After this year, various engine technologies have been tried to use hydrogen as fuel.

Hydrogen is not a natural fuel, but a synthetic fuel that can be produced from different raw materials such as water, fossil fuels and biomass, using primary energy sources. There are many alternative hydrogen production technologies such as steam recovery, waste gas purification, electrolysis, photo processes, thermochemical processes, and radiolysis. The produced hydrogen can be transported over great distances by pipelines or tankers.

The fuel of the heat that the sun and other stars give to the thermonuclear reaction is hydrogen and it is the main energy source of the universe. H gas is typically stored as liquefied at about  $-253\text{ }^{\circ}\text{C}$  ( $-423\text{ }^{\circ}\text{F}$  or  $20\text{ K}$ ). The volume of liquid hydrogen is only 1/700 of its gaseous volume. Hydrogen has the highest energy content per unit mass of all known fuels.

Hydrogen is not found free in nature, it exists in compounds. The most well-known compound is water. In energy systems where hydrogen, which is clean and easy to use in all areas requiring heat and explosion energy, is used as fuel, the product thrown into the atmosphere is only water and / or water vapor. It is an average 1.33 times more efficient fuel than hydrogen petroleum fuels. During the production of energy from hydrogen, there is no production of any gas and harmful chemicals other than water vapor that can pollute the environment and increase the greenhouse effect. Hydrogen gas can be obtained by different methods, as well as with water, solar energy or its derivatives, wind, wave and biomass.

Research shows that hydrogen is about three times more costly than other gases under current conditions and its use as a ordinary energy source will turn on cost-saving technological developments in the production of hydrogen. However, storing excess electrical energy as hydrogen in regular or seasonal intervals can be considered as a viable option today. The widespread use of energy stored in this manner depends, for example, on the development of fuel cell-based automotive technologies for public transport purposes. Hydrogen energy has no effect that could threaten human and environmental health. Hydrogen, which is obtained from

fossil resources such as coal and natural gas as well as water and biomass, is considered to be an energy carrier rather than an energy source.

Although solar energy is converted into heating and photovoltaic electrical energy, this energy must be stored in order to be used effectively because it is intermittent. For photovoltaic or thermal storage of solar energy, thermal energy storage, battery energy storage, storage as hydrogen energy, pumped hydro-based energy storage, compressed air-based energy storage systems are used. Hydrogen energy, which can be used as fuel in heating, transportation, and electricity generation, is an ideal energy carrier for humanity.

### **1.3.1. Electrolysis**

Electrolysis is a process in which a chemical reaction that does not occur spontaneously is carried out with electrical energy. The process is done in electrolytic cells. It is the release of metal ions on the cathode and non-metallic ions on the anode as a result of the chemical decomposition that occurs when the electric current is passed through aqueous or molten electrolytes as shown in Figure 1.16.

The energy required for the electrolysis process should be a direct current source. In the electrolysis experiment of water, a little salt or acid is added to make the water a good conductor. Tubes are filled with this water to the brim and put into the water in the container by inverting. Two electrodes are placed inside the tubes and connected to the ends of a battery as shown in the figure. When the load starts to pass through the circuit, gases begin to accumulate in the inverted tubes (Chi J. and Yu H., 2018).

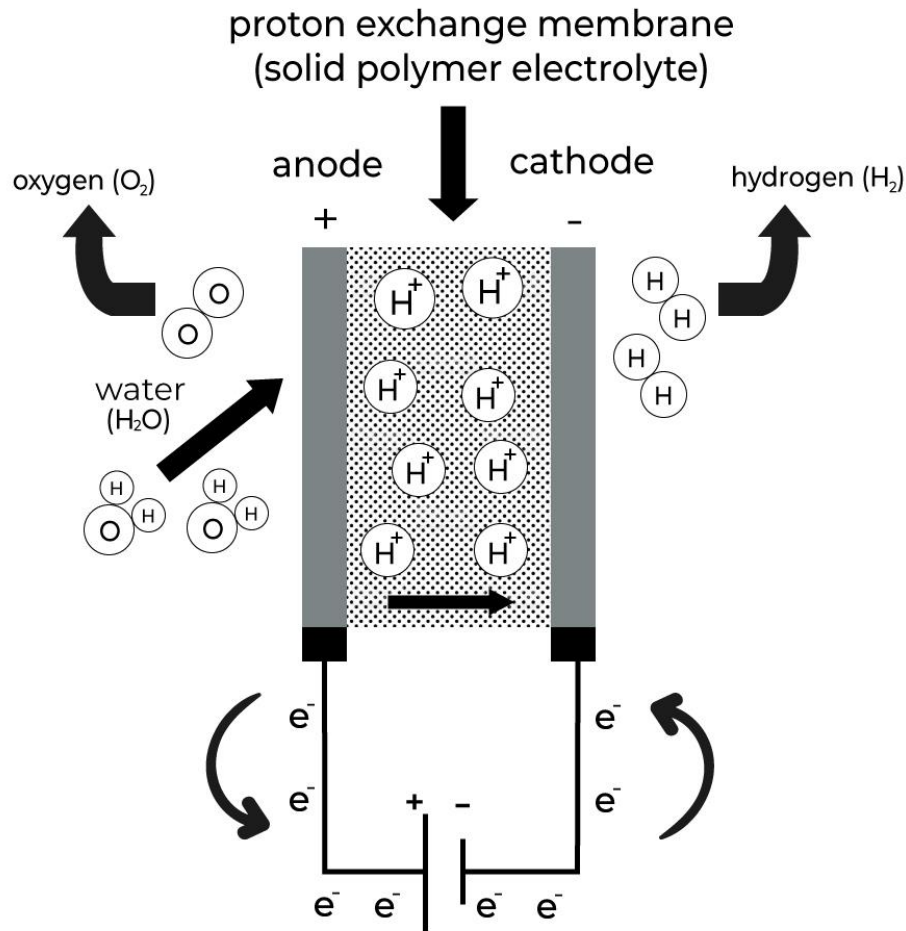


**Figure 1.16.** Hydrogen production by water electrolysis (Acar and Dincer 2019).

The volume of gas collected becomes  $V$  with the anode and  $2V$  at the cathode. Accordingly, (+) oxygen was accumulated at the anode and hydrogen at the (-) cathode. The 1 C load that passes through the circuit causes an accumulation of approximately 0.06 cm<sup>3</sup> of oxygen and 0.12 cm<sup>3</sup> of hydrogen. If the tube in which the oxygen gas is accumulated is deactivated, the system is called the hydrogen container. It can be found the amount of gas collected in the tubes and the current strength in the circuit.

Dincer and Zamfirescu (2016) explained in detail the electrolysis methods, which are the most basic method of hydrogen production.

Basically, three different electrolytes can be mentioned. And five different electrolysis methods can be applied with these electrolytes as seen in Figure 1.17.

- Alkaline electrolytes
- Acidic electrolytes (Sulfuric acid electrolysis and Proton Exchange Membrane Electrolysis are divided into PEM)
- Solid oxide electrolytes (SOEC)

Solid Oxide Electrolysis of these is still in the research phase. It is not practiced commercially. The most commonly used method in practice is alkaline electrolysis and Proton Exchange Membrane (PEM) electrolysis.

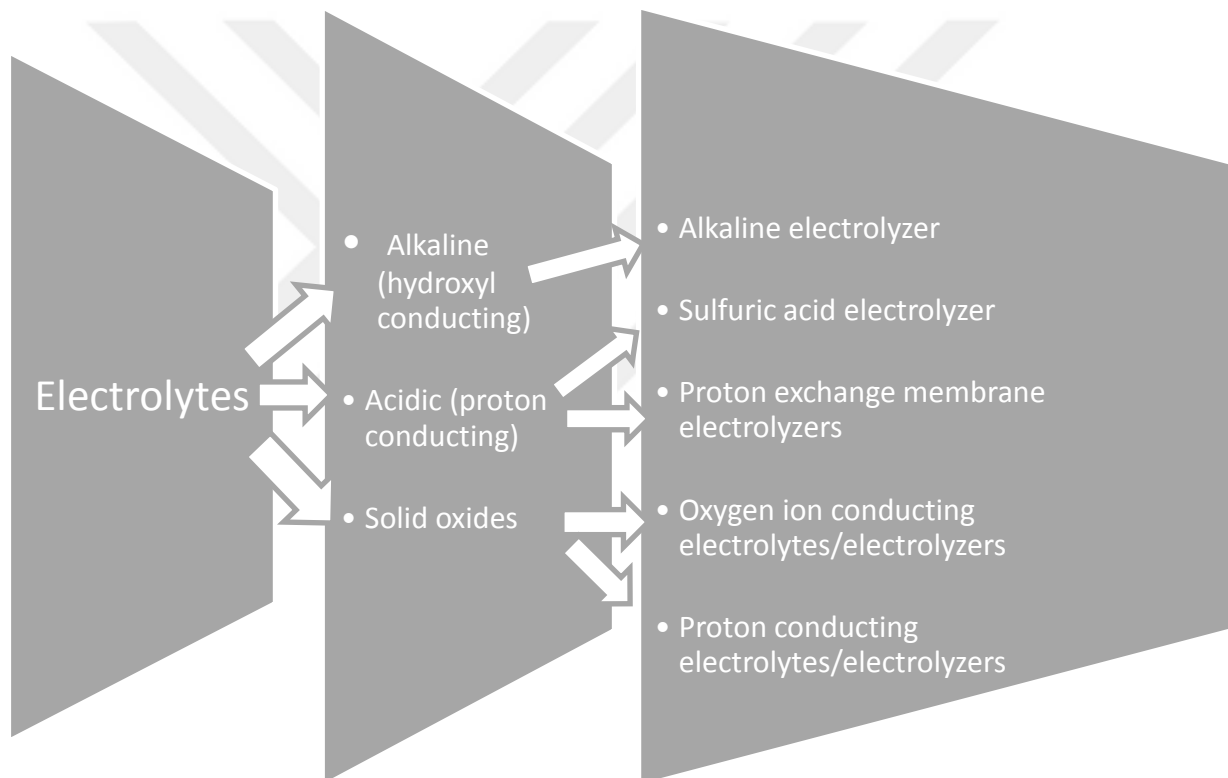


**Figure 1.17.** Classification of electrolysis methods (Dincer and Zamfirescu, 2016).

**Table 1.1** Current state of development of electrolysis methods (Dincer and Zamfirescu, 2016).

Technology		Development status	T(°C)	P(bar)	SEC(kWh/kgH <sub>2</sub> )
Alkaline	Large Scale	Commercial	70-90	1-25	48-60
	High Pressure	Commercial	70-90	Up to 690	56-60
	Advanced	Pre-commercial	80-140	Up to 120	42-48
PEM		Commercial	80-150	Up to 400	40-60
SOEC		Prototype	900-1000	Up to 30	28-39

### 1.3.2. Electrocatalysis

Electrocatalysis can be defined as the heterogeneous catalysis of electrochemical reactions that are created by taking advantage of the electrode's ability to receive and donate electrons in the electrolysis process.

The rate of an electrode reaction is determined by the rate of charge transfer event. The rate of charge transfer depends on the type and concentration of the material reacting with the electrode and the type of the electrode material with the voltage applied to the electrode.

In cases where the charge transfer step is slow, changes can be made in the structure of the electrode or some substances can be added to the solution instead of applying excessive voltages to the electrode to accelerate the electrode reaction.

With this application called electrocatalysis, it is possible to shift the electrode reaction towards thermodynamic voltages and carry out higher current densities. The production of H<sub>2</sub>, O<sub>2</sub> and Cl<sub>2</sub> gases by electrolysis, the electrodegradation of the O<sub>2</sub> molecule and the electrooxidation of methanol, which are of great importance in practice, require excessive voltage and it is important to accelerate these events by electrocatalytic ways (Yildiz, 2000).

### **1.3.3. Hydrogen economy**

The hydrogen economy is a vision of future energy in transportation, industry and homes, where the energy consumed is stored as hydrogen, not when it is produced, but when it is needed as seen in Figure 1.18.

Studies in the field of energy point to hydrogen as the fuel of the future, as the carbon emissions in the world, have reached or even passed on dangerous levels. The economic model that this new energy concept will create is called the hydrogen economy. This concept was first used in the 1950s as an integral element in large-scale nuclear power generation.

In 1974, during the first conference on hydrogen economy, the hydrogen economy Miami Energy Conference (THEME), a consensus was reached on the idea that the hydrogen energy system was timely and the meeting came to the question of whether a formal organization on hydrogen energy is required. As a result of the discussions, towards the end of the same year, the "International Hydrogen Energy Agency" was established and started to work. (Goltsov et al, 2001), (Veziroglu and Nejat, 2000)

Hydrogen can be used to facilitate the entry of renewable energy sources. Because it can be used both as an energy carrier and as a storage medium to balance the spacing nature of many renewable resources. By using renewable resources and hydrogen, services can be provided to both the electricity sector and the transportation sector.

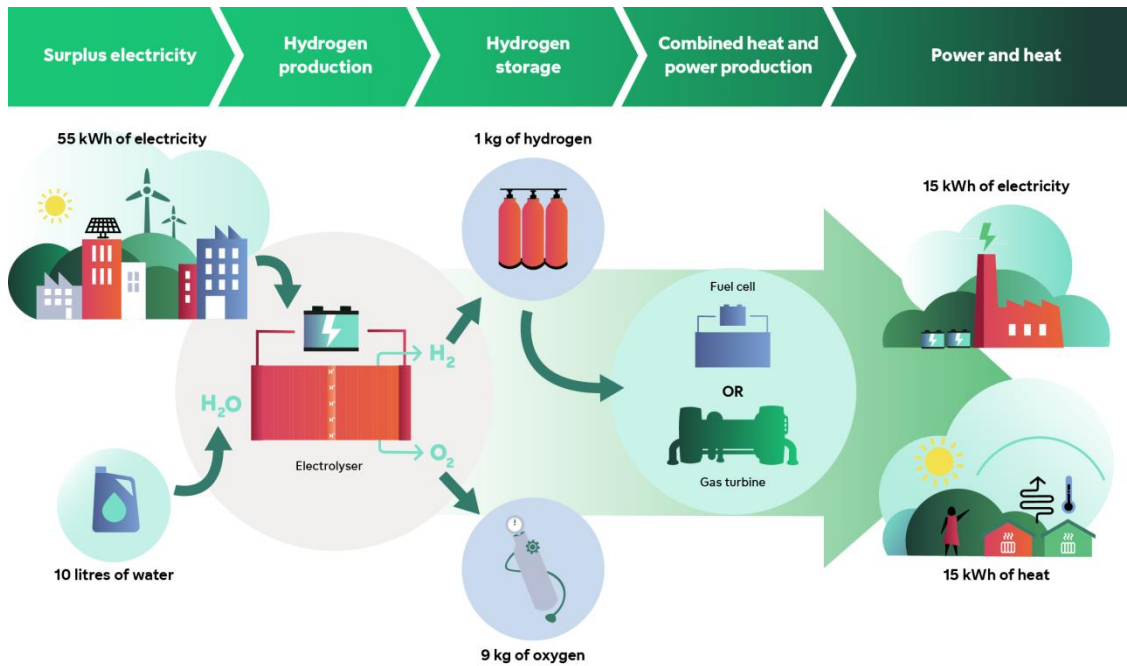


**Figure 1.18.** An example of an energy system in hydrogen economy (Goltsov et al, 2001).

### 1.3.4. Storage and novel applications of hydrogen

Perhaps the most important feature of hydrogen is that it is storable. As it is known, a suitable method has not been found to store large amounts of energy today. If it were possible to store energy from hydroelectric power plants today, it would be possible to solve the energy problem to some extent. The hydrogen storage methods are schematized in Figure 1.18.

However, the best known storage method for electrical energy is still nothing more than acidic batteries. Hydrogen can be stored as gas or liquid in pure form, as well as physically stored in carbon nanotubes or chemically in the form of hydride.

Hydrogen can be stored as gas or liquid in suitable steel tanks. However, tank weights cause problems in gas storage due to high pressure. Perhaps the cheapest method of storing hydrogen gas is to store it underground in depleted oil or gas reservoirs, similar to natural gas. A somewhat costly form of storage is to store in caves in mines. (Ozdemir and Mutlubas,2019)

Hydrogen takes up space 4 times more amount than oil; it is necessary to store hydrogen in liquid form in order to reduce the capacity seized by hydrogen. For this, high pressure and

cooling process is required. Liquefied hydrogen may be reserved under high pressure in cutting tubes. This method is the most used method for medium or small scale storage. However, it is a very expensive method for large quantities. Because approximately of the energy of hydrogen should be spent for the liquefaction process.

Another practical solution is to store liquid hydrogen in low temperature tanks. Liquid hydrogen, which is constantly used as rocket fuel in space programs, is stored by this method. The largest liquid hydrogen tank in the world is at the Kennedy Space Center and can receive 3400 m<sup>3</sup> of liquid hydrogen. This amount corresponds to the value of hydrogen as a fuel of 29 million Mega Joules or 8 million kWh.

As a result of recent studies, hydrogen can also be reserved in carbon nanotubes. Carbon nanotubes are concisely converted into tubes of graphite sheets. Their diameters are in the order of a few nanometers or 10-20 nanometers, and their length is in the order of microns.

Hydrogen can be chemically stored as hydride in metals, alloys and intermediate metals. Although metal hydrides are a very suitable method for storing hydrogen, their own weights pose a serious problem. Complex hydrides containing aluminum and boron have been studied extensively, especially for the last 10 years due to their high storage capacity. Complex hydrides containing boron are also important due to their use in liquid conditions. Boron-based systems are mainly based on sodium boron hydride. NaBH<sub>4</sub> contains 10.5% hydrogen by weight in solid form. (Shi et al, 2020)

In solution, sodium boron hydride gives hydrogen and converts to sodium metaborate according to the following reaction Equation (3).



With the addition of H<sub>2</sub>O and NaOH the amount of sodium boron hydride in the liquid can be between 20-35% by weight, which allows the storage of 4.4-7.7% by weight of hydrogen in the system. (Aghababaei et al, 2020)

The most important advantage of storing hydrogen in sodium boron hydride is that the stored hydrogen can be recovered at room temperature and the recovery can be easily controlled with the help of a catalyst. The most important bottleneck in the use of sodium boron hydride for hydrogen purposes is the conversion of the formed metaborate to  $\text{NaBH}_4$ .

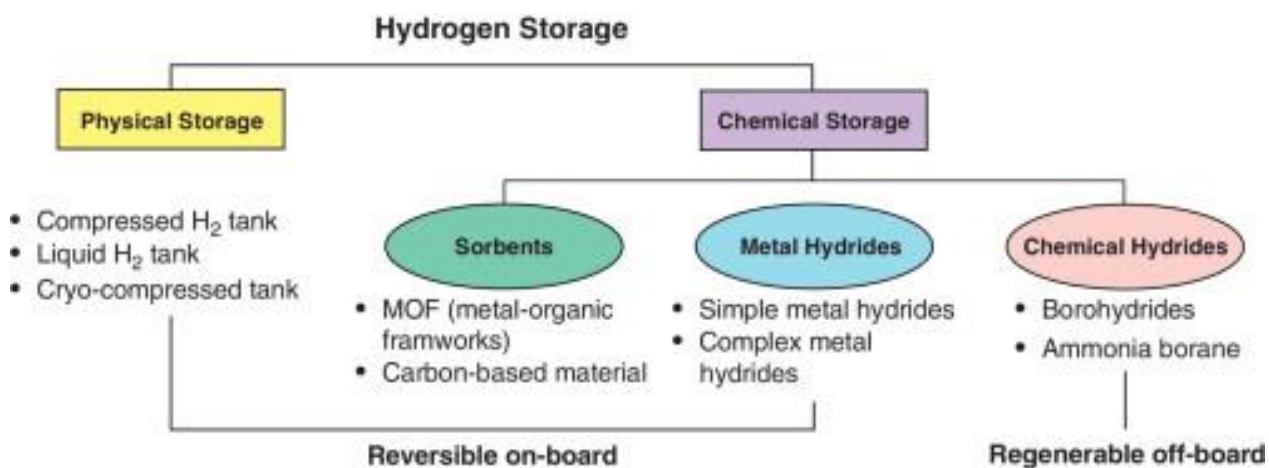


**Figure 1.19.** Hydrogen storage methods (Hwang and Varma, 2014).

Today, energy can be obtained from hydrogen through two methods, namely combustion and fuel cell. These two technologies determine the uses of hydrogen energy. Combustion Technologies; can be burned like hydrogen, gasoline and natural gas. The advantage of petroleum derivatives compared to fuels is that their emissions are less. Hydrogen turbines for military and industrial purposes and internal combustion engines for vehicles are being developed. A gasoline-powered car takes on average 65 liters (47 kg) of gasoline, which corresponds to 17 kg of hydrogen as energy fuel cell technologies; fuel cells are materials that work as the opposite of electrolysis. Electric current is obtained by combining hydrogen and oxygen in the air (forming anode and cathode). It is more efficient than burning and it is the more preferred method.

Fuel cells, which started to be used in space studies by NASA in the late 1950s, have been successfully used in industry and service sectors, especially in the transportation sector. Fuel cells can be used for portable applications such as laptop computers and mobile phones as well as suitable power supplies for power plants. Due to their high efficiency and low emissions, they have found wide use in the transportation sector.

## 2. LITERATURE REVIEW

The primary parameter affecting the efficiency of a photovoltaic panel is the temperature after the solar radiation level. Numerous studies have examined the effect of temperature on the efficiency of solar panels.

In the one of these studies, Ghazi and Ip (2014) investigated that the influence of weather situations on the yield of PV panels in the southeast of UK. With this study It is concluded that even when the dust accumulated on the panel is minimum, it decreases the panel efficiency by 5%.

Another study of Elminshawy et al (2019) investigated the effect of temperature on panel yield. Accordingly, only 20% of the solar radiation is transformed into electrical energy, and the rest of energy turns into temperature. Therefore, increasing temperature means a decrease in efficiency. As a result of the study, each temperature increasing in degrees causes a loss between 0.25% and 0.5% in panel efficiency.

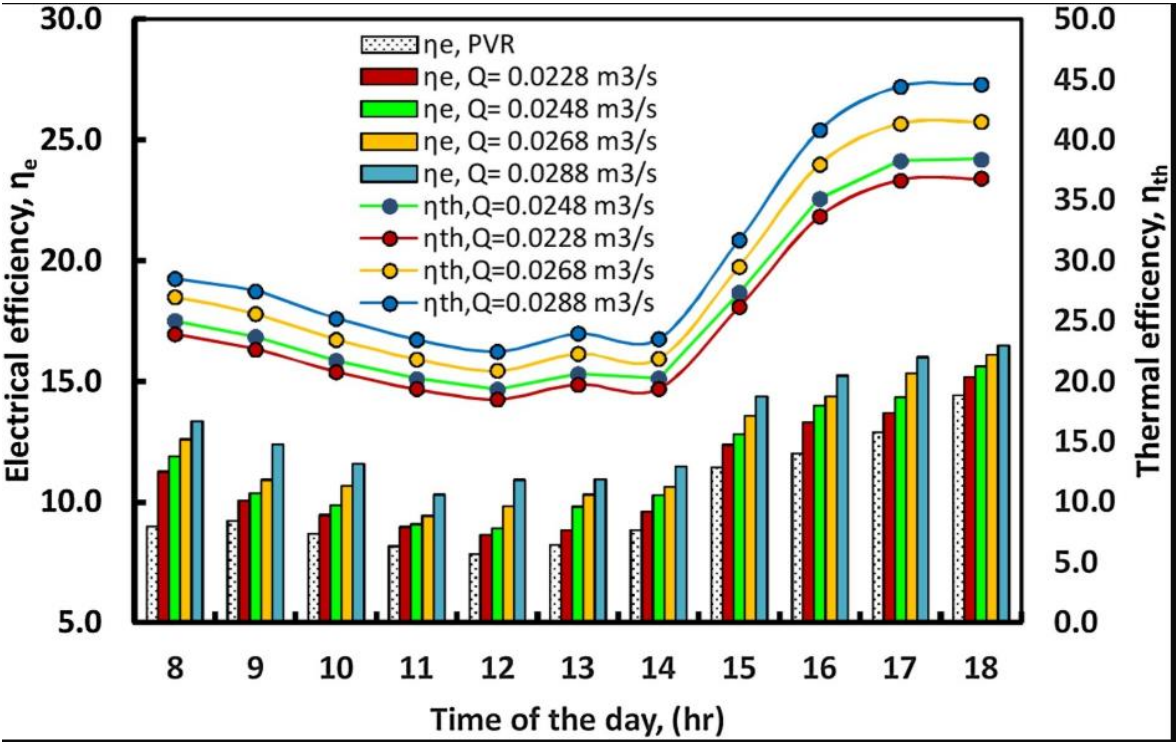


Figure 2.1. PV cells electrical and thermal yielding in 35 °C. (Elminshawy et al., 2019).

As can be seen, most of the radiation turns into heat energy, so it is important to control the panel temperature.

Ngoh and Njomo (2012) have pointed out that hydrogen production from solar energy in the market can reach more energy prices with more advanced methods. According to the study, the electrolysis process powered by solar power seems to be more advantageous because less processes are needed and no external power source is required when compared to electro-thermic, chemical and thermochemical technologies.

Hossains M. et al (2019) have focused on the parametric effect of hydrogen generation by solar powered water electrolysis using the variance analysis method. In the study, a realistic experiment was carried out using the Response Surface Methodology by creating three-dimensional surfaces and shapes. As a result of the experiment, 20 Nm<sup>3</sup> of hydrogen was obtained in 24 hours with 500 W of solar energy.

Touili et al (2018) created a simulation using The Global Horizontal Irradiation (GHI), data from local meteorological stations and CAMS-Rad satellite data to conduct a techno-economic analysis of Morocco's hydrogen production potential from solar energy.

**Table 2.1.** Hydrogen generating expense in some places and with some renewable energy resources (Touili et al, 2018).

<b>Table 4 – Hydrogen production cost in different locations and with different sources of electricity.</b>		
Location	Source of energy	Hydrogen cost (\$/Kg)
In Salah, Algeria	Geothermal	8.24
Garoua, Cameroun	High temperature electrolysis (PV)	5.23
Kirkklareli, Turkey	Wind energy	16.4638–21.9642 (12 m hub height)
		12.1019–16.2488 (36 m hub height)
Northeast of Algeria		4.679
Southwest of Algeria	Geothermal	8.706
Cordoba, Argentina	Wind energy	3.10–7.21 (depending on the price of electricity)
Ouargla, Algeria	PV	7
	Geothermal	5-15 (depending on the plant size)
	Solar chimney	12–25
Algeria:		(For a 7% market penetration)
Algier		5.78
Oran		5.69
Setif		5.57
Ouargla		5.31
Tamanrasset	PV	4.61
	Geothermal	
Algier		4.51
Oran		3.37
Setif		3.94
Ouargla		4.53
Tamanrasset		6.98

In Ahmed and Dincer’s study (2018), hydrogen production by photoelectrochemical method was examined in terms of efficiency. The contribution of developments in semiconductor technology to the efficiency of solar energy and hydrogen production has been studied with rational engineering principles. The commercial future of photoelectrochemical reactors, which can also be applied, is discussed. In the study, single, double and cascade connections are simulated in hydrogen production by photoelectrochemical method as seen in Figure 2.2.

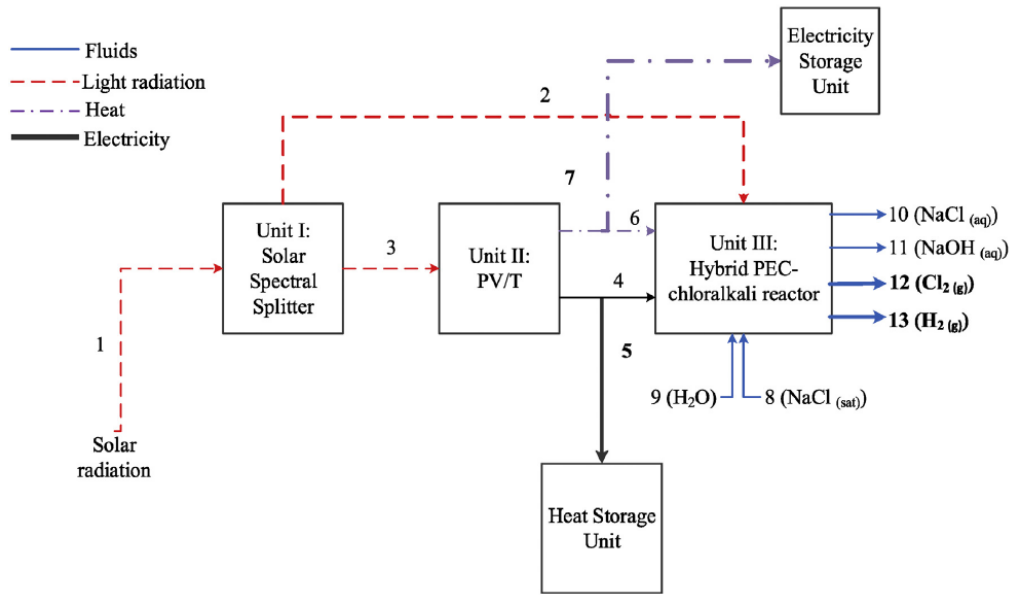


**Figure 2.2.** Block diagram of integrated system (Ahmet and Dincer, 2018).

In Senthilraja et al's study (2019), the efficiency of photovoltaic thermal collectors used in hydrogen production has been discussed. For this, a solar assisted water separation system has been created as seen in Figure 2.3. This design consists of the array of photovoltaic (PV) cells with 0.303 m<sup>2</sup> surface area, a spiral flow thermal collector with 12.7 mm outer diameter, 10.26 mm internal diameter, 10 m length copper tube and Hoffman voltmeter. As a result, it has been observed that as the water flow increases, the collector outlet temperature and output voltage and output power increase, and the PV module temperature decreases with the increase in flow rate.



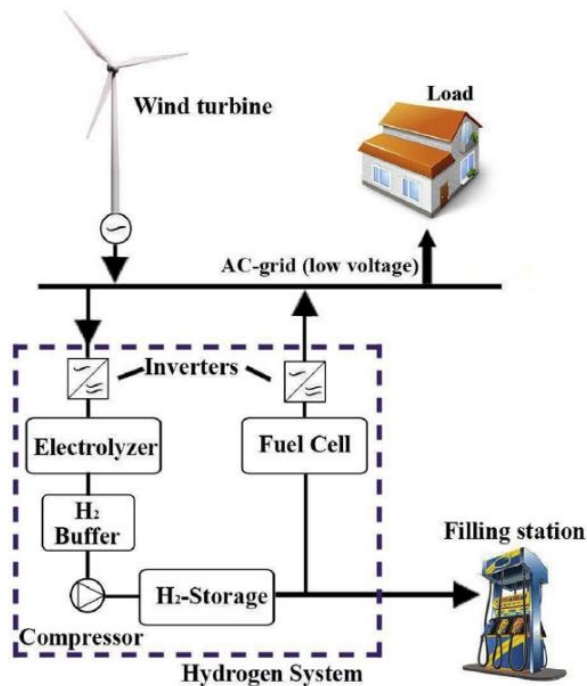


**Figure 2.4.** Schematic of hydrogen production through wind energy (Nematollahi et al, 2019).

sh

Al-Sharafi et al. (2017) evaluated hydrogen production potential based on wind and solar energy data from various regions of Saudi Arabia, Canada and Australia. For this, simulation consisting of PV - battery bank, wind - battery bank, PV - wind - battery bank, PV - FC (Fuel Cell), wind - FC and PV - wind - FC variations are designed. As a result, it was seen that the best configuration was the integration of 2 kW PV array, 3 wind turbines, 2 kW converter and battery storage banks.

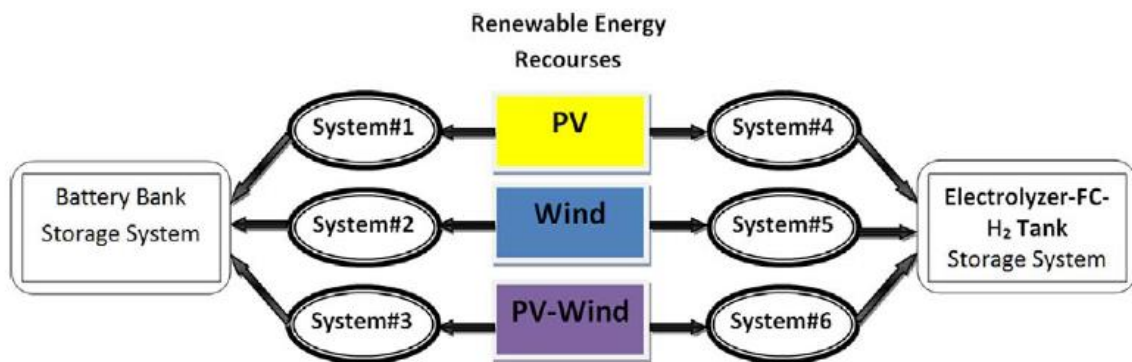


**Figure 2.5.** Different renewable energy systems that are considered for the simulations. (Al-Sharafi et al, 2017).

Kovak et al. (2019) aimed to achieve the most efficient hydrogen production possible with the bipolar alkaline electrolysis method, in addition to parameters such as the best sun angle, the highest radiation time with the 960 Wp solar module. In the study, where 1.138 g of hydrogen was obtained in one hour, a total of 1.234 MWh of energy was produced, meeting the energy needs of 122 houses and the environment, which corresponds to 23 trees in terms of meeting their carbon emissions.

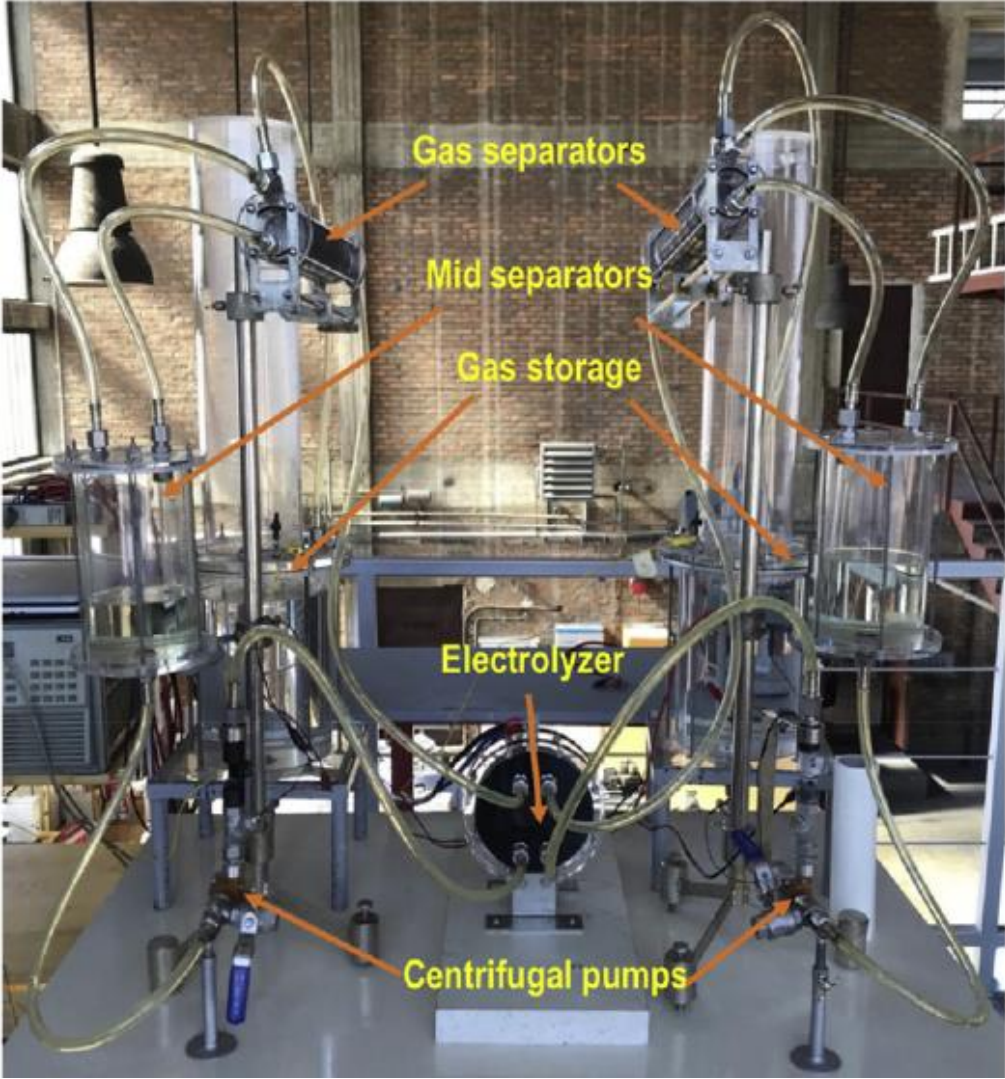


**Figure 2.6.** Hydrogen production system (Kovak et al, 2019).

In Gondal et al. study (2017), the energy crisis of Pakistan, one of the developing economies, has been discussed. In this context, the focus is on hydrogen production from renewable energy sources such as biomass, solar, wind, solid waste and geothermal. As a result, it has been seen that the most feasible renewable energy is biomass for Pakistan, and then solar and solid waste alternatives respectively are efficient options.

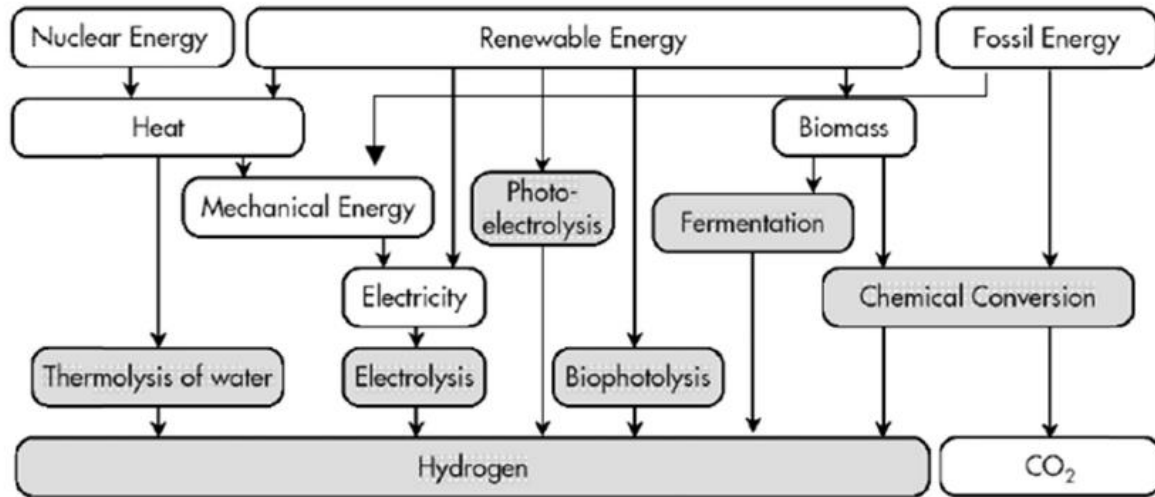


**Figure 2.7.** Some pathways for hydrogen production (Gondal et al, 2017).

In Alrabie et al's work (2018), on the energy problem of another developing country Jordan, a mathematical model was developed using a combination of solar cell - proton electron membrane (PEM) electrolysis. In the study, it was concluded that hydrogen production with solar energy PEM electrolysis would contribute significantly to the solution of Jordan's energy problem.

Allanne and Cao (2017) discussed the hydrogen economy and zero energy point concepts with rapidly developing hydrogen fuel vehicles. In the study, a topology for the use of hydrogen in transportation and smart grids has been developed. The current and overnight state of hydrogen economy has been redefined by referring to the Gartner hype curve and qualitative content analysis method.

Acar and Dincer (2019) dealt with different hydrogen production sources such as wind, geothermal, biomass, solar in a comparative way in economic, environmental, social and

technical aspects. As hydrogen production methods, biological, thermal, photonic, and electrical are the selected and hydrogen storage methods are chemical hydrides, compressed gas, cryogenic liquid, metal hydrides, and nanomaterials are the selected. In the study, each method was evaluated on a scale from 1 to 10 and the most effective hydrogen production source was the sun with 8/10.

Moliner et al. (2016) discussed hydrogen economy in terms of production, distribution and consumption and presented models for solving the problems in these processes. In the study, why hydrogen cannot be a fuel alternative at the expected speed is discussed and a future projection for hydrogen economy is drawn.

Danaehpour and Mehrpooya (2018) achieved hydrogen production by combining a solar thermal photovoltaic device with a solid oxide electrolysis system. They aimed at high efficiency by creating steam electrolysis with a high thermal potential solar thermal photovoltaic device. They achieved 17% efficiency in electricity generation from solar energy, which provided enough energy to feed the solid oxide electrolysis assembly. As a result of the sensitivity analysis, it was seen that; 7458 kg of hydrogen was produced per hour with an efficiency rate of 54% electrical energy to the solid oxide electrolysis system. Thus, the total efficiency of the system was 34%. This hybrid system in hydrogen production has the potential to be competitive.

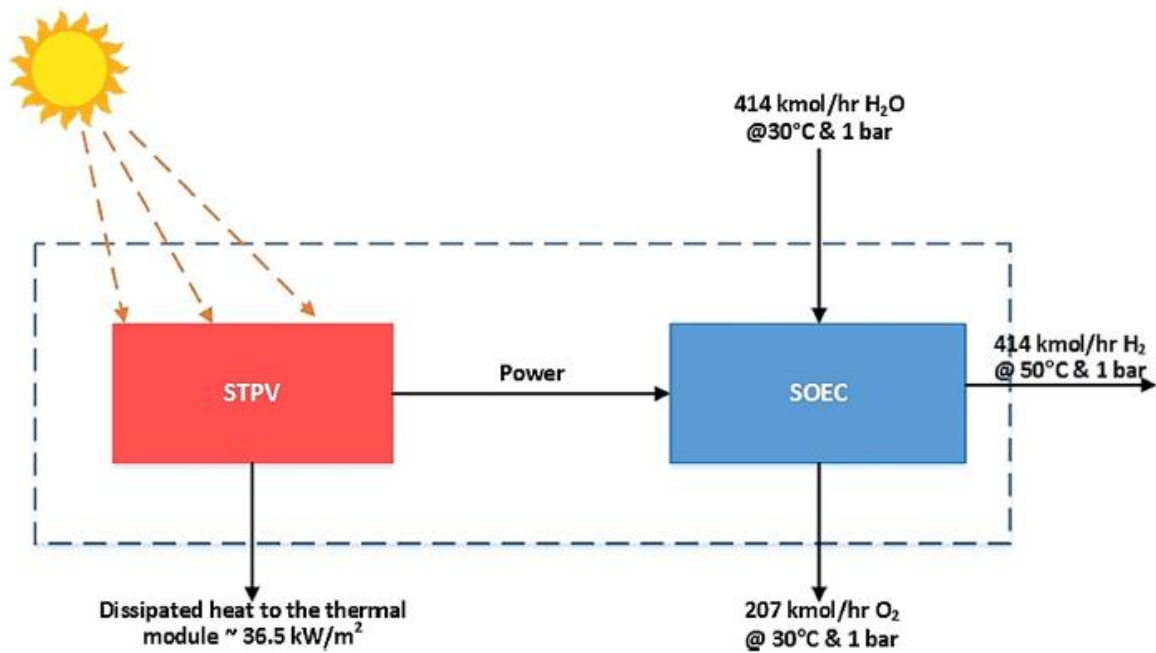


**Figure 2.8.** Block diagram of the proposed topology (Danaehpour and Mehrpooya, 2018).

Xing et al. (2013) have discussed photoelectrochemical and photochemical methods in hydrogen production and developed a kind of photoreactor design. A masked cylindrical batchtype reactor and a fixed quartz window is proposed for the photochemical water separation method, due to its low cost and easy production.

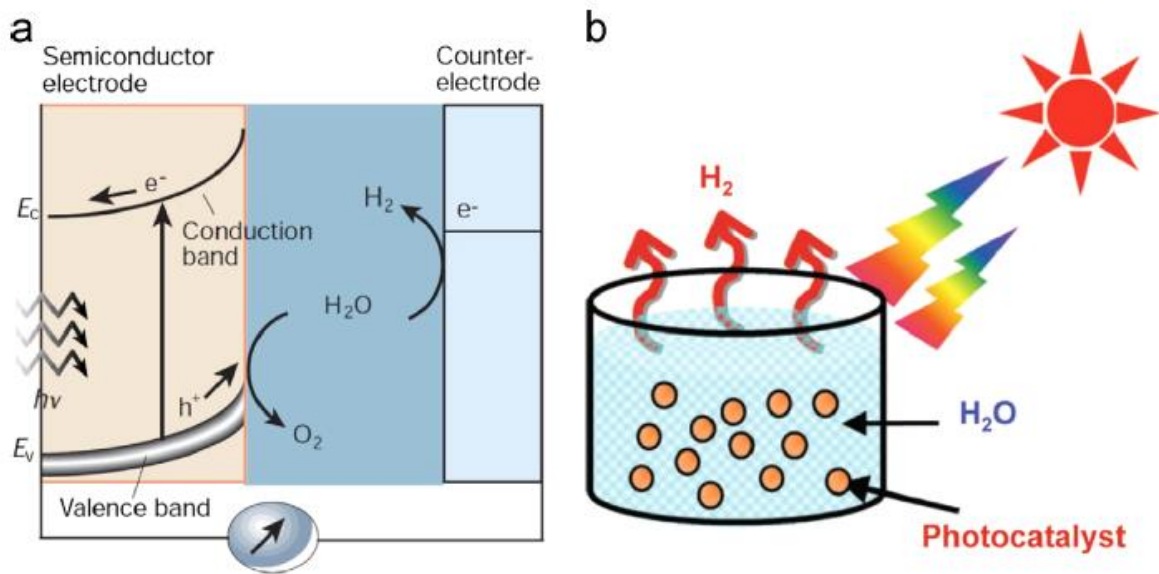


**Figure 2.9.** PEC and photochemical water separation methods (Xing et al, 2013).

Ozcan and Ersoz (2019), the potential of solar energy in three major regions in Turkey were evaluated in terms of a comparative photovoltaic system applications. Solar radiation data, optimal sun angles and GEPA data in these regions were brought together and annual production potentials were calculated in pvsyst program. With these calculations, the return period of the investment has been estimated by making financial analysis.

In the study of Omar and Altinisik (2016), hydrogen production from water electrolysis was simulated with the help of a hybrid solar collector. Borland Delphi 7 program was used in the numerical analysis of the simulation. 3 regions of Turkey; Erzurum, Istanbul, Konya were selected. The solar radiation potentials of these 3 regions are compared with each other. When different pressure and temperature levels are applied to these 3 regions, the most efficient hydrogen production with solar energy fed electrolysis has been achieved in Konya Province.

Benli (2015), using meteorological and geographical data of 6 different cities in Turkey demonstrated the potential of solar water heating potential of the sun. Two different collector types, galvanized plate and vacuum tube, have been compared. As a result of the collector made of galvanized material for heating water with solar energy it has been proven to be the most efficient option for Turkey.

In another study, Mumcular in the south of Turkey made with the help of a simulation software Pvsyst solar panel dam is built on the lake. With the energy generated from this panel, it has been tried to meet the energy need of a small residential area. A hydrogen fuel cell was used to use it when there was no sun, while hydrogen was obtained by converting the energy obtained from the solar panel into hydrogen production through electrolysis. The following advantages of a system established in this way have been demonstrated:

- Increasing the efficiency of the panel with the cooling effect of water on the solar panel
- Thanks to the shading function of the panel on the water, helping to preserve the amount of water by decreasing the evaporation in the water.
- To provide cleaner water by preventing the formation of algae in the water.

- To be able to use energy with the hydrogen fuel cell when the energy is needed by converting the energy produced when the sun is available to hydrogen production by electrolysis of water (Temiz and Javani, 2018)

Davis et al. (2017) talked about alkaline electrolysis with polymer electrolyte membrane (PEM) electrolysis, which are the two most used electrolysis methods to convert the energy obtained from an independent solar power panel into hydrogen energy. In this method, only one side of the cage electrode coated with catalysis was used and an asymmetrical positioning was made. Thus, the cross over rate remained at only 1 percent. This ratio was realized at the level of 7% in the electrode system coated with double side catalysis. An electrolysis system with an independent and floating solar panel was included in this asymmetric electrode system and the hydrogen generation efficiency from solar energy was 5.3% for 1 solar illumination intensity. Since the system is membrane-free, it can be applied at a very low cost.

Gorjian et al. (2021) emphasized in their study that floating solar panel systems have been in demand since 2016. They predicted that floating solar panel applications would grow by 31% in 2024 as governments encouraged this system. In the study, a detailed comparison of floating solar panels and land-mounted solar panels has been made. They emphasized that the floating solar panel is 25% more expensive than the traditional panel system, but this rate will decrease with increasing installed power. They examined in detail the contribution of the reduction of the panel temperature, which is the most important advantage of the floating solar panel, to the panel efficiency.



**Figure 2.10.** The largest floating PV system in the world which is installed in China (Gorjian et al, 2021).

Another study examined the advantages of the floating solar panel system. The components that make up the floating system are discussed in detail both electrically and mechanically. The deficiencies in the literature have been identified by making a compilation of existing studies. Considered as one of these shortcomings; The efficiency and cost comparison of the floor mounted system and the floating system was made. In order to connect the system to the distribution network, the application of multi-layer DC-DC converter is emphasized. In one of the studies cited, a floating solar panel system with a power of 10 kW connected to the grid and a ground-mounted solar panel system with a power of 10 kW connected to the grid. As a result, in the floating system, a decrease of 9.6% in losses due to panel heat in summer was observed, while a decrease of 3% was observed in winter. Interconnection methods of floating panels have been discussed and the efficiency of these methods has been compared. (Ranjbaran et al, 2019)

### 3. MATERIALS AND METHODS

#### 3.1. Solar panel experiments materials

Experiments were made at the center located in Adana in southern Turkey. Air temperature data were taken from Turkey Meteorological web page.

Initially, the 10W solar panel, specified below, is fixed on a flat land, at an optimal angle. Then the 10W solar panel same as above is fixed on a water-filled container, allowing it to float at an optimal angle. And then two values will be compared. Then, the current panel data and meteorological conditions were run on the Simulink plug-in from the MATLAB program and the results were obtained. These results were compared with the results of the experimental study.

**Table 3.1.** Technical datas of the solar panel.

Parameter:	Value:
Pmax	10W
Brand	LEXRON
Model Type	LXR-10P
Power Tolerance Range	5%
Open Circuit Voltage(Voc)	22.10V
Max Power Voltage (Vmp)	18.00V
Short Circuit Current (Isc)	0.67A
Max Power Current	0.56A
Max System Voltage	1000V
Max Series Fuse Rating	10.0A
Weight	1.5 kg
Module Application	Class A
All technical data at standard test condition:	
A	1.5
E	1000W/m <sup>2</sup>

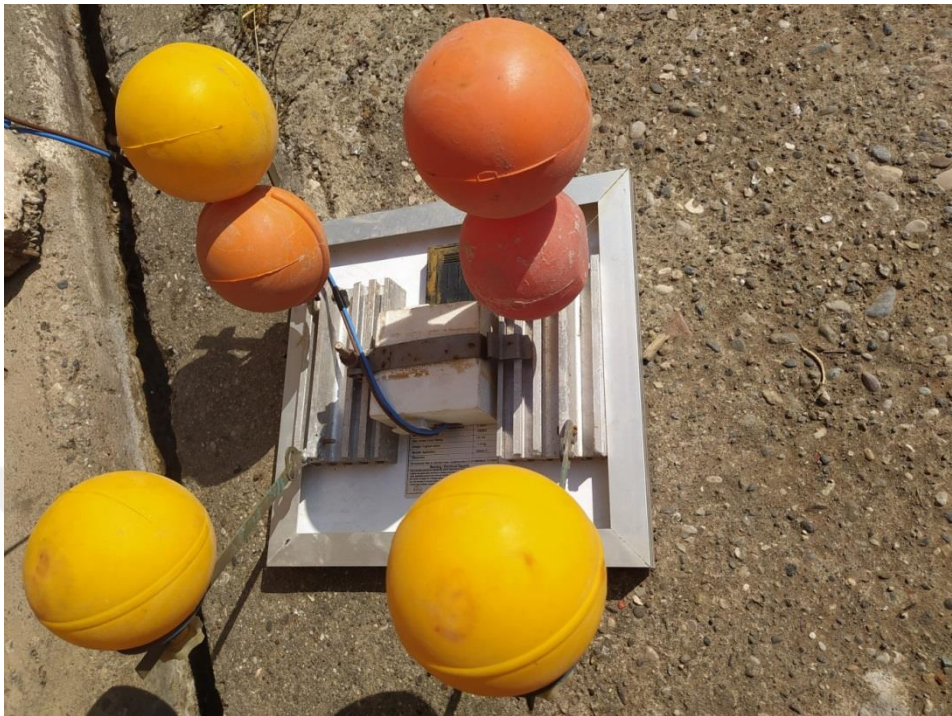


**Figure 3.1.** The appearance of solar panel back.



**Figure 3.2.** The Appearance of solar panel from side.



**Figure 3.3.** Installed solar panel floating on water.

### 3.2. Hydrogen production experiment materials

**Electrolyte:** 1 M KOH solution was used as the electrolyte in electrolysis cell.

The nickel plating bath composition was 30% NiSO<sub>4</sub>·7H<sub>2</sub>O, 1% NiCl<sub>2</sub>·6H<sub>2</sub>O, 1.25% H<sub>3</sub>BO<sub>3</sub>.

The cobalt decoration bath composition was % 30 CoSO<sub>4</sub>·7H<sub>2</sub>O, % 1 CoCl<sub>2</sub>·6H<sub>2</sub>O, % 1.25 H<sub>3</sub>BO<sub>3</sub>.

**Working electrodes:** Graphite(G), Nickel plated graphite (G/Ni), Cobalt decorated nickel plated graphite (G/NiCo) was used.

**Reference electrode:** Ag/AgCl was used as a reference electrode.

**Counter electrode:** Platinum (Pt) with a surface area of 2 cm<sup>2</sup> was used as counter electrode.

**DC source:** 0.01V step adjustable direct current source was used to provide constant voltage to be applied to the electrolysis circuit.

**Multimeter:** It was used to measure the DC electric current passing through the electrolysis circuit.

**Magnetic stirrer:** It was used to homogenize solutions.

**Sandpaper:** Used for polishing the electrode surfaces.

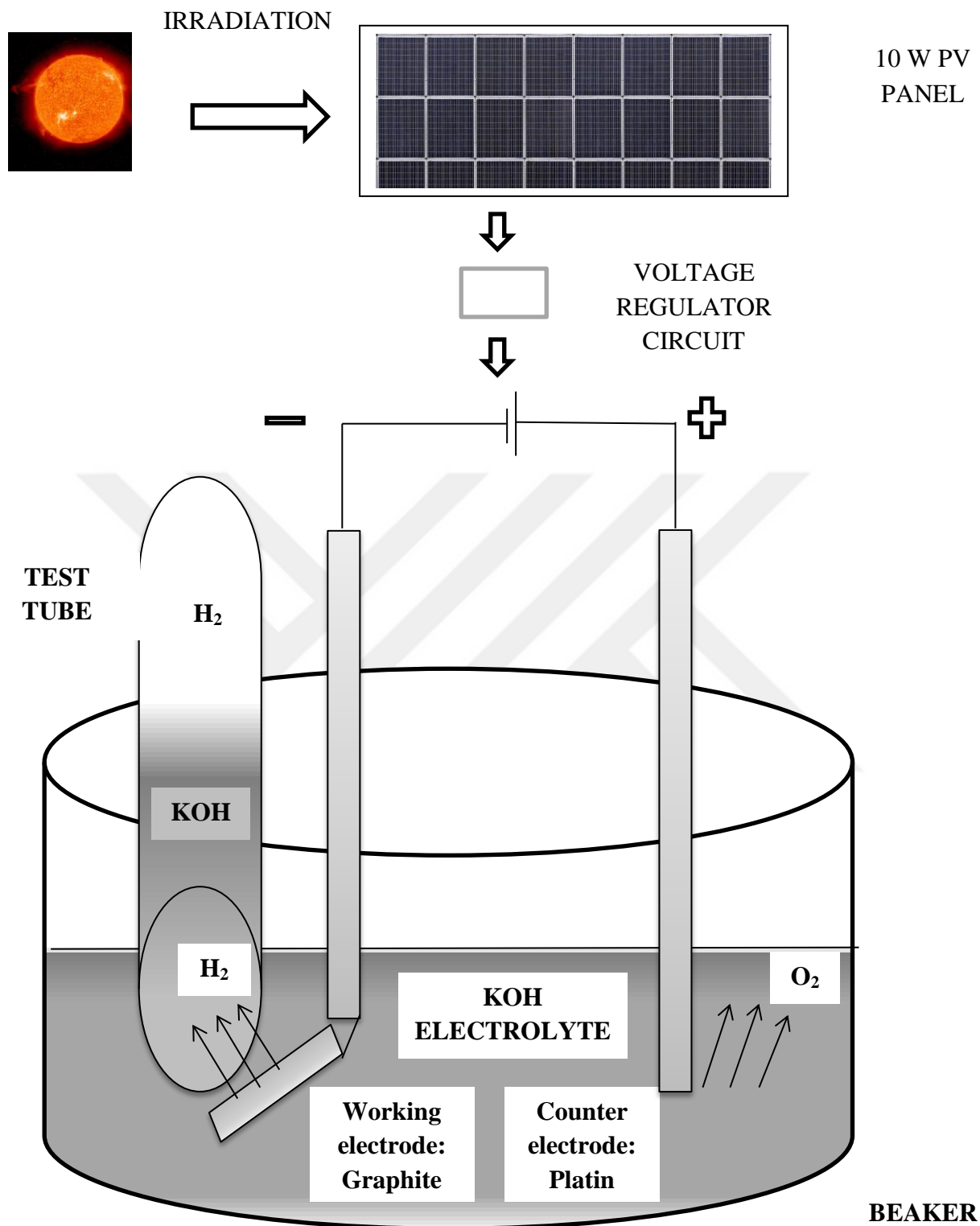


Figure 3.4. View of the experimental setup.

### 3.3. Methods

Two commercial graphite material (Alfa Aesar and Sigma-aldrich Adana), are supplied, 0.36 cm<sup>2</sup> (referred to G-I) and 0.86 cm<sup>2</sup> (referred to G-II) so that two different surface areas can be compared. In order to remove possible contamination on the electrode surface, the electrodes were first washed with pure water, then polished with sandpaper and fixed in the test tube by passing through pure water again. The same procedure was applied again after each experiment with hydrogen evolution.

To prepare a 1 M KOH solution, 56 grams of KOH, the weight of one mole, was weighed and put into the beaker. The beaker was then filled with distilled water until it reached the level of 1 liter. In order to ensure the homogeneity of the solution obtained, the solution was mixed with the help of magnetic stirrer.

In order to prepare Ni bath, 30 grams NiSO<sub>4</sub>·7H<sub>2</sub>O, 1 gram NiCl<sub>2</sub>·6H<sub>2</sub>O, 1.25 grams H<sub>3</sub>BO<sub>3</sub> were weighed and put into the volumetric flask. The volume of solution was 100 mL. The 10 μm thick Ni coating was achieved via galvanostatic method by Ivium stat electrochemical analyzer. The current density was 50 mA/cm<sup>2</sup>. A three-electrode system was used Ni electrode was used as counter electrode, Ag / AgCl (3M KCl) as reference electrode, and graphite as working electrode.

In order to prepare Co bath, 30 grams CoSO<sub>4</sub>·7H<sub>2</sub>O, 1 gram CoCl<sub>2</sub>·6H<sub>2</sub>O, 1.25 grams H<sub>3</sub>BO<sub>3</sub> were weighed and put into the volumetric flask. The volume of solution was 100 mL. The 10 μg Co decorated per 1 cm<sup>2</sup> of electrode surface with the help of galvanostatic method by Ivium stat electrochemical analyzer. The current density was 50 mA/cm<sup>2</sup>. A three-electrode system was used Pt electrode was used as counter electrode, Ag / AgCl (3M KCl) as reference electrode, and graphite as working electrode.

The determination of discharge potential of all electrodes was achieved in 1M KOH solution with a two-electrode configuration in which G, G/Ni, and G/NiCo were cathode and Pt was anode. The hydrogen gas performances of these electrodes at different potentials (between 2.3 and 3.0 V) were determined with the help of electrolysis cell which was supplied via PV system (Figure 3.4)

### 3.4. Simulation and experimental system

The experiments were also simulated by defining the same conditions in the MATLAB Simulink program. The MATLAB version used is MATLAB R2020B. The solar panel consists of 36 serially connected solar cells. Solar irradiance has been chosen as  $1000 \text{ W / m}^2$ . Short circuit current is  $0.66 \text{ A}$  and open circuit voltage is  $0.6 \text{ V}$  in accordance with the panel's catalog values. The quality factor is set at 1.5. Voltage was executed for 60 minutes after the circuit was built and the results were graphically obtained. The calculated ratio of error is 1:20. Below (Figure 3.5.) is the equivalent circuit of the experimental system prepared in Matlab Simulink.



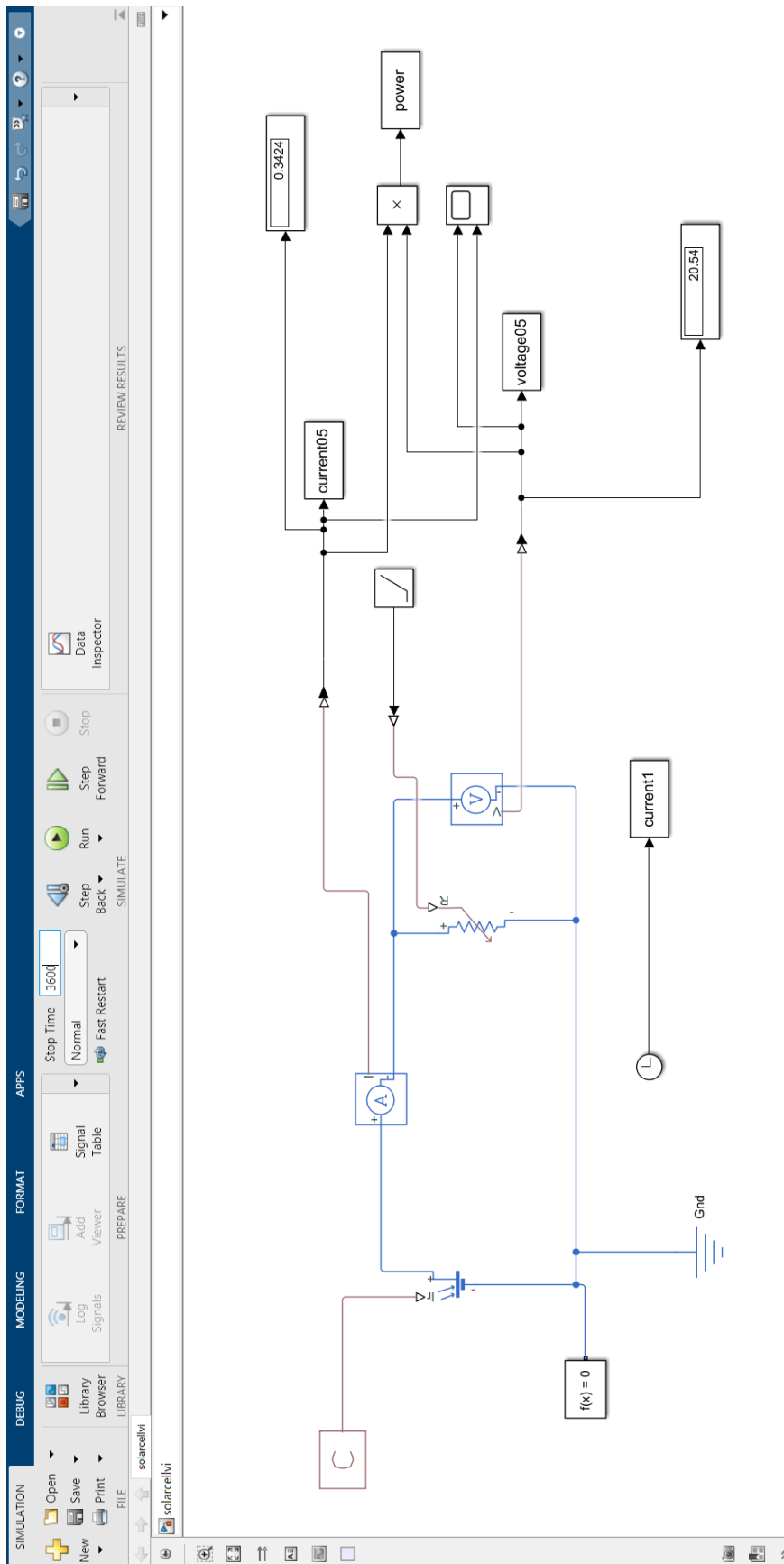


Figure 3.5. MATLAB Simulink equivalent circuit of panel.

## 4. RESULTS AND DISCUSSIONS

In order to provide the energy required in hydrogen production experiments, two 10 W solar panels, one mounted on the ground and the other mounted on water, were installed. Since the warm Mediterranean climate is observed in the Adana region, data at four different temperature values consisting of 6°C, 16°C, 24°C and 37°C were collected. These temperature values have been chosen in this way in order to compare the efficiencies of floating and land-mounted solar panels, especially in cold, cool, normal and hot weather conditions. Turkey Meteorological data were obtained from the web pages of the publication of daily temperature values.

### 4.1. Solar energy production in non-floating design

**Table 4.1.** Obtained current(I/A) and potential(U/V) values at temp 6°C in non-floating design.

U(V)	I (A)	P (W)
0.0	0.61	0.000
1.9	0.61	1.159
3.1	0.61	1.891
5.2	0.61	3.172
7.1	0.61	4.331
8.3	0.61	5.063
9.0	0.61	5.490
10.4	0.61	6.344
11.0	0.61	6.710
13.4	0.60	8.040
14.0	0.60	8.400
15.2	0.00	0.000
17.5	0.00	0.000
17.9	0.00	0.000

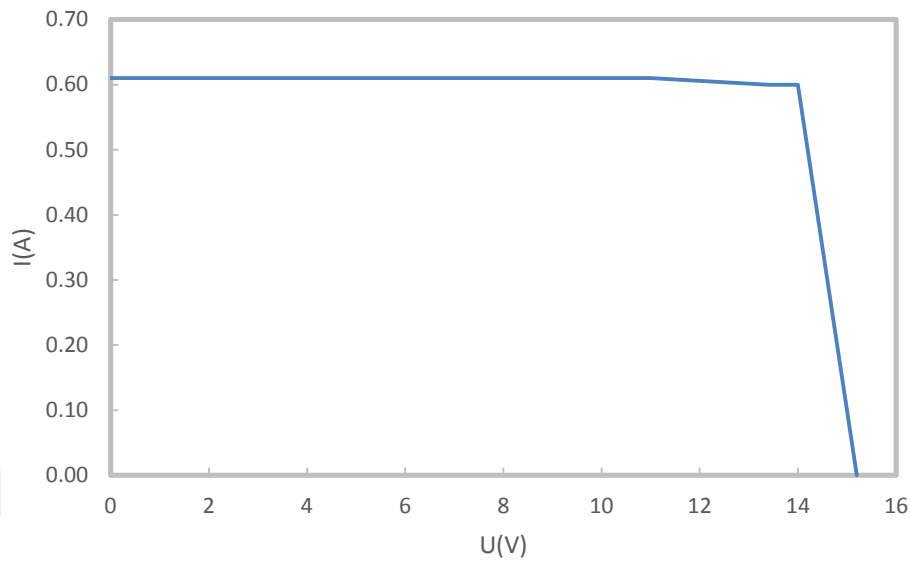


**Figure 4.1.** Obtained curve belonging to potential (U/V) and current (I/A) at 6°C.

Since the experiments started in the winter period, the data at 6°C temperature were observed first. At this temperature value, the current value after 15.2 volts could not be observed as seen in table 4.1

**Table 4.2.** Obtained current(I/A) and potential(U/V) values at temp 16°C in non-floating design.

U(V)	I (A)	P
0.0	0.62	0.000
1.9	0.62	1.178
3.1	0.62	1.922
5.2	0.62	3.224
7.1	0.62	4.402
8.3	0.62	5.146
9.0	0.62	5.580
10.4	0.62	6.448
11.0	0.62	6.820
13.4	0.62	8.308
14.0	0.62	8.680
15.2	0.62	9.424
17.5	0.00	0.000
17.9	0.00	0.000

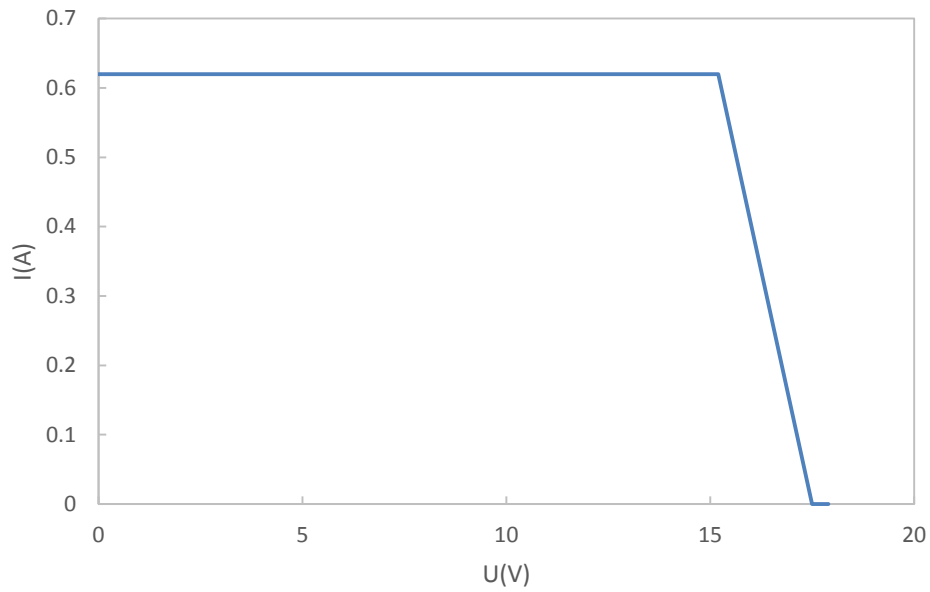


**Figure 4.2.** Obtained curve belonging to potential (U/V) and current (I/A) at 16°C.

As seen in Figure 4.2 and Table 4.2, the highest power value was reached at 15.5 volts.

**Table 4.3.** Obtained current(I/A) and potential(U/V) values at temp 24°C in non-floating design.

U(V)	I (A)	P
0.0	0.64	0.000
1.9	0.64	1.216
3.1	0.64	1.984
5.2	0.64	3.328
7.1	0.64	4.544
8.3	0.64	5.312
9.0	0.64	5.760
10.4	0.64	6.656
11.0	0.64	7.040
13.4	0.64	8.576
14.0	0.64	8.960
15.2	0.64	9.728
17.5	0.64	11.200
17.9	0.00	0.000

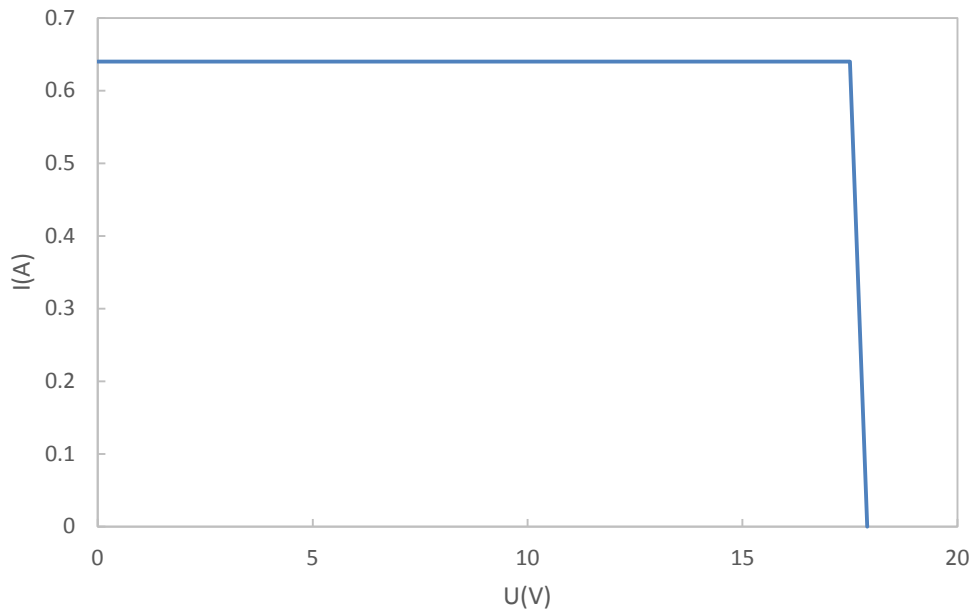


**Figure 4.3.** Obtained curve belonging to potential (U/V) and current (I/A) at 24°C.

As seen in Figure 4.3. and Table 4.3., the highest power value was reached at 16.7 volts.

**Table 4.4.** Obtained current(I/A) and potential(U/V) values at temp 37°C in non-floating design.

U(V)	I (A)	P
0.0	0.66	0.000
1.9	0.66	1.254
3.1	0.66	2.046
5.2	0.66	3.432
7.1	0.66	4.686
8.3	0.66	5.478
9.0	0.66	5.940
10.4	0.66	6.864
11.0	0.66	7.260
13.4	0.66	8.844
14.0	0.66	9.240
15.2	0.66	10.032
17.5	0.66	11.550
17.9	0.65	11.635
18.5	0.00	0.000

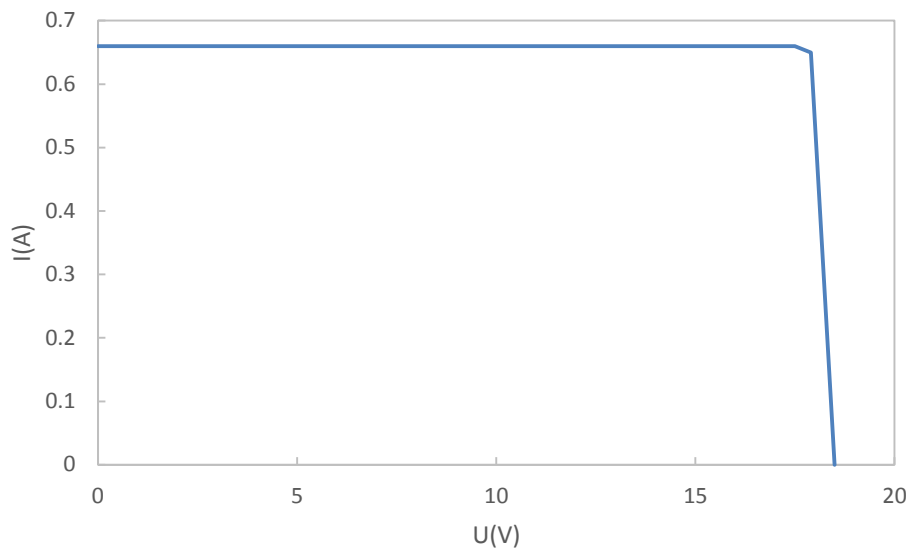


**Figure 4.4.** Obtained curve belonging to potential (U/V) and current (I/A) at 37°C.

As seen in Figure 4.4 and Table 4.4, the highest power value was reached at 16.5 Volts.

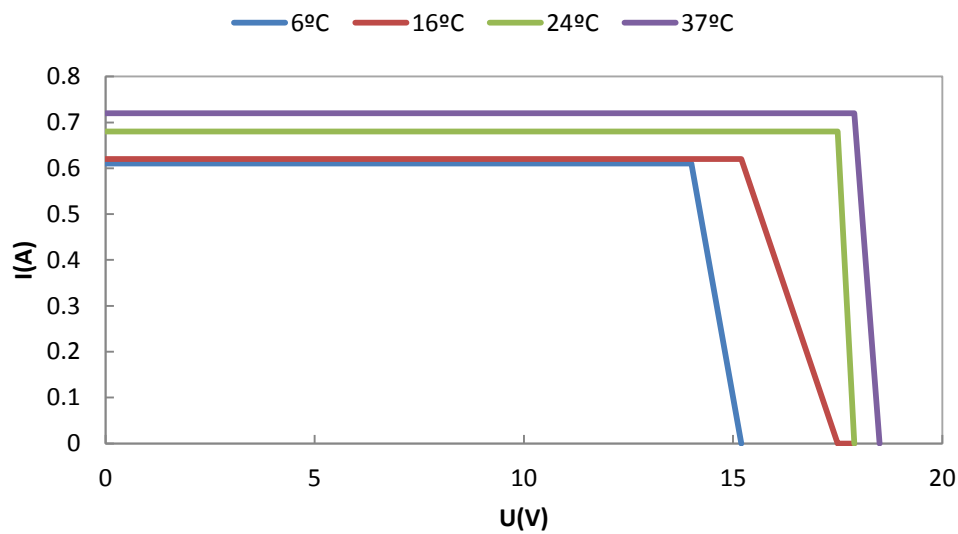


**Figure 4.5.** Obtained curve belonging to potential (U/V) and current (I/A) at different temperatures (combined appearance).

As seen in figure 4.5. in the land mounted system, the highest power value was achieved at 37°C. It is seen that the power obtained from the solar panel increases with the increase of the solar radiation value as the temperature increases.

## 4.2.Solar energy production in floating design

**Table 4.5.** Obtained current(I/A) and potential(U/V) values at temp 6°C in floating design.

U(V)	I (A)	P(Watt)
0.0	0.61	0.000
1.9	0.61	1.159
3.1	0.61	1.891
5.2	0.61	3.172
7.1	0.61	4.331
8.3	0.61	5.063
9.0	0.61	5.490
10.4	0.61	6.344
11.0	0.61	6.710
13.4	0.61	8.174
14.0	0.61	8.540
15.2	0.00	0.000
17.5	0.00	0.000
17.9	0.00	0.000

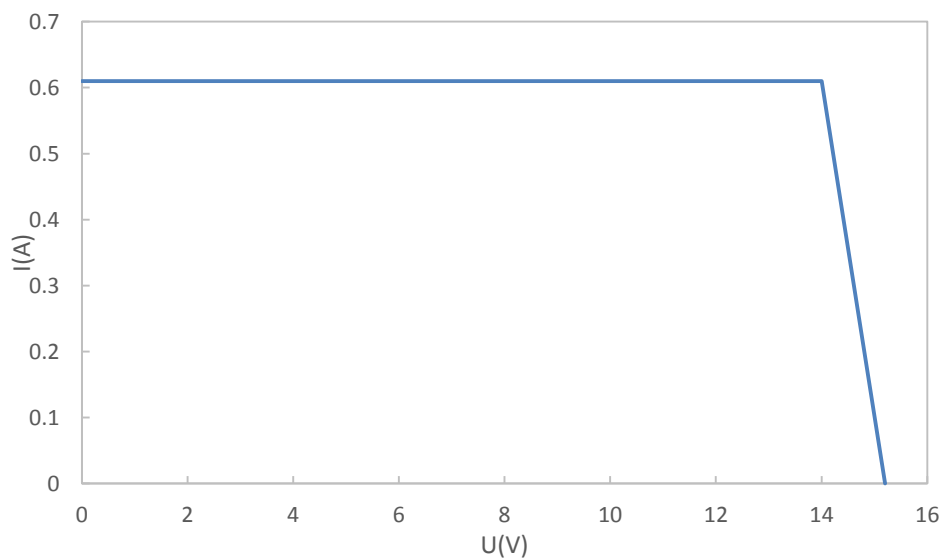


**Figure 4.6.** Obtained curve belonging to potential (U/V) and current (I/A) at 6°C in floating design.

As seen in Figure 4.6. and Table 4.5., the highest power value was reached at 14 Volts.

**Table 4.6.** Obtained current(I/A) and potential(U/V) values at temp 16°C in floating design.

U(V)	I (A)	P(Watt)
0.0	0.62	0.000
1.9	0.62	1.178
3.1	0.62	1.922
5.2	0.62	3.224
7.1	0.62	4.402
8.3	0.62	5.146
9.0	0.62	5.580
10.4	0.62	6.448
11.0	0.62	6.820
13.4	0.62	8.308
14.0	0.62	8.680
15.2	0.62	9.424
17.5	0.00	0.000
17.9	0.00	0.000

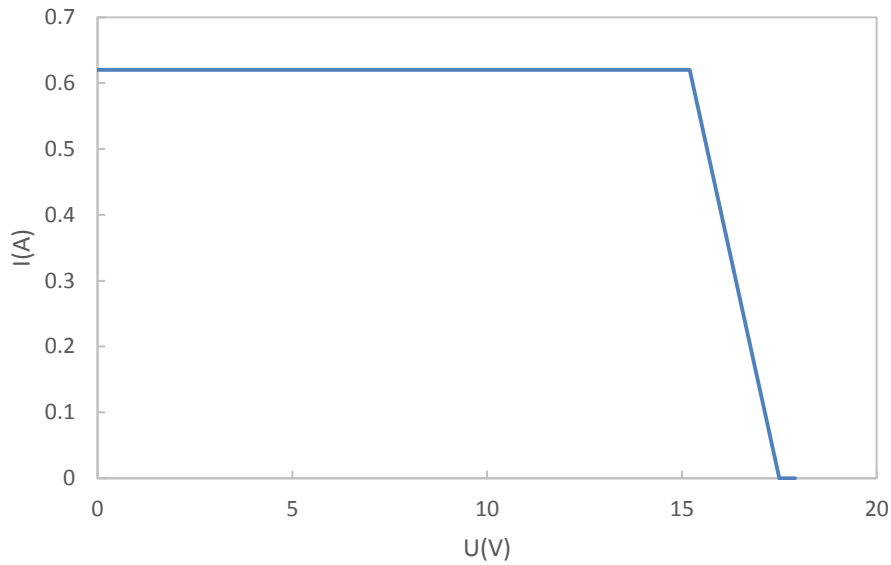


**Figure 4.7.** Obtained curve belonging to potential (U/V) and current (I/A) at 16°C in floating design.

As seen in Figure 4.7. and Table 4.6, the highest power value was reached at 15.2 Volts.

**Table 4.7.** Obtained current(I/A) and potential(U/V) values at temp 24°C in floating design.

U(V)	I (A)	P
0.0	0.68	0.000
1.9	0.68	1.292
3.1	0.68	2.108
5.2	0.68	3.536
7.1	0.68	4.828
8.3	0.68	5.644
9.0	0.68	6.120
10.4	0.68	7.072
11.0	0.68	7.480
13.4	0.68	9.112
14.0	0.68	9.520
15.2	0.68	10.336
17.5	0.68	11.900
17.9	0.00	0.000

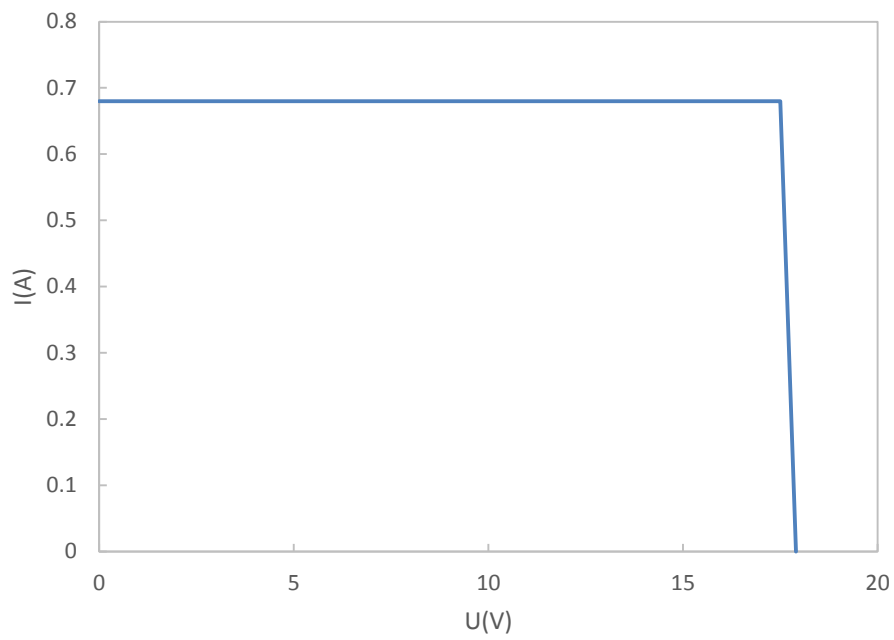


**Figure 4.8.** Obtained curve belonging to potential (U/V) and current (I/A) at 24°C in floating design.

As seen in Figure 4.8. and Table 4.7., the highest power value was reached at 17.5 Volts.

**Table 4.8.** Obtained current(I/A) and potential(U/V) values at temp 37°C in floating design.

U(V)	I (A)	P
0.0	0.72	0.000
1.9	0.72	1.368
3.1	0.72	2.232
5.2	0.72	3.744
7.1	0.72	5.112
8.3	0.72	5.976
9.0	0.72	6.480
10.4	0.72	7.488
11.0	0.72	7.920
13.4	0.72	9.648
14.0	0.72	10.080
15.2	0.72	10.944
17.5	0.72	12.600
17.9	0.72	12.880
18.5	0.00	0.000

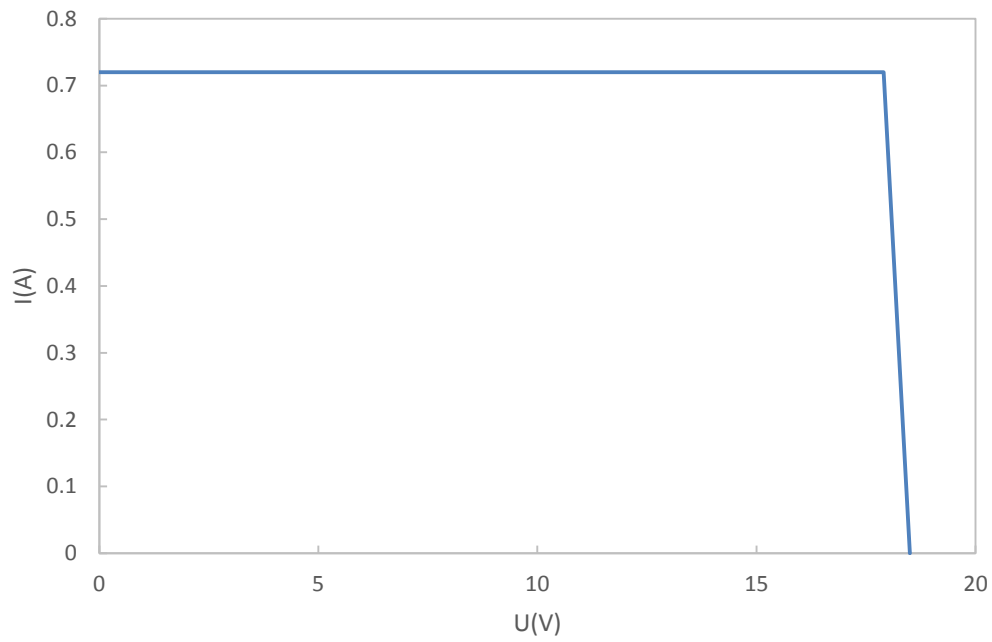


**Figure 4.9.** Obtained curve belonging to potential (U/V) and current (I/A) at 37°C in floating design.

As seen in Figure 4.9. and Table 4.8., the highest power value was reached at 17.9 Volts.

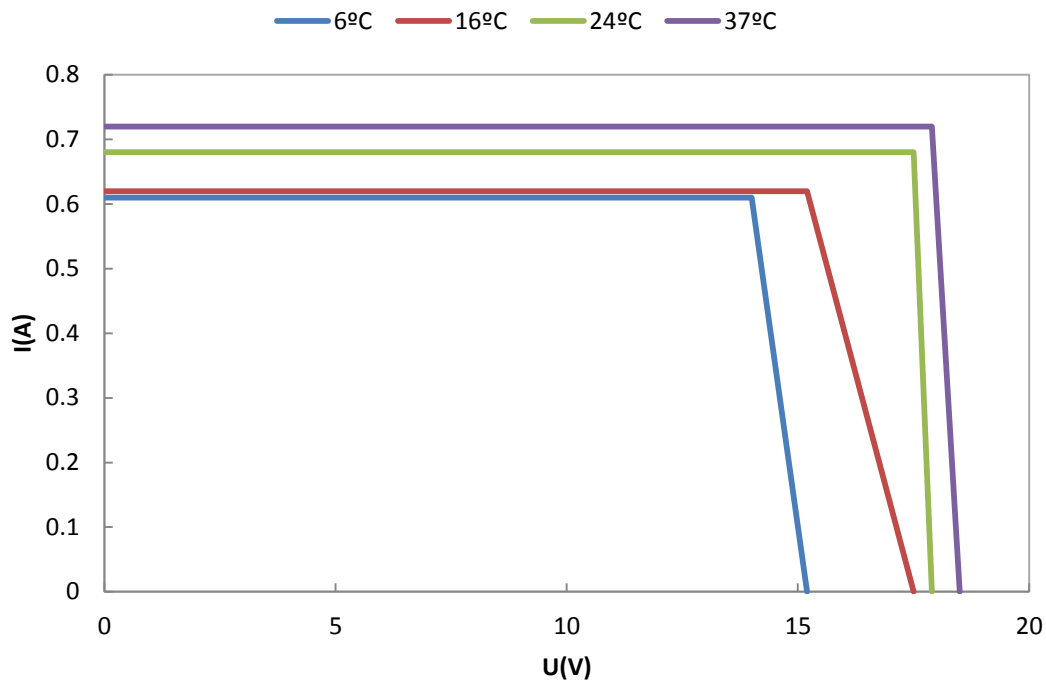


**Figure 4.10.** Obtained curve belonging to potential (U/V) and current (I/A) at different temperatures in floating design (combined appearance).

As seen in Figure 4.10, the obtained power value increased as the temperature and thus the solar radiation increased in the floating system.

### 4.3. Comparison of floating solar panel and land mounted solar panel

The I-V(Current-Potential) curves of the floating solar panel system and the land-mounted solar panel, which does not come into contact with water, that are formed at different temperatures, are seen in Figures 4.1-4.10, the traditional I-V behavior is same and there is no significant difference in the curve formations. However, it has been observed that the current strengths at the same voltage levels increase in the floating solar panel, especially at high temperatures.

The maximum power values obtained from floating and non-floating solar panels at different temperatures are pointed out in Table 4.9.

**Table 4.9.** Pmax values at different temperatures in two design.

Temperature	Pmax (non floating)	Pmax (floating)	Difference	% Dif.
6°C	8.400	8.540	0.140	1.666
16°C	9.424	9.424	0.000	0.000
24°C	11.200	11.900	0.700	6.250
37°C	11.635	12.880	1.245	10.700

The measurement results of the solar panel, which were made in two different designs, floating and non-floating at four different temperature values, were tabulated and graphed in Table 4.9 and Figure 4.11.

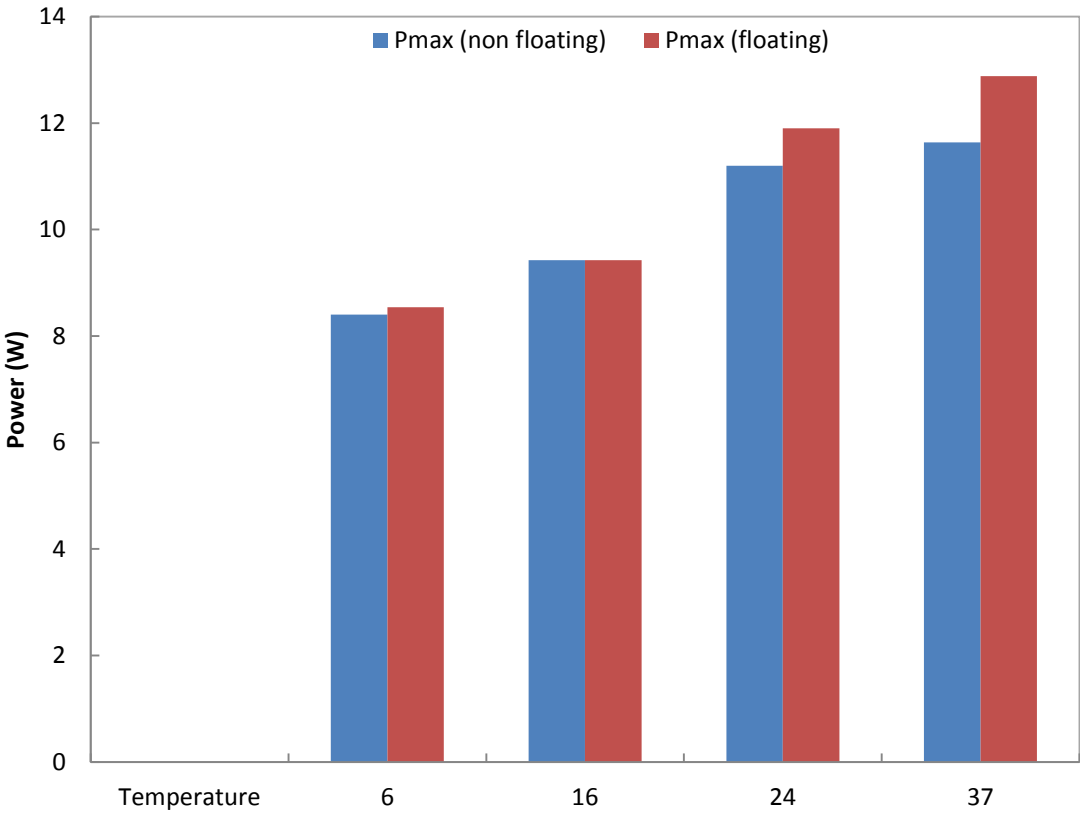


**Figure 4.11.** Pmax comparison floating with non-floating design.

In Figure 4.11, the floating and non-floating designs were compared. There was no significant increase in the power obtained from the solar panel at 6°C and 16°C temperatures. However, a power increase of 6.25% and 10.075% was achieved, respectively, in the panel that floats at 24°C and 37°C temperatures and is in contact with water compared to the land-mounted panel, which is not in contact with water.

The parameters belonging to the same solar panel were run in MATLAB Simulink program this time.

Current (I / A) and Voltage (U / V) graphs obtained at different temperature values as a result of running the program are as follows.

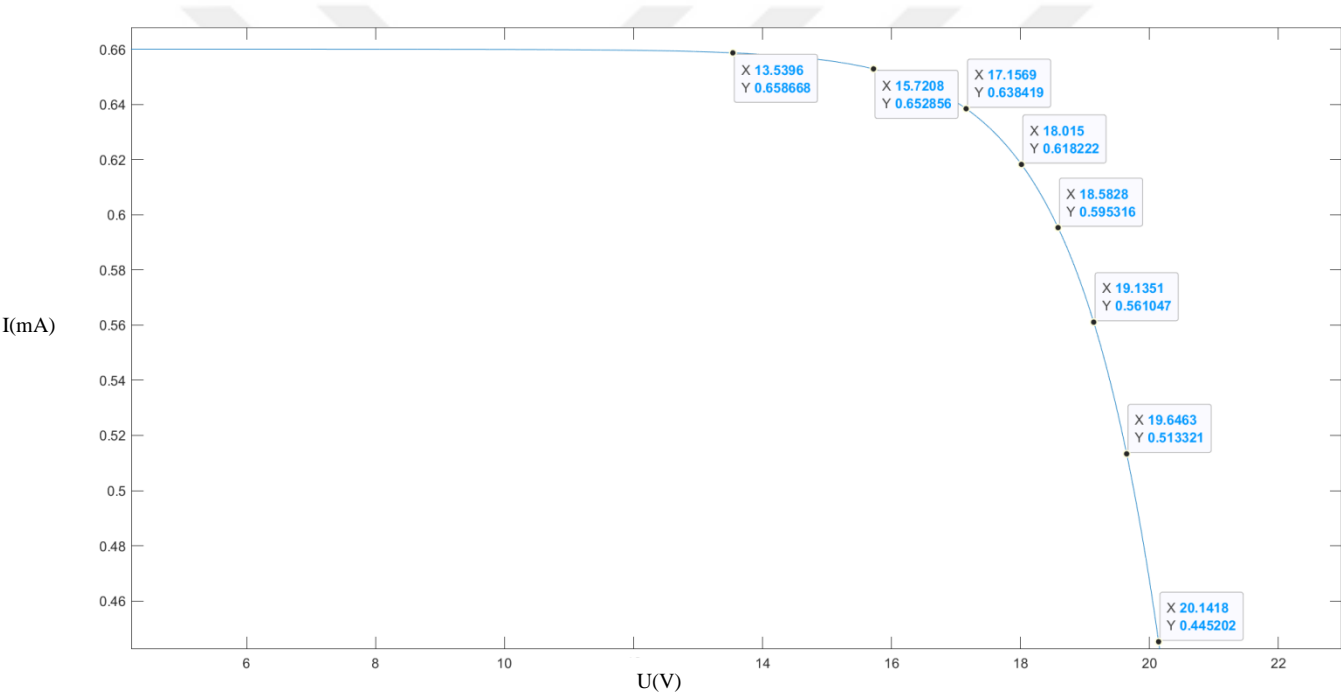


**Figure 4.12.** Current (I / A) - voltage (U / V) graph obtained as a result of 6°C temperature in MATLAB Simulink.

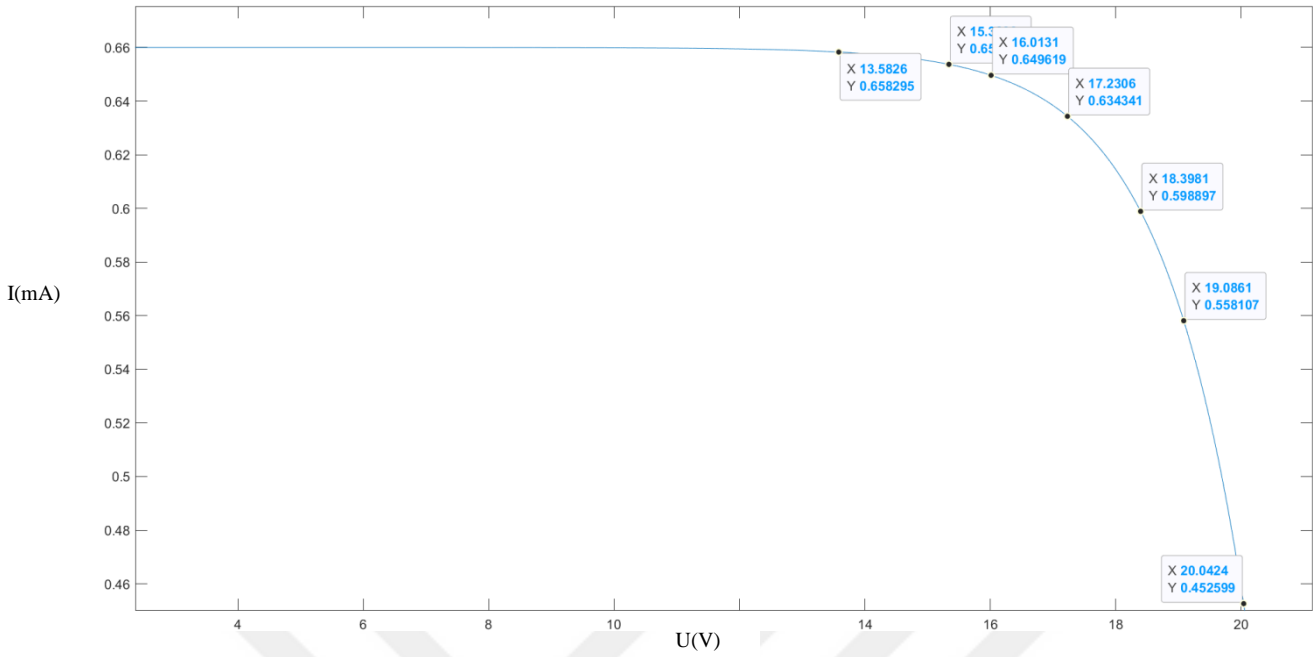


**Figure 4.13.** Current ( $I / A$ ) - voltage ( $U / V$ ) graph obtained as a result of 16 °C temperature in MATLAB Simulink.

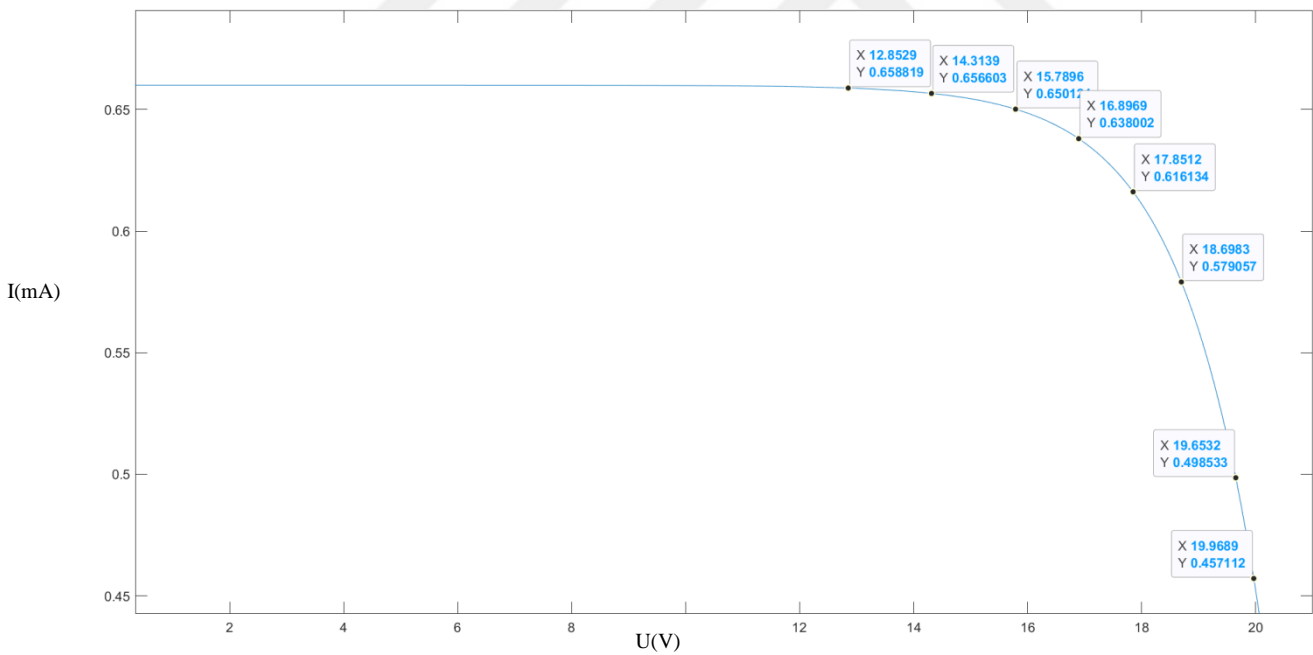


**Figure 4.14.** Current ( $I / A$ ) - voltage ( $U / V$ ) graph obtained as a result of 24 °C temperature in MATLAB Simulink.

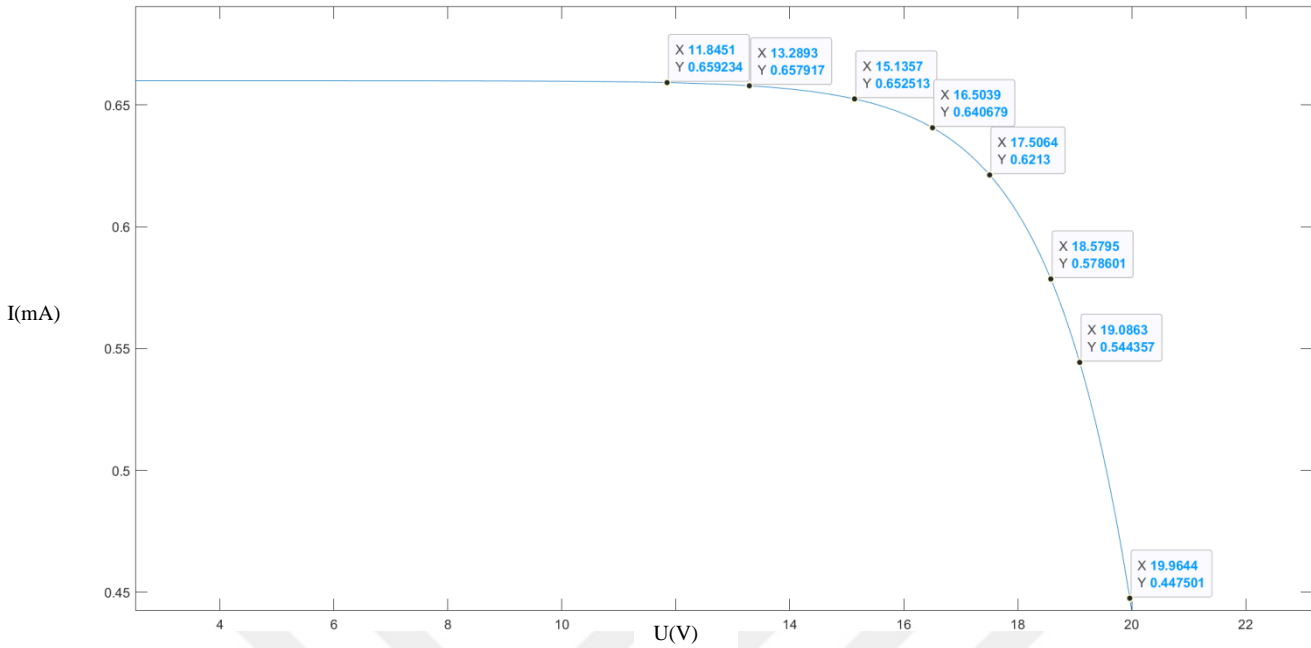


**Figure 4.15.** Current (I / A) - voltage (U / V) graph obtained as a result of 36 °C temperature in MATLAB Simulink.

The experiments performed in the field and the simulation studies performed in MATLAB Simulink were compared. Accordingly, very close results were obtained in the current value in the graphs obtained, and the voltage value was higher in MATLAB Simulink. The reason is considered to be the difference between the field conditions in which the experiment was carried out and the ideal conditions in the simulation.

In the study by Kamuyu et al. (2018), the effect of temperature on panel efficiency was investigated using MATLAB. For this, the land-mounted panel model and the floating panel model were compared. As a result, it has been revealed that the floating solar panel system is 10% more yielding than the land-mounted system due to the decrease in temperature effect. This overlaps with the data in our experimental study.

In another study by Sahu et al. (2016), it was revealed that the floating solar panel system is 11% more yielding with the effect of lowering the panel temperature compared to the ground-mounted system. Again, this value is very close to the experimental work and MATLAB simulation study done by us.

## 4.4. Hydrogen production experiment

### 4.4.1. The performance of graphite

The discharge potential and hydrogen gas volume were determined with a two-electrode configuration. Pt was used as anode, two different commercial bare graphite electrodes (G-I and G-II) were used as a cathode in this system. Hydrogen gas was determined via graduated cylinder which was filled with 1 M KOH electrolyte. It was inverted over the cathode. The hydrogen performance of G-I and G-II were compared.

Before the experiments the surface of electrodes were mechanically abraded with sharpener paper (320–1200 grain size), then washed up with distilled water. In order to minimize human-induced measurement errors, experiments were repeated 6 times and the values were averaged. In the experiment, the current increased with increasing potential and the highest current density was obtained at 3V as 354.16 mA/cm<sup>2</sup> and 179.06 mA/cm<sup>2</sup> for G-I and G-II, respectively.

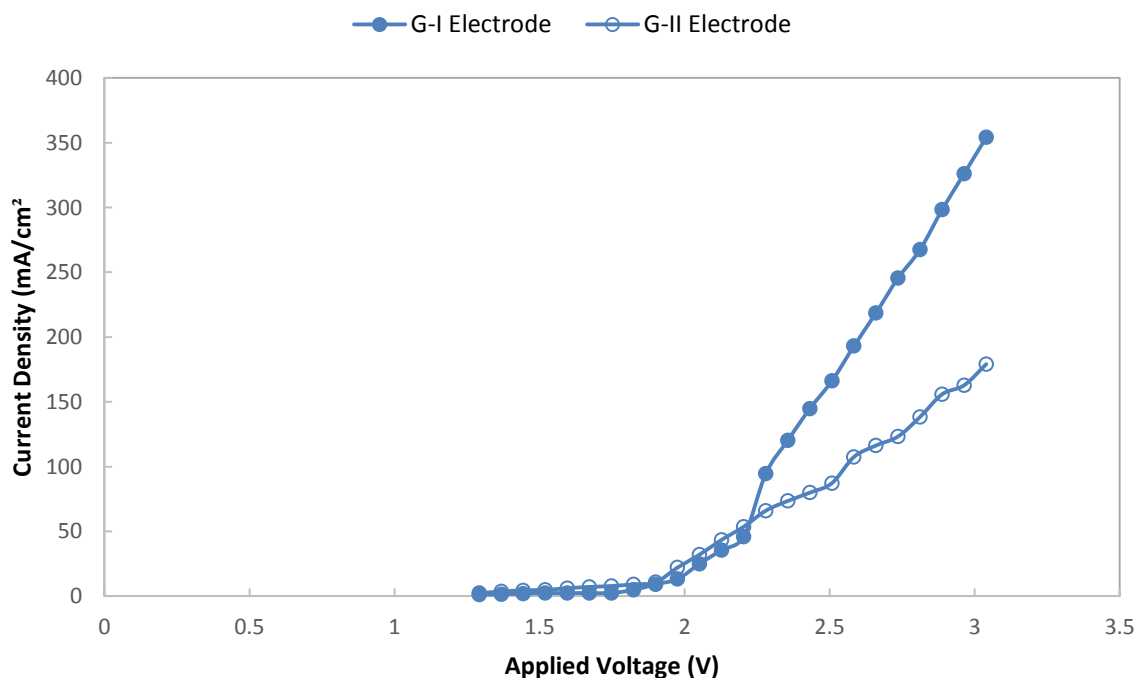


**Figure 4.16.** The voltage - current density curve of G-I/bare (●) and G-II/bare (○) in 1 M KOH at 298 K.

In Figure 4.16, the electrodes were compared, it was seen that the G-I electrode had higher current density. Therefore, G-I electrode was preferred.

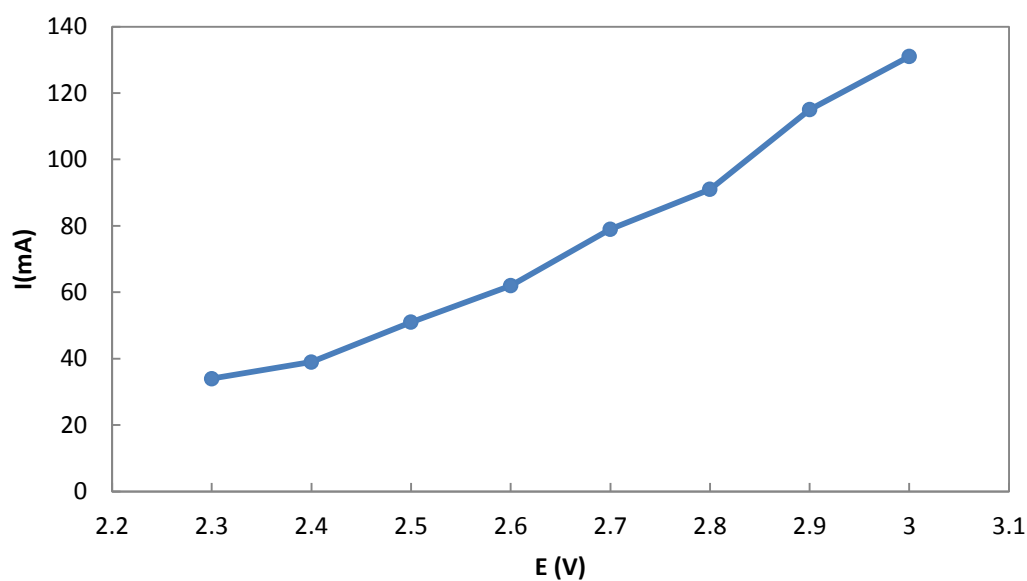


**Figure 4.17.** The voltage - current curve of G-I/bare (●) in 1 M KOH at 298 K.

**Table 4.10.** Produced hydrogen volume with G-I/bare at the end of 30 minutes.

Applied Potential (V)	I(mA)	Produced Hydrogen Volume (mL)
2.3	32.0	7.0
2.4	37.7	9.5
2.5	48.2	12.5
2.6	59.5	15.0
2.7	77.8	18.0
2.8	90.3	21.0
2.9	115.2	28.0
3.0	127.5	30.0

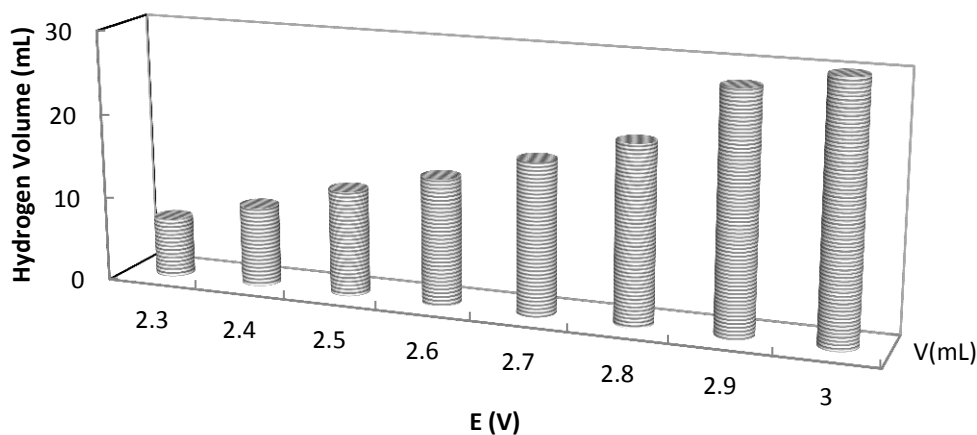


**Figure 4.18.** Hydrogen production volume by applied voltage with G-I/bare.

In the electrolysis cell, graphite electrode (G-I) with  $0.363 \text{ cm}^2$  surface area was used as the cathode electrode, Pt was used as the anode electrode, the constant voltage from 2.3 V to 3 V was applied to the circuit in 0.1 V steps, respectively. The highest hydrogen production was obtained at 3 V voltage. As can be seen in Table 4.10, 30 mL of hydrogen was produced at the end of 30 minutes with a voltage of 3 V.

In the study of Türkmen (2016), 3.5% NaCl solution was used, platinum was used as the anode electrode and at the end of the 60-minute test period, the maximum hydrogen production was obtained with nickel-zinc coated mild steel as 45.7 mL. In the experiment using nickel-zinc coated mild steel as the counter electrode, 22.85 mL of hydrogen could be produced according to the current test period. This means a better efficiency in the current experiment with the graphite electrode.

In the study of Koca et al. (2019), 1 M KOH solution was used as the electrolyte, Platinum (Pt) was used as the reference electrode, CF, CF / Ni, CF / NiGa were used as the cathode electrodes and 3V DC voltage was used in the electrolysis circuit for 30 minutes. has been applied. At the end of the experiment, the highest hydrogen production occurred when CF / NiGa electrode was used with 27.5 mL. From this, it can be said that the use of CF/NiGa

electrodes can achieve almost the same amount of hydrogen production with the use of graphite electrodes.

In the study of Chakik et al. (2017), 20g / L NaOH solution was used as the electrolyte, and zinc (Zn) alloys in various proportions were used as cathodes. As a result of the experiment, the highest hydrogen production was obtained when Zn90% Cr10% alloy was used as cathode. When 3 V constant DC voltage was applied, 1 mL hydrogen production was achieved in 246 seconds, 2 mL hydrogen production in 382 seconds, 3 mL hydrogen production in 536 seconds. It is seen that the amount of hydrogen produced remains low compared to the present experiment.

#### 4.4.2. The performance of nickel plated graphite (G/Ni)

The electrodeposition of nickel (Ni) was performed by galvanostatically using Iviumstat Electrochemical Interface (with serial number AO6063) with a three-electrode configuration. In this system, G-I was used as working electrode, nickel as counter electrode and an Ag/AgCl (3 M KCl) electrode was used as the reference electrode. The nickel deposition bath composition was 30% NiSO<sub>4</sub>.7H<sub>2</sub>O, 1% NiCl<sub>2</sub>.6H<sub>2</sub>O, 1.25% H<sub>3</sub>BO<sub>3</sub>. The deposition current density was 50 mA cm<sup>-2</sup>. The thickness was 10 μm. The coating was obtained according to Equation 4.



The polarization measurements were achieved with two electrode configurations in this system G-I/Ni was used as cathode and Pt was used as anode. The obtained voltage-current density E (V) / I<sub>d</sub> (mA/cm<sup>2</sup>) graph is as in Figure 4.19.

The same procedure was repeated, which was presented in section 4.4.1 for Ni plated graphite electrode. The obtained voltage-current density E (V) / I<sub>d</sub> (mA/cm<sup>2</sup>) graph was presented in Figure 4.19. In Figure 4.20, the current densities obtained in the separation experiments with G-I / bare and G-I / Ni are compared. In the experiment with nickel coating, higher current density was obtained at the same potentials compared to the experiment with bare graphite.

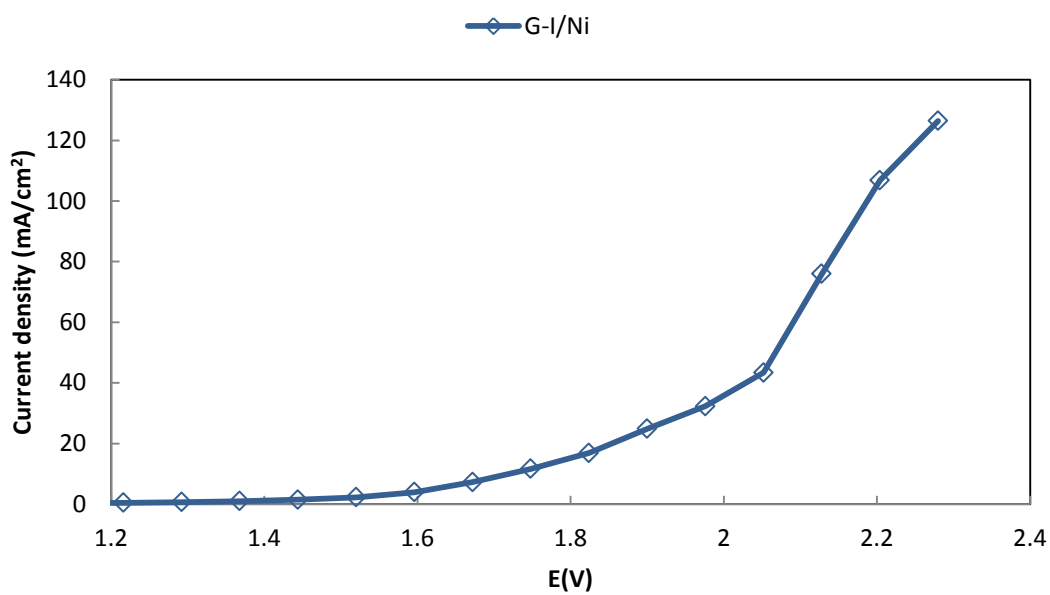


**Figure 4.19.** The voltage - current density curve of G-I/Ni ( $\diamond$ ) in 1 M KOH at 298 K.

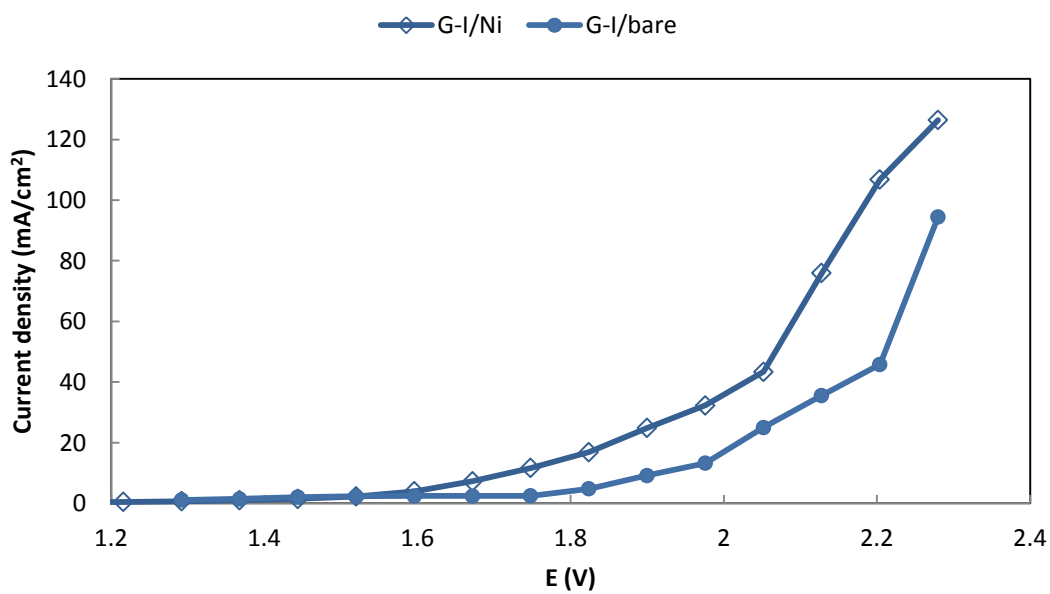


**Figure 4.20.** The voltage - current density curve of G-I/bare ( $\bullet$ ) and G-I/Ni ( $\diamond$ ) in 1 M KOH at 298 K.

**Table 4.11.** Produced hydrogen volume with G/Ni at the end of 30 minutes.

Applied Potential (V)	I(mA)	Produced Hydrogen Volume (mL)
2.3	34.9	9.25
2.4	55.5	14.25
2.5	59.6	15.00
2.6	75.0	18.50
2.7	89.0	21.50
2.8	107.5	26.50
2.9	116.2	28.00
3.0	126.0	31.00

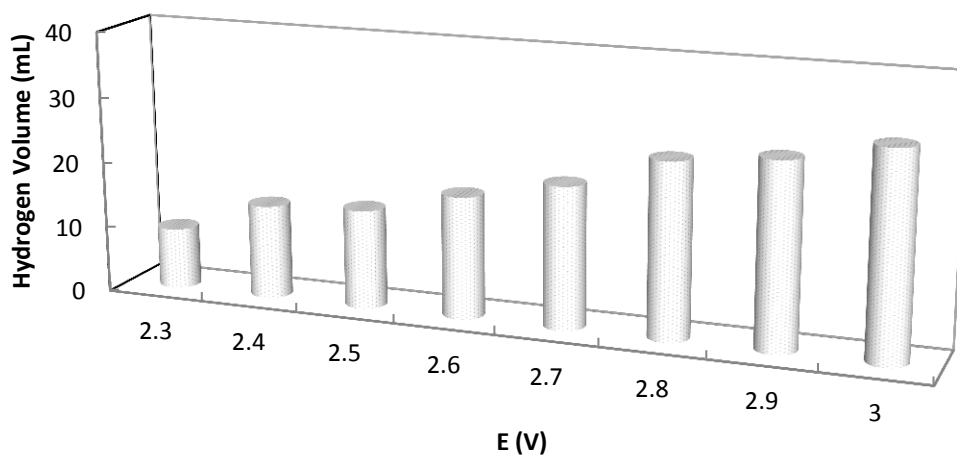


**Figure 4.21.** Hydrogen production volume by applied voltage with G-I/Ni.

In Figure 4.20, a significantly higher current density was obtained with nickel-coated graphite compared to bare graphite. In Table 4.11 and Figure 4.21, the amount of hydrogen obtained

with currents at different potentials and different durations are shown. There was a partial increase in the study with the G-I / Ni electrode compared to the G-I / bare electrode.

In the study by Mert et al. (2019), 6 M KOH was used as a solution, Cu / NiMo with a surface area of 0.283 cm<sup>2</sup> was used as the cathode electrode, 12 V voltage was applied for 8 hours and 8180 mL of hydrogen was produced. If it is assumed that 511.25 mL of hydrogen will be produced in 30 minutes, which is the current test period, it can be seen that a considerable amount of hydrogen is produced compared to the present experiment. However, it should not be forgotten that this experiment was conducted in four separate containers with 12 V voltage.

In the study of Mert (2005), the maximum hydrogen production in 30 minutes was obtained in NaOH solution as 30.8 mL with Nickel-plated silver electrode in the case of Platinum anode. 11.4 mL of hydrogen was produced with the bare silver electrode. This coincides with the values in the current experiment using the graphite electrode.

#### **4.4.3. The performance of cobalt decorated nickel plated graphite (G-I/NiCo)**

In order to decorate G-I/Ni surface, Co plating bath was used which was 30% CoSO<sub>4</sub>.7H<sub>2</sub>O, 1% CoCl<sub>2</sub>.6H<sub>2</sub>O, 1.25 H<sub>3</sub>BO<sub>3</sub>. The operation performed by galvanostatically using Iviumstat Electrochemical Interface with a three-electrode configuration. In this system, G-I/Ni was used as working electrode, Pt electrode was used as counter electrode and an Ag/AgCl (3 M KCl) electrode was used as the reference electrode. The deposition current density was 50 mA cm<sup>-2</sup>. The electrode surface was decorated according to Equation 5,



The polarization measurements were achieved with two electrode configurations in this G-I/NiCo was used as cathode and Pt was used as anode. The obtained voltage-current density E (V) / I<sub>d</sub> (mA/cm<sup>2</sup>) graph is as in Figure 4.22. In Figure 4.23., the current densities obtained in the separation experiments with G-I / bare, G-I / Ni and G-I/NiCo are compared.

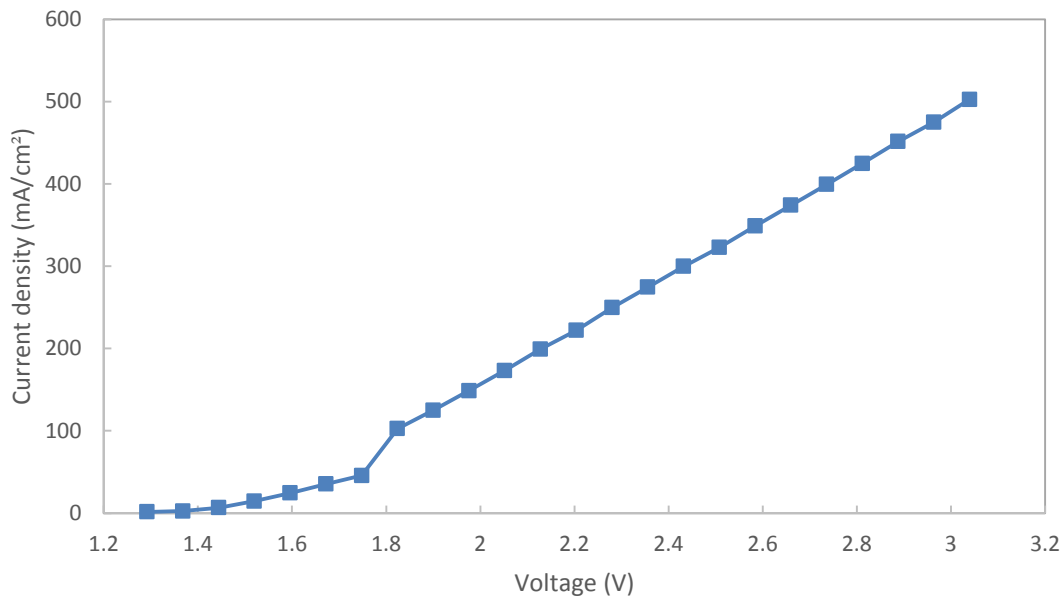


**Figure 4.22.** The voltage - current density curve of G-I/NiCo (■) in 1 M KOH at 298 K.

Theoretically, the voltage at which water begins to decompose is 1.229 V. (Döner, 2005) Due to over potentials ( $E_{\text{over}}$ ) the decomposition voltage of G-I, G-I / Ni and G-I/NiCo was 2.1 V; 1.9 V and 1.7 V, respectively. According to experimental data in Figure 4.19., 4.20. and 4.22; over potentials are;

For G-I/bare;

$$\begin{aligned}
 E_{\text{over}} &= E_d - 1.3 && (6) \\
 &= 2.1 - 1.3 \\
 E_{\text{over}} &= 0.8 \text{ V}
 \end{aligned}$$

For G-I/Ni

$$\begin{aligned}
 E_{\text{over}} &= E_d - 1.3 \\
 &= 1.9 - 1.3 \\
 E_{\text{over}} &= 0.6 \text{ V}
 \end{aligned}$$

For G-I/NiCo

$$\begin{aligned}
 E_{\text{over}} &= E_d - 1.3 \\
 E_{\text{over}} &= 0.4 \text{ V}
 \end{aligned}$$

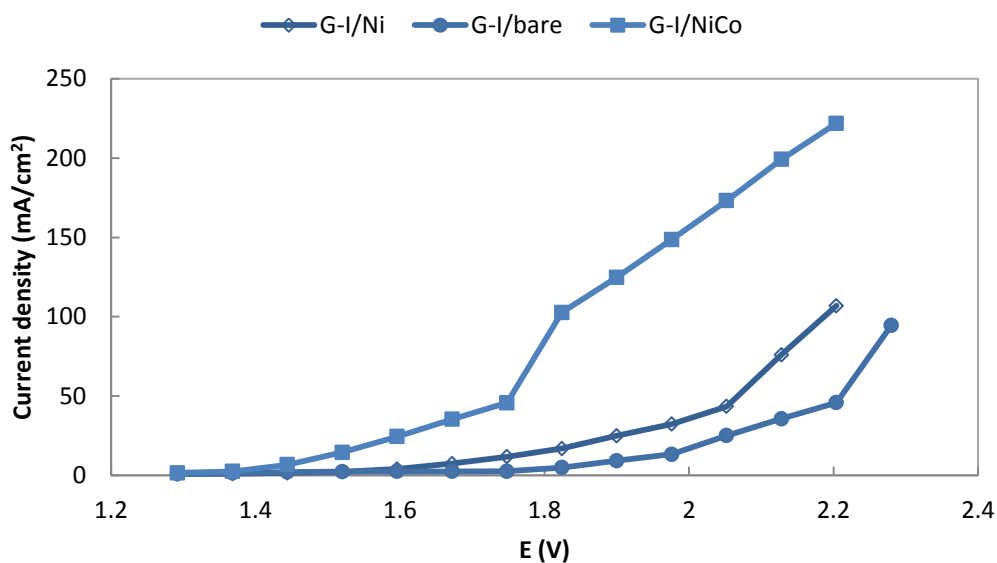


**Figure 4.23.** The voltage - current density curve of G-I/bare (●), G-I/Ni (◇) and G-I/NiCo (■) in 1 M KOH at 298 K.

As can be pointed in Figure 4.23, the highest current density and lower decomposition voltage is seen for G-I/NiCo.

**Table 4.12.** Produced hydrogen volume with G-I/NiCo at the end of 30 minutes.

Applied Potential (V)	I(mA)	Produced Hydrogen Volume (mL)
2.3	92.7	22.00
2.4	97.3	24.00
2.5	106.8	27.00
2.6	112.8	29.00
2.7	132.2	33.00
2.8	147.8	35.00
2.9	154.2	37.50
3.0	180.0	42.00

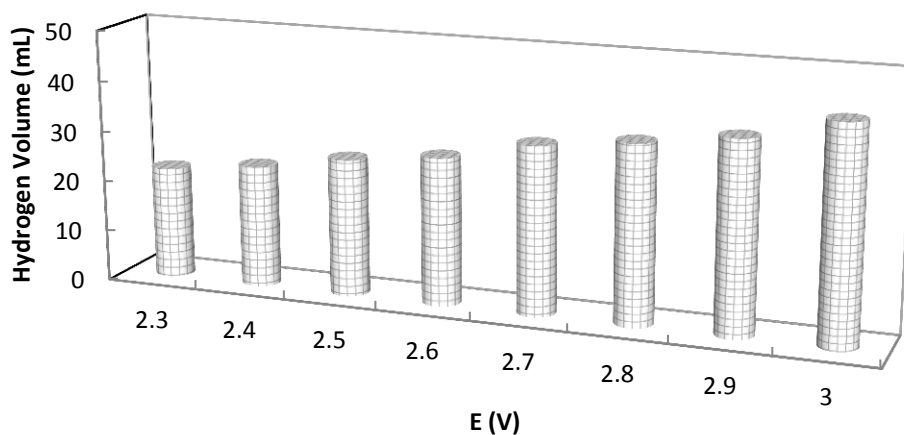


**Figure 4.24.** Hydrogen production volume by applied voltage with G-I/NiCo.

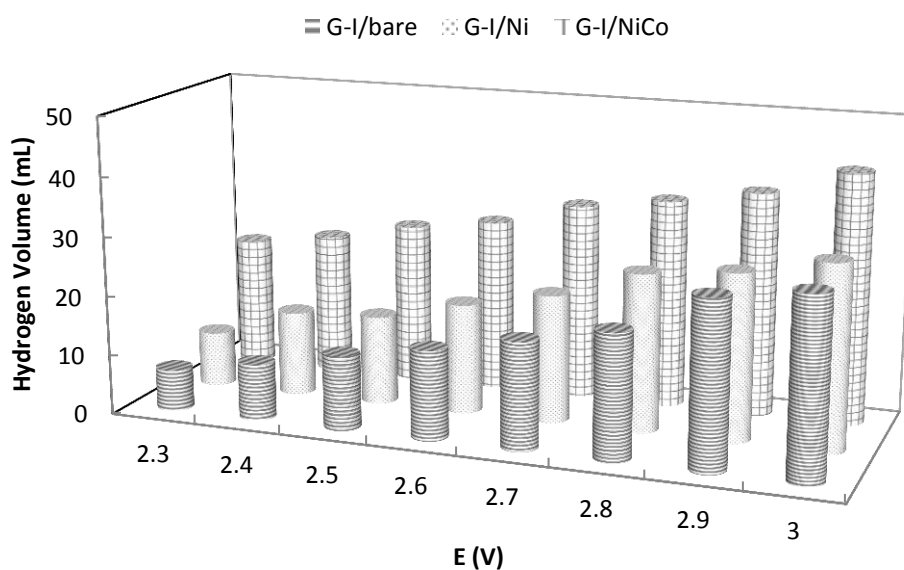


**Figure 4.25.** Comparison of the hydrogen amounts generated by the G-I/bare, G-I/Ni and G-I / NiCo electrodes.

In the experiment with Ni coated graphite electrode decorated with Co, a much higher volume of hydrogen was found compared to Ni coated graphite and bare surface graphite. At the end of 30 minutes, 42 mL of hydrogen was obtained by applying 3 V potential with the G-I /

NiCo electrode. The increase in hydrogen production in the G-I / Ni electrode compared to the G-I / bare electrode remained low.

In the study of Döner (2008), platinum was used as anode in 1 M KOH solution, and Cu, Cu / Cu, Cu / Ni, Cu / Co, Cu / NiCo electrodes were used as cathodes. In the experiments, the maximum amount of hydrogen was obtained in 141 mL with Cu / NiCu electrode in 60 minutes. Considering the production amount in 30 minutes, which is the current test period, assuming that 70.5 mL of hydrogen will be produced, it can be said that a higher hydrogen production has occurred compared to the present experiment. However, it should be noted that the cost of the Cu / NiCu electrode used is higher than the graphite electrode.

In the study of Yuvaraj and Santharaj (2013), the effect of molarity, temperature, time, applied voltage and specified cathode types on hydrogen production was investigated in the experiment with KOH solution. In the experiment where SS 316L, graphite, EN8 and carbon were used as cathodes, the highest hydrogen production was realized when using 55 mL graphite per minute with 12 V constant DC voltage and 1.2 A current. Since it is operated with much higher voltage and current, it is usual to produce much more hydrogen than the current experiment.

In the study of Mert (2018), nickel-cobalt-bismuth (NiCoBi) coating was created on the copper surface by electrochemical method. The performance of the coating in hydrogen production was investigated with the electrochemical decomposition experiment in which alkali water was used as an electrolyte. When bare copper (Cu) was used as cathode, when 3 V constant potential was applied, the amount of hydrogen obtained after 30 minutes was 8.43 mL. This amount increased to 11.52 mL in the same potential and time as nickel plated copper, 15.33 mL hydrogen was obtained with Nickel-Bismuth coated copper, Nickel-Cobalt coated copper 18.61 mL. The highest hydrogen volume was obtained with Cu / NiCoBi as 20.51 mL. The advantage of the selected electrode type can be seen, considering that 42 mL of hydrogen was obtained at the same potential at the same time in the current experiment with nickel-plated, cobalt-decorated graphite (G / NiCo). In addition, the cost of graphite is much lower than the cost of copper (Cu).

In the study by Solmaz and Kardaş (2008), bare surface and nickel plated stainless steel, silver and brass electrodes were used as working electrodes in 0.5 M H<sub>2</sub>SO<sub>4</sub> solution, the current densities and the amount of hydrogen produced were compared. The lowest current density was measured in experiments with nickel-plated electrodes, and the highest hydrogen content was obtained with nickel-plated silver at 5 V constant potential at the end of 30 minutes as 153.6 mL. Although the amount of hydrogen produced is higher than the amount of hydrogen obtained in the present study, it can be concluded that nickel-coated cobalt decorated graphite is more advantageous when the costs of the electrodes used and the applied potential are compared.

Consequently, the performance of the produced G-I/NiCo electrode is comparable with literature and it has profitable advantages while as a cathode in an alkaline electrolysis cell which is supplied by a floating PV system.

## 5. CONCLUSIONS

In this study, we aimed to set – up alternative energy application depends on the solar and hydrogen-based system in order to decrease the global warming problem that threatens the world. The issue of efficiency decreases due to temperature increase, which is one of the biggest problems of electricity generation from solar energy, has been discussed. For this reason, the floating solar panel system, whose applications have been increasing both in the private sector and in the public sector, has been carried out both in the field and simulated in matlab simulink and the results have been examined.

In the experimental section, the ground-mounted solar panel with the same features was installed and a floating solar panel was installed on a large water-filled container in order to make a comparison. Both solar panels were exposed to the sun at the same angle and current and voltage measurements were made at the same temperature values. Four different temperature values were chosen to measure the panel response at different temperatures. These are 6°C, 16°C, 24°C and 37°C. In the observations made, it was seen that the power taken from the panel output increased due to the increasing sunlight with temperature. On the other hand, it was observed that the panel efficiency decreased due to the increase in panel temperature compared to the level of radiation. Therefore, there is no significant difference between the solar panel floating in cool weather like 6°C and 16°C and the solar panel mounted on the land, while the power obtained from the floating solar panel in hot and very hot weather such as 24°C and 37°C is 6.25% and 10.075%, respectively such increases have occurred.

One of the problems with renewable energy is that it is difficult to produce energy at the moment it is consumed, in other words, it cannot be stored. One of the most striking solutions to this problem in recent years is the conversion of the produced energy to hydrogen production by chemical separation methods and the burning of the produced hydrogen in fuel cells when needed and converting it into electrical energy. The world, especially the European Union and the USA, is building its new energy plans on the hydrogen economy. Therefore, obtaining hydrogen by electrolysis method constituted an important part of our work.

KOH was chosen as the electrolyte solution in the electrolysis processes, and graphite was chosen as the working electrode because of its low cost and the independent performance from corrosion in aqueous environment. Initially, the graphite performance was examined 30 mL of hydrogen was obtained after 30 minutes at a potential of 3 V. Results are remarkable when compared with similar studies. Then the graphite surface was coated with 10  $\mu\text{m}$  Ni and the same experiments were repeated and the volume of 32 mL. Finally, the Nickel coated graphite surface was decorated with Co. As a result of the experiments, 42 mL of hydrogen was obtained at the same potential and at the same operation time.

Consequently, we can declare that a profitable system was set up for hydrogen production with the combining floating PV system and alkaline electrolysis.

We created this system and imagined it as a charging station for marine vessels in future applications.

## **6. RECOMMENDATIONS**

Floating solar panels naturally keep costs higher than land-mounted solar panels. Therefore, there is a need for studies in which the yield obtained is compared with the recovery period of the investment. For hydrogen production, the experiments should also be carried with alternative electrodes which have more electrocatalytic efficiency.



## REFERENCES

- Abdalla, A., Khan, I., Sohail, M., & Qurashi, A. (2019). Au/Ga<sub>2</sub>O<sub>3</sub>/ZnO heterostructure nanorods arrays for effective photoelectrochemical water splitting. *Solar Energy*, *181*, 333–338. doi:[10.1016/j.solener.2019.01.065](https://doi.org/10.1016/j.solener.2019.01.065)
- Acar, C., & Dincer, I. (2019a). Review and evaluation of hydrogen production options for better environment. *Journal of Cleaner Production*, *218*, 835–849. doi:[10.1016/j.jclepro.2019.02.046](https://doi.org/10.1016/j.jclepro.2019.02.046)
- Acar, C., & Dincer, I. (2019b). Review and evaluation of hydrogen production options for better environment. *Journal of Cleaner Production*, *218*, 835–849. doi:[10.1016/j.jclepro.2019.02.046](https://doi.org/10.1016/j.jclepro.2019.02.046)
- Ahmed, M., & Dincer, I. (2019). A review on photoelectrochemical hydrogen production systems: Challenges and future directions. *International Journal of Hydrogen Energy*, *44*(5), 2474–2507. doi:[10.1016/j.ijhydene.2018.12.037](https://doi.org/10.1016/j.ijhydene.2018.12.037)
- Alanne, K., & Cao, S. (2017). Zero-energy hydrogen economy (ZEH 2 E) for buildings and communities including personal mobility. *Renewable and Sustainable Energy Reviews*, *71*, 697–711. doi:[10.1016/j.rser.2016.12.098](https://doi.org/10.1016/j.rser.2016.12.098)
- Aleem, S. A., Hussain, S. M. S., & Ustun, T. S. (2020). A Review of Strategies to Increase PV Penetration Level in Smart Grids, 28. Retrieved from Zotero
- Alrabie, K., & Saidan, M. N. (2018). A preliminary solar-hydrogen system for Jordan: Impacts assessment and scenarios analysis. *International Journal of Hydrogen Energy*, *43*(19), 9211–9223. doi:[10.1016/j.ijhydene.2018.03.218](https://doi.org/10.1016/j.ijhydene.2018.03.218)

Al-Sharafi, A., Sahin, A. Z., Ayar, T., & Yilbas, B. S. (2017). Techno-economic analysis and optimization of solar and wind energy systems for power generation and hydrogen production in Saudi Arabia. *Renewable and Sustainable Energy Reviews*, 69, 33–49.

doi:[10.1016/j.rser.2016.11.157](https://doi.org/10.1016/j.rser.2016.11.157)

articles.exe. (n.d.).

Badea, G., Naghiu, G. S., Giurca, I., Aşchilean, I., & Megyesi, E. (2017). Hydrogen Production Using Solar Energy - Technical Analysis. *Energy Procedia*, 112, 418–425.

doi:[10.1016/j.egypro.2017.03.1097](https://doi.org/10.1016/j.egypro.2017.03.1097)

Bareiß, K., de la Rua, C., Möckl, M., & Hamacher, T. (2019). Life cycle assessment of hydrogen from proton exchange membrane water electrolysis in future energy systems. *Applied Energy*, 237, 862–872. doi:[10.1016/j.apenergy.2019.01.001](https://doi.org/10.1016/j.apenergy.2019.01.001)

Benli, H. (2016). Potential application of solar water heaters for hot water production in Turkey. *Renewable and Sustainable Energy Reviews*, 54, 99–109. doi:[10.1016/j.rser.2015.09.061](https://doi.org/10.1016/j.rser.2015.09.061)

Bhattacharyya, R., Misra, A., & Sandeep, K. C. (2017). Photovoltaic solar energy conversion for hydrogen production by alkaline water electrolysis: Conceptual design and analysis. *Energy Conversion and Management*, 133, 1–13. doi:[10.1016/j.enconman.2016.11.057](https://doi.org/10.1016/j.enconman.2016.11.057)

Buttler, A., & Spliethoff, H. (2018). Current status of water electrolysis for energy storage, grid balancing and sector coupling via power-to-gas and power-to-liquids: A review. *Renewable and Sustainable Energy Reviews*, 82, 2440–2454. doi:[10.1016/j.rser.2017.09.003](https://doi.org/10.1016/j.rser.2017.09.003)

C6-Hydrogen gas evolution at nickel coated.pdf. (n.d.).

Cao, S., Piao, L., & Chen, X. (2020). Emerging Photocatalysts for Hydrogen Evolution. *Trends in Chemistry*, 2(1), 57–70. doi:[10.1016/j.trechm.2019.06.009](https://doi.org/10.1016/j.trechm.2019.06.009)

- Chi, J., & Yu, H. (2018). Water electrolysis based on renewable energy for hydrogen production. *Chinese Journal of Catalysis*, 39(3), 390–394. doi:[10.1016/S1872-2067\(17\)62949-8](https://doi.org/10.1016/S1872-2067(17)62949-8)
- Daneshpour, R., & Mehrpooya, M. (2018). generation and solid oxide electrolyser for hydrogen production. *Energy Conversion and Management*, 13. Retrieved from Zotero
- David, M., Ocampo-Martínez, C., & Sánchez-Peña, R. (2019). Advances in alkaline water electrolyzers: A review. *Journal of Energy Storage*, 23, 392–403.  
doi:[10.1016/j.est.2019.03.001](https://doi.org/10.1016/j.est.2019.03.001)
- Davis, J. T., Qi, J., Fan, X., Bui, J. C., & Esposito, D. V. (2018). Floating membraneless PV-electrolyzer based on buoyancy-driven product separation. *International Journal of Hydrogen Energy*, 43(3), 1224–1238. doi:[10.1016/j.ijhydene.2017.11.086](https://doi.org/10.1016/j.ijhydene.2017.11.086)
- Demirbas, A., & Bakis, R. (2004). Energy from Renewable Sources in Turkey: Status and Future Direction. *Energy Sources*, 26(5), 473–484. doi:[10.1080/00908310490429759](https://doi.org/10.1080/00908310490429759)
- Dincer, I., & Zamfirescu, C. (2012). Sustainable hydrogen production options and the role of IAHE. *International Journal of Hydrogen Energy*, 37(21), 16266–16286.  
doi:[10.1016/j.ijhydene.2012.02.133](https://doi.org/10.1016/j.ijhydene.2012.02.133)
- Dincer, I., & Zamfirescu, C. (2016). Hydrogen Production by Electrical Energy. In *Sustainable Hydrogen Production* (pp. 99–161). Elsevier. doi:[10.1016/B978-0-12-801563-6.00003-0](https://doi.org/10.1016/B978-0-12-801563-6.00003-0)
- Döner, A. (n.d.). ÇUKUROVA ÜNİVERSİTESİ FEN BİLİMLERİ ENSTİTÜSÜ, 128. Retrieved from Zotero
- Đukić, A., & Firak, M. (2011). Hydrogen production using alkaline electrolyzer and photovoltaic (PV) module. *International Journal of Hydrogen Energy*, 36(13), 7799–7806.  
doi:[10.1016/j.ijhydene.2011.01.180](https://doi.org/10.1016/j.ijhydene.2011.01.180)

- Elminshawy, N. A. S., Mohamed, A. M. I., Morad, K., Elhenawy, Y., & Alrobaian, A. A. (2019). Performance of PV panel coupled with geothermal air cooling system subjected to hot climatic. *Applied Thermal Engineering*, 148, 1–9. doi:[10.1016/j.applthermaleng.2018.11.027](https://doi.org/10.1016/j.applthermaleng.2018.11.027)
- Fawzy, S. M., Omar, M. M., & Allam, N. K. (2019). Photoelectrochemical water splitting by defects in nanostructured multinary transition metal oxides. *Solar Energy Materials and Solar Cells*, 194, 184–194. doi:[10.1016/j.solmat.2019.02.011](https://doi.org/10.1016/j.solmat.2019.02.011)
- Ghazi S., Ip K., (2014) The effect of weather conditions on the efficiency of PV panels in the southeast of UK *Renewable Energy Volume 69, September 2014, Pages 50-59* doi:[10.1016/j.renene.2014.03.018](https://doi.org/10.1016/j.renene.2014.03.018)
- Gil, J. J., Aguilar-Martínez, O., Piña-Pérez, Y., Pérez-Hernández, R., Santolalla-Vargas, C. E., Gómez, R., & Tzompantzi, F. (2020). Efficient ZnS–ZnO/ZnAl-LDH composite for H<sub>2</sub> production by photocatalysis. *Renewable Energy*, 145, 124–132. doi:[10.1016/j.renene.2019.06.001](https://doi.org/10.1016/j.renene.2019.06.001)
- Gondal, I. A., Masood, S. A., & Khan, R. (2018). Green hydrogen production potential for developing a hydrogen economy in Pakistan. *International Journal of Hydrogen Energy*, 43(12), 6011–6039. doi:[10.1016/j.ijhydene.2018.01.113](https://doi.org/10.1016/j.ijhydene.2018.01.113)
- Gorjian, S., Sharon, H., Ebadi, H., Kant, K., Scavo, F. B., & Tina, G. M. (2021). Recent technical advancements, economics and environmental impacts of floating photovoltaic solar energy conversion systems. *Journal of Cleaner Production*, 278, 124285. doi:[10.1016/j.jclepro.2020.124285](https://doi.org/10.1016/j.jclepro.2020.124285)
- Haug, P., Kreitz, B., Koj, M., & Turek, T. (2017). Process modelling of an alkaline water electrolyzer. *International Journal of Hydrogen Energy*, 42(24), 15689–15707. doi:[10.1016/j.ijhydene.2017.05.031](https://doi.org/10.1016/j.ijhydene.2017.05.031)

- He, Y., & Wang, D. (2018). Toward Practical Solar Hydrogen Production. *Chem*, 4(3), 405–408.  
doi:[10.1016/j.chempr.2018.02.013](https://doi.org/10.1016/j.chempr.2018.02.013)
- Hien, T. T., Quang, N. D., Kim, C., & Kim, D. (2019). Energy diagram analysis of photoelectrochemical water splitting process. *Nano Energy*, 57, 660–669.  
doi:[10.1016/j.nanoen.2018.12.093](https://doi.org/10.1016/j.nanoen.2018.12.093)
- Hoffmann, J. E. (2019). On the outlook for solar thermal hydrogen production in South Africa. *International Journal of Hydrogen Energy*, 44(2), 629–640.  
doi:[10.1016/j.ijhydene.2018.11.069](https://doi.org/10.1016/j.ijhydene.2018.11.069)
- Hossain, M. S., Rahim, N. A., Aman, M. M., & Selvaraj, J. (2019). Application of ANOVA method to study solar energy for hydrogen production. *International Journal of Hydrogen Energy*, 44(29), 14571–14579. doi:[10.1016/j.ijhydene.2019.04.028](https://doi.org/10.1016/j.ijhydene.2019.04.028)
- Hu, Q., Shen, Y., Chew, J. W., Ge, T., & Wang, C.-H. (2020). Chemical looping gasification of biomass with Fe<sub>2</sub>O<sub>3</sub>/CaO as the oxygen carrier for hydrogen-enriched syngas production. *Chemical Engineering Journal*, 379, 122346. doi:[10.1016/j.cej.2019.122346](https://doi.org/10.1016/j.cej.2019.122346)
- Ito, H., Maeda, T., Nakano, A., & Takenaka, H. (2011). Properties of Nafion membranes under PEM water electrolysis conditions. *International Journal of Hydrogen Energy*, 36(17), 10527–10540. doi:[10.1016/j.ijhydene.2011.05.127](https://doi.org/10.1016/j.ijhydene.2011.05.127)
- Jin, Q., Shen, Y., Cai, Y., Chu, L., & Zeng, Y. (2020). Resource utilization of waste V<sub>2</sub>O<sub>5</sub>-based deNO<sub>x</sub> catalysts for hydrogen production from formaldehyde and water via steam reforming. *Journal of Hazardous Materials*, 381, 120934. doi:[10.1016/j.jhazmat.2019.120934](https://doi.org/10.1016/j.jhazmat.2019.120934)

- Joy, J., Mathew, J., & George, S. C. (2018). Nanomaterials for photoelectrochemical water splitting – review. *International Journal of Hydrogen Energy*, 43(10), 4804–4817.  
doi:[10.1016/j.ijhydene.2018.01.099](https://doi.org/10.1016/j.ijhydene.2018.01.099)
- Kamuyu, W. C. L., Lim, J. R., Won, C. S., & Ahn, H. K. (2018). Prediction Model of Photovoltaic Module Temperature for Power Performance of Floating PVs, 13. Retrieved from Zotero
- Kaygusuz, K. (2011). Prospect of concentrating solar power in Turkey: The sustainable future. *Renewable and Sustainable Energy Reviews*, 15(1), 808–814. doi:[10.1016/j.rser.2010.09.042](https://doi.org/10.1016/j.rser.2010.09.042)
- Keleş, S., & Bilgen, S. (2012). Renewable energy sources in Turkey for climate change mitigation and energy sustainability. *Renewable and Sustainable Energy Reviews*, 16(7), 5199–5206.  
doi:[10.1016/j.rser.2012.05.026](https://doi.org/10.1016/j.rser.2012.05.026)
- Koumi Ngoh, S., & Njomo, D. (2012). An overview of hydrogen gas production from solar energy. *Renewable and Sustainable Energy Reviews*, 16(9), 6782–6792.  
doi:[10.1016/j.rser.2012.07.027](https://doi.org/10.1016/j.rser.2012.07.027)
- Li, H., Wang, X., Xi, J., Du, G., Li, Z., & Ji, Z. (2019). Efficient photoelectrochemical water splitting of stainless steel electrocatalyst modified TiO<sub>2</sub> films. *Journal of Alloys and Compounds*, 803, 546–553. doi:[10.1016/j.jallcom.2019.06.315](https://doi.org/10.1016/j.jallcom.2019.06.315)
- Li, W., Wang, K., Yang, X., Zhan, F., Wang, Y., Liu, M., ... Liu, Y. (2020). Surfactant-assisted controlled synthesis of a metal-organic framework on Fe<sub>2</sub>O<sub>3</sub> nanorod for boosted photoelectrochemical water oxidation. *Chemical Engineering Journal*, 379, 122256.  
doi:[10.1016/j.cej.2019.122256](https://doi.org/10.1016/j.cej.2019.122256)

- Lin, M., & Haussener, S. (2017). Techno-economic modeling and optimization of solar-driven high-temperature electrolysis systems. *Solar Energy*, 155, 1389–1402.  
doi:[10.1016/j.solener.2017.07.077](https://doi.org/10.1016/j.solener.2017.07.077)
- Liu, Y., Lin, R., Man, Y., & Ren, J. (2019). Recent developments of hydrogen production from sewage sludge by biological and thermochemical process. *International Journal of Hydrogen Energy*, 44(36), 19676–19697. doi:[10.1016/j.ijhydene.2019.06.044](https://doi.org/10.1016/j.ijhydene.2019.06.044)
- Mahmood, N., Yao, Y., Zhang, J.-W., Pan, L., Zhang, X., & Zou, J.-J. (2018). Electrocatalysts for Hydrogen Evolution in Alkaline Electrolytes: Mechanisms, Challenges, and Prospective Solutions. *Advanced Science*, 5(2), 1700464. doi:[10.1002/advs.201700464](https://doi.org/10.1002/advs.201700464)
- Marini, S., Salvi, P., Nelli, P., Pesenti, R., Villa, M., Berrettoni, M., ... Kirov, Y. (2012). Advanced alkaline water electrolysis. *Electrochimica Acta*, 8. Retrieved from Zotero
- Marmara University Technology Faculty Electric-Electronic Engineering Department, Ziverbey Campus 34722 Goztepe, Istanbul, & Oyman Serteller, N. F. (2018). Examination and Comparison of Nuclear Energy with other Available Energy Sources for Electricity Production in Turkey. *International Journal of Humanities and Social Science Research*, 3, 38–42. doi:[10.6000/2371-1655.2017.03.04](https://doi.org/10.6000/2371-1655.2017.03.04)
- May, M. M., Lackner, D., Ohlmann, J., Dimroth, F., van de Krol, R., Hannappel, T., & Schwarzburg, K. (n.d.). On the Benchmarking of Multi-Junction Photoelectro- chemical Fuel Generating Devices, 13. Retrieved from Zotero
- Mert, M. E. (n.d.-a). ÇUKUROVA ÜNİVERSİTESİ FEN BİLİMLERİ ENSTİTÜSÜ, 120.  
Retrieved from Zotero

Mert, M. E. (n.d.-b). ÇUKUROVA ÜNİVERSİTESİ FEN BİLİMLERİ ENSTİTÜSÜ, 96.

Retrieved from Zotero

Mockaitis, G., Bruant, G., Guiot, S. R., Peixoto, G., Foresti, E., & Zaiat, M. (2020). Acidic and thermal pre-treatments for anaerobic digestion inoculum to improve hydrogen and volatile fatty acid production using xylose as the substrate. *Renewable Energy*, *145*, 1388–1398. doi:[10.1016/j.renene.2019.06.134](https://doi.org/10.1016/j.renene.2019.06.134)

Moliner, R., Lázaro, M. J., & Suelves, I. (2016). Analysis of the strategies for bridging the gap towards the Hydrogen Economy. *International Journal of Hydrogen Energy*, *41*(43), 19500–19508. doi:[10.1016/j.ijhydene.2016.06.202](https://doi.org/10.1016/j.ijhydene.2016.06.202)

Nematollahi, O., Alamdari, P., Jahangiri, M., Sedaghat, A., & Alemrajabi, A. A. (2019). A techno-economical assessment of solar/wind resources and hydrogen production: A case study with GIS maps. *Energy*, *175*, 914–930. doi:[10.1016/j.energy.2019.03.125](https://doi.org/10.1016/j.energy.2019.03.125)

Nouicer, I., Khellaf, A., Menia, S., Yaiche, M. R., Kabouche, N., & Meziane, F. (2019). Solar hydrogen production using direct coupling of SO<sub>2</sub> depolarized electrolyser to a solar photovoltaic system. *International Journal of Hydrogen Energy*, *44*(39), 22408–22418. doi:[10.1016/j.ijhydene.2018.11.106](https://doi.org/10.1016/j.ijhydene.2018.11.106)

Omar, M. A., & Altinişik, K. (2016). Simulation of hydrogen production system with hybrid solar collector. *International Journal of Hydrogen Energy*, *41*(30), 12836–12841. doi:[10.1016/j.ijhydene.2016.05.166](https://doi.org/10.1016/j.ijhydene.2016.05.166)

Park, J., Deshmukh, P. R., Sohn, Y., & Shin, W. G. (2019). ZnO-TiO<sub>2</sub> core-shell nanowires decorated with Au nanoparticles for plasmon-enhanced photoelectrochemical water splitting. *Journal of Alloys and Compounds*, *787*, 1310–1319. doi:[10.1016/j.jallcom.2019.02.061](https://doi.org/10.1016/j.jallcom.2019.02.061)

- Perez-Trujillo, J. P., Elizalde-Blancas, F., Pietra, M. D., & McPhail, S. J. (2018). carbonate cell operating in fuel cell mode and electrolysis mode. *Applied Energy*, 19. Retrieved from Zotero
- Perlin M. (2013). Sanism and the law, *American Medical Association Journal of Ethics* October 2013, Volume 15, Number 10: 878-885.  
doi: 10.1001/virtualmentor.2013.15.10.msoc1-1310 · Source: PubMed
- Ranjbaran, P., Yousefi, H., Gharehpetian, G. B., & Astaraei, F. R. (2019). A review on floating photovoltaic (FPV) power generation units. *Renewable and Sustainable Energy Reviews*, 110, 332–347. doi:[10.1016/j.rser.2019.05.015](https://doi.org/10.1016/j.rser.2019.05.015)
- Sahu, A. (2016). Floating photovoltaic power plant\_ A review. *Renewable and Sustainable Energy Reviews*, 10. Retrieved from Zotero
- Sakr, I. M., Abdelsalam, A. M., & El-Askary, W. A. (2017). Effect of electrodes separator-type on hydrogen production using solar energy. *Energy*, 140, 625–632.  
doi:[10.1016/j.energy.2017.09.019](https://doi.org/10.1016/j.energy.2017.09.019)
- Sellami, M. H., & Loudiyi, K. (2017). Electrolytes behavior during hydrogen production by solar energy. *Renewable and Sustainable Energy Reviews*, 70, 1331–1335.  
doi:[10.1016/j.rser.2016.12.034](https://doi.org/10.1016/j.rser.2016.12.034)
- Senthilraja, S., Gangadevi, R., Marimuthu, R., & Baskaran, M. (2020). Performance evaluation of water and air based PVT solar collector for hydrogen production application. *International Journal of Hydrogen Energy*, 45(13), 7498–7507. doi:[10.1016/j.ijhydene.2019.02.223](https://doi.org/10.1016/j.ijhydene.2019.02.223)
- Sheikhabaei, V., Baniasadi, E., & Naterer, G. F. (2018). Experimental investigation of solar assisted hydrogen production from water and aluminum. *International Journal of Hydrogen Energy*, 43(19), 9181–9191. doi:[10.1016/j.ijhydene.2018.03.196](https://doi.org/10.1016/j.ijhydene.2018.03.196)

- Shiva Kumar, S., & Himabindu, V. (2019). Hydrogen production by PEM water electrolysis – A review. *Materials Science for Energy Technologies*, 2(3), 442–454.  
doi:[10.1016/j.mset.2019.03.002](https://doi.org/10.1016/j.mset.2019.03.002)
- Singh, V., & Chatterjee, T. (2013). Study on splitting of water for production of hydrogen gas using solar energy. *Recent Research in Science and Technology*, 3. Retrieved from Zotero
- Solmaz, R. (n.d.). ÇUKUROVA ÜNİVERSİTESİ FEN BİLİMLERİ ENSTİTÜSÜ, 181.
- Sun, X., Xu, K., Fleischer, C., Liu, X., Grandcolas, M., Strandbakke, R., ... Chatzitakis, A. (2018). Earth-Abundant Electrocatalysts in Proton Exchange Membrane Electrolyzers. *Catalysts*, 8(12), 657. doi:[10.3390/catal8120657](https://doi.org/10.3390/catal8120657)
- Tavares, R., Monteiro, E., Tabet, F., & Rouboa, A. (2020). Numerical investigation of optimum operating conditions for syngas and hydrogen production from biomass gasification using Aspen Plus. *Renewable Energy*, 6. Retrieved from Zotero
- Tayebi, M., & Lee, B.-K. (2019). Recent advances in BiVO<sub>4</sub> semiconductor materials for hydrogen production using photoelectrochemical water splitting. *Renewable and Sustainable Energy Reviews*, 111, 332–343. doi:[10.1016/j.rser.2019.05.030](https://doi.org/10.1016/j.rser.2019.05.030)
- Temiz, M., & Javani, N. (2020). Design and analysis of a combined floating photovoltaic system for electricity and hydrogen production. *International Journal of Hydrogen Energy*, 45(5), 3457–3469. doi:[10.1016/j.ijhydene.2018.12.226](https://doi.org/10.1016/j.ijhydene.2018.12.226)
- Touili, S., Alami Merrouni, A., Azouzoute, A., El Hassouani, Y., & Amrani, A. (2018). A technical and economical assessment of hydrogen production potential from solar energy in Morocco. *International Journal of Hydrogen Energy*, 43(51), 22777–22796.  
doi:[10.1016/j.ijhydene.2018.10.136](https://doi.org/10.1016/j.ijhydene.2018.10.136)

Türkmen, Ü. (n.d.). ÇUKUROVA ÜNİVERSİTESİ FEN BİLİMLERİ ENSTİTÜSÜ, 104.

Vincent, I., & Bessarabov, D. (2018). Low cost hydrogen production by anion exchange membrane electrolysis: A review. *Renewable and Sustainable Energy Reviews*, *81*, 1690–1704. doi:[10.1016/j.rser.2017.05.258](https://doi.org/10.1016/j.rser.2017.05.258)

Wang, L., Tong, Y., Feng, J., Hou, J., Li, J., Hou, X., & Liang, J. (2019). G-C<sub>3</sub>N<sub>4</sub>-based films: A rising star for photoelectrochemical water splitting. *Sustainable Materials and Technologies*, *19*, e00089. doi:[10.1016/j.susmat.2018.e00089](https://doi.org/10.1016/j.susmat.2018.e00089)

Wang, P., Yin, Z., Gao, L., Li, H., Zhang, T., Shen, Q., ... Zou, Z. (2020). Thiourea-assisted coating of dispersed copper electrocatalysts on Si photocathodes for solar hydrogen production. *Journal of Energy Chemistry*, *40*, 75–80. doi:[10.1016/j.jechem.2019.02.012](https://doi.org/10.1016/j.jechem.2019.02.012)

Wittstock, G., Rastgar, S., & Scarabino, S. (2019). Local studies of photoelectrochemical reactions at nanostructured oxides. *Current Opinion in Electrochemistry*, *13*, 25–32. doi:[10.1016/j.coelec.2018.10.007](https://doi.org/10.1016/j.coelec.2018.10.007)

Xing, Z., Zong, X., Pan, J., & Wang, L. (2013). On the engineering part of solar hydrogen production from water splitting: Photoreactor design. *Chemical Engineering Science*, *104*, 125–146. doi:[10.1016/j.ces.2013.08.039](https://doi.org/10.1016/j.ces.2013.08.039)

Yang, Y., Liu, M., Wei, Q., Li, J., & Zhao, L. (2017). Toward the enhancement of activity and stability of CdXZn<sub>1-X</sub>S photocatalyst for solar hydrogen production. *International Journal of Hydrogen Energy*, *42*(43), 26597–26604. doi:[10.1016/j.ijhydene.2017.09.010](https://doi.org/10.1016/j.ijhydene.2017.09.010)

Yuvaraj, A. L., & Santhanaraj, D. (n.d.). A Systematic Study on Electrolytic Production of Hydrogen Gas by Using Graphite as Electrode. *Materials Research*, *5*. Retrieved from Zotero